UNIVERSITÉ DU QUÉBEC À TROIS-RIVIÈRES

DAF-18/PTEN prévient le gaspillage des ovocytes chez *C. elegans* en prévenant la relaxation spontanée du col de la spermathèque lorsqu'elle est dépourvue de spermatozoïdes

C. elegans DAF-18/PTEN prevents oocyte wastage by preventing spontaneous dilation of the sperm-less spermatheca neck

THÈSE PRÉSENTÉE
COMME EXIGENCE PARTIELLE DU
DOCTORAT EN BIOLOGIE CELLULAIRE ET MOLÉCULAIRE

PAR
JICHAO DENG

DEC 2023

UNIVERSITÉ DU QUÉBEC À TROIS-RIVIÈRES

UNIVERSITÉ DU QUÉBEC À TROIS-RIVIÈRES

BIOLOGIE CELLULAIRE ET MOLÉCULAIRE (DOCTORAT)

Direction de recherche :

Patrick Narbonne — Directeur de recherche

Jury d'évaluation de la thèse :

Patrick Narbonne — Directeur de recherche

Erwan Pernet — Évaluateur interne by Président du jury

Jean-Philippe Leduc Gaudet — Évaluateur interne

Jean-Claude Labbé — Évaluateur externe

Thèse soutenue le 5 décembre 2023

I dedicate my thesis to my mother, father,
family, and friends

ACKNOWLEDGEMENTS

I would like to express my heartfelt appreciation and gratitude to my esteemed professor, Patrick Narbonne, for his exceptional mentorship and unwavering support throughout my doctoral journey. He has displayed numerous admirable traits that have had a profound impact on my academic and personal growth. His kindness, forgiveness, friendliness and understanding have helped me navigate the challenges of life and academia with resilience and determination. His guidance and teachings have enriched my knowledge, skills, and perspective, shaping me into a better researcher and individual. Under his excellent mentorship, I have learned how to delve deep into a research project, think critically, and push the boundaries of my intellectual capabilities. Moreover, his unwavering support during the unprecedented COVID-19 pandemic has been truly invaluable. He went above and beyond to assist me in balancing my personal and professional responsibilities, providing guidance, and instilling confidence in my abilities. I am immensely grateful for his dedication, expertise, and genuine care as my mentor. His profound influence on my academic and personal growth is immeasurable, and I am honoured to have had him as my guide throughout my PhD journey. “Professor Patrick Narbonne, I can't thank you enough from the bottom of my heart for believing in me and giving me this incredible opportunity. I'm truly grateful for all the guidance and support you've provided throughout my doctoral journey. I'm honoured to have had you by my side. Thank you so much!”

My deepest gratitude goes to my beloved family for their unwavering support and love throughout my doctoral journey. Despite the challenges posed by the COVID-19 pandemic and the distance that separated us, my family has shown incredible strength and resilience. To my dear mom and dad, I know that you have faced health issues and other difficulties during the past four years, and I am sorry for not being able to be physically present with you. Your unwavering belief in my abilities, your constant encouragement, and your comforting words during difficult situations have been my guiding light. Your sacrifices, understanding, and love have been instrumental in my

achievements, and I am deeply grateful for your endless support. Mom, dad, I am truly blessed to have you as my parents, and I cherish your love and guidance more than words can express. I wish I could be your son again in the next life, and I am forever grateful for your presence in my life.

I would like to take a moment to express my appreciation to the most important person in this journey - myself. I thank myself for staying motivated and pushing through despite the challenges I encountered along the way. My sincere gratitude goes to myself for being my own biggest supporter, believing in my abilities, and never giving up on my dreams. I would also like to acknowledge my own maturity and growth throughout this journey. I am grateful for the lessons I have learned, the skills I have developed, and the wisdom I have gained.

I would like to thank all my friends and colleagues Alexandre Clouet, Lloyd Venceslas Fotso Dzuna, Pier-Olivier Martel, Armi Chaudhari, Matthieu Valet, Xavier Lechasseur, Sarah Turmel-Couture, Maria L. Naranjo, Lucie Beaulieu, Erika Emond, Janina Rieger, Rustelle Janse Van Vuuren, and Mohamad Ali EI Mortada for creating a supportive and positive work environment in the lab. Their good work vibe and camaraderie have been invaluable in making my research journey enjoyable and motivating. I am grateful for their generosity in sharing their knowledge and experience of experiments, which has greatly contributed to the success of my research. I would also like to thank Benjamin Dufour, Vincent Roy, Olivier Gagné, Andres F. Rodriguez, Pier-Olivier Martel, and Armi Chaudhari for their valuable contributions to my PhD work.

I would like to extend my appreciation to the other labs at UQTR, particularly the Hugo Germain and Isabel Desgagne-Penix's Lab, the Alexandre Fisette and Eric Asselin's Lab, for their willingness to share research equipment and resources. Their collaboration and support have been instrumental in expanding the scope of my research and enhancing the quality of my work. I would also like to extend my thanks to Drs Erin J. Cram, Mei Zhen and Florence Solari lab for generously providing reagents, which have greatly enriched my research and contributed to the success of my doctoral

thesis. I am grateful for their willingness to share their resources and expertise. Additionally, I would like to express my appreciation to the *Caenorhabditis* Genetics Centre (CGC) for providing the plethora of *C. elegans* strains that have been essential to my experiments.

I am deeply grateful to the NSERC (RGPIN-2019-06863, RGPAS-2019-00017, DGECR-2019-00326) and the CIHR (PJT-169138) and the FRQS (J2-310643) for their invaluable support to the Narbonne Laboratory. Their financial assistance has provided me with the means to pursue my doctoral thesis, allowing me to focus on my passion for science without distractions. I am honoured to acknowledge their contribution to my research and express my heartfelt appreciation for their invaluable support to fundamental research.

In addition, I express my deepest gratitude to all my friends for their presence in my life. I would like to thanks my old friends Depeng Dai, Lifang Liao, Lijun He for being on my side as I was confused with my life. I would like to thank Hongmei Liu, Qiangbing Yang, Bing Yao, Yuxin Zhang, and Shihao Pei for being my companions as I ventured into uncharted territories outside of the lab. Their friendship and companionship have given me a renewed sense of purpose and joy, and I am truly blessed to have them in my life.

Finally, I want to declare that I used ChatGPT to assist in proofreading and refining this thesis.

My sincere thanks to all my well-wishers!

RÉSUMÉ

La phosphatase et homologue de TENsin PTEN est un important suppresseur de tumeur, sa perte étant associée à divers types de cancer. En clinique, le syndrome des tumeurs hamartomateuses PTEN (PHTS) comprend le syndrome de Cowden (CS), le syndrome de Bannayan-Riley-Ruvalcaba (BRRS), et le syndrome de Protée lié à PTEN (PS). *Caenorhabditis elegans* (*C. elegans*) est un organisme modèle largement utilisé pour l'étude de divers processus biologiques en raison de ses nombreux avantages, tels que son génome simple et sa courte durée de vie, qui permettent une manipulation génétique facile et une observation rapide des changements au fil du temps. Chez *C. elegans*, l'orthologue de PTEN est codé par le gène *daf-18*, qui est hautement homologue au gène PTEN chez l'humain, de sorte que dans certains cas, PTEN peut remplacer fonctionnellement la fonction de DAF-18 chez *C. elegans*. *C. elegans* constitue donc un excellent système modèle pour étudier le rôle de PTEN. Chez les *C. elegans* hermaphrodites qui manquent de sperme, DAF-18 est nécessaire pour que les ovocytes s'arrêtent et s'accumulent dans la gonade proximale, et pour la régulation homéostatique concomitante de la prolifération des cellules souches germinales, afin d'éviter une surproduction d'ovocytes. En tant que tels, les mutants *daf-18(ø)* sans sperme subissent une oogenèse complète uniquement pour pondre et gaspiller tous les ovocytes résultants. Lorsque la ponte est empêchée, ces ovocytes s'accumulent indéfiniment pour former une tumeur bénigne différenciée pouvant éventuellement rompre la gonade et tuer l'animal. Comment DAF-18 agit pour permettre l'arrêt et l'accumulation des ovocytes en l'absence de spermatozoïdes, pour finalement supprimer la prolifération des cellules souches germinales, reste cependant inconnu.

À ce jour, malgré des preuves accablantes soutenant unilatéralement les rôles cellulaires autonomes du suppresseur de tumeur cellulaire PTEN dans divers types cellulaires et organismes, nous rapportons ici comment nous sommes tombés sur une situation où l'orthologue de PTEN chez *C. elegans*, *daf-18*, agit de manière cellulaire non autonome pour prévenir la tumorigenèse bénigne.

Dans notre étude, nous avons utilisé des transgènes pour sauver spécifiquement *daf-18* dans l'intestin, les neurones, l'hypoderme, les muscles, la gonade somatique proximale et la lignée germinale des mutants *daf-18(ø)* sans sperme. Nous avons trouvé de manière intéressante que l'expression de *daf-18* dans les muscles ou dans la gonade somatique proximal était suffisante pour permettre aux ovocytes non fécondés de s'arrêter et de s'accumuler chez les animaux sans spermatozoïdes. Bien que les cellules spermathécales ressemblent à des cellules musculaires, nous avons constaté que le sauvetage de *daf-18* spécifiquement dans la spermathèque distale, mais pas dans la valve spermathèque-utérine (sp-ut), était suffisant pour permettre l'arrêt des ovocytes. Nous apportons également des preuves que *daf-18* pourrait prévenir la dilatation de la spermathèque distale en inhibant la signalisation d'AKT dans la spermathèque distale. Dans l'ensemble, nos résultats montrent que DAF-18 peut prévenir la dilation de la spermathèque distale pour médiatiser de manière non autonome l'arrêt des ovocytes en l'absence de spermatozoïdes et permettre leur accumulation dans la gonade proximale. Ces résultats fournissent un tout nouveau mécanisme par lequel PTEN peut prévenir la formation de tumeurs.

Mots-clés: DAF-18/PTEN, *C. elegans,* tumeur, spermathèque distale, PLC-1/signalisation Ca^{2+}, signalisation AKT-1,2

ABSTRACT

The Phosphatase and TENsin homolog PTEN is an important tumour suppressor, its loss being associated with various types of cancers. In the clinic, the PTEN hamartoma tumour syndrome (PHTS) includes Cowden syndrome (CS), Bannayan-Riley-Ruvalcaba syndrome (BRRS), and PTEN-related Proteus syndrome (PS). *Caenorhabditis elegans (C. elegans)* is a widely used model organism for studying various biological processes due to its numerous advantages, such as a simple genome and short lifespan, which enable easy genetic manipulation and rapid observation of changes over time. In *C. elegans* the PTEN ortholog is encoded by the *daf-18* gene, which is highly homologous to human PTEN, such that in some cases, human PTEN can functionally replace DAF-18's function in *C. elegans*. *C. elegans* therefore provides an excellent model system to study the role of human PTEN. In *C. elegans* hermaphrodites that lack sperm, DAF-18 is required for oocytes to arrest and accumulate in the proximal gonad, and for the concomitant homeostatic downregulation of germline stem cell proliferation to prevent oocyte overproduction. As such, sperm-less *daf-18(ø)* mutants undergo full blown oogenesis only to lay, and waste, all the resulting oocytes. When laying is prevented, these oocytes accumulate indefinitely to form a disorganized differentiated benign tumour that can eventually rupture the gonad and kill the animal. How DAF-18 acts to permit oocyte arrest and accumulation in the absence of sperm, to eventually suppress germline stem cell (GSC) proliferation, however remains unknown.

To date, despite overwhelming evidence unilaterally supporting cell autonomous tumour suppressor roles for PTEN across cell types and organisms, we report here how we came across a situation where the *C. elegans* PTEN ortholog *daf-18* acts cell non-autonomously to prevent benign tumorigenesis.

In our study, we used transgenes to specifically rescue *daf-18* in the gut, neurons, hypodermis, muscles, proximal somatic gonad, and in the germline of sperm-less *daf-*

18(ø) mutants. Interestingly, we found that *daf-18* expression in the muscles, or in the proximal somatic gonad, was sufficient to allow unfertilized oocytes to arrest and accumulate in sperm-less animals. While the spermathecal cells are muscle-like cells, we found that rescuing *daf-18* specifically in the distal spermatheca, but not in the spermatheca-uterine (sp-ut) valve, was sufficient to permit oocyte arrest. We further provide evidence that *daf-18* may prevent the dilation of the distal spermatheca through inhibiting AKT signaling in the distal spermatheca. Overall, our results demonstrate that DAF-18 may prevent the dilation of the distal spermatheca to non-autonomously mediate oocyte arrest in the absence of sperm, and allow for their accumulation in the proximal gonad. These results provide an entirely new mechanism by which PTEN can prevent tumour formation.

Key words: DAF-18/PTEN, *C. elegans,* tumor, distal spermatheca, PLC-1/Ca^{2+} signaling, AKT-1,2 signaling

CONTENTS

LIST OF FIGURES AND TABLE

LIST OF ABBREVIATIONS AND ACRONYMS

AC	Anchor Cell
ATP	Adenosine TriphosPhate
BRRS	Bannayan-Riley-Ruvalcaba syndrome
Ca^{2+}	Calcium
CaM	Calmodulin
cAMP	cyclic Adenosine Monophosphate
cECs	circular ExtraChromosomal arrays
C. elegans	*Caenorhabditis elegans*
COs	CrossOvers
CS	Cowden Syndrome
DAG	DiAcyl Glycerol
DAPI	4'6-DiAmidino-2-Phenylindole
DIC	Differential Interference Contrast
DTCs	Distal Tip Cells
DSBs	Double-Strand Breaks
ECs	Extrachromosomal arrays
EGF	Epidermal Growth Factor
EGFR	Epidermal Growth Factor Receptor
*Eph*R	*Eph* Receptor
ER	Endoplasmic Reticulum
eunc-54	Enhanced *unc-54*
FBEs	FBF-binding Elements
FBF-1	*Fem-3* mRNA Binding Factor-1
FBF-2	*Fem-3* mRNA Binding Factor-2
GSC	Germline Stem Cell
HDR	Homology-Directed Repair
lECs	Linear Extrachromosomal arrays
IIS	Insulin-like/IGF-1 Signalling

ILPs	Insulin-Like Peptides
IP_3	Inositol-(1,4,5)-trisphosphate
IP_3R	Inositol-(1,4,5)-trisphosphate receptor
IR	Insulin receptor
LF	Lost Function
MI	Mitotic Index
MLCK-1	Myosin Light Chain Kinase
mNG	mNeonGreen
MSP	Major Sperm Protein
NGM	Nematode Growth Media
NHEJ	Non-Homologous End-Joining
PCR	Polymerase Chain Reaction
PDEs	Phosphodiesterases
PFA	Paraformaldehyde
PI_3K	Phosphoinositide 3-Kinase
PIP_2	Phosphatidylinositol 4,5-bisphosphate
PIP_3	Phosphatidylinositol-3,4,5-triphosphate
PKA	Protein Kinase A
PS	Proteus Syndrome
PTEN	The Phosphatase and TENsin homolog
qRT-PCR	quantitative Real-Time Polymerase Chain Reaction
Rho GAP	Rho GTPase Activating Protein
RNAi	RNA interference
RT-PCR	Reverse Transcription-Polymerase Chain Reaction
SC	Synaptonemal Complex
SCs	Sheath Cells
SGBs	Somatic Gonad Blast cells
Sp	Spermatheca
Sp-Ut	Spermatheca-Uterine

SPV-1	Sperm-specific Protein with VWFA and Cache Domains-1
Ut	Uterus
UTRs	UnTranslated Regions
VU	Ventral Uterine
WT	Wild-Type

CHAPTER I

INTRODUCTION

1.1 An overview of *C. elegans*

C. elegans is a microscopic, free-living nematode that can be found worldwide. Due to their small size, these worms are often observed and manipulated using dissecting microscopes. This allows researchers to study the behaviors and development of individual nematodes as they move, eat, develop, mate, and lay eggs. In the laboratory, *C. elegans* is commonly grown on agar plates that contain *Escherichia coli*, a bacterium that provides the nutrients necessary for the nematodes to develop. *C. elegans* has a rapid developmental cycle, with hatched larvae developing through 4 larval stages, termed L1-L4, into egg-laying adults within just a few days. Once an adult, a single hermaphrodite *C. elegans* can lay up to 300 eggs, such that a single animal is enough to rapidly generate a large population [1]. Temperature is an important factor that affects the growth and development of *C. elegans*. The nematodes can be grown at temperatures ranging from 12°C to 25°C [2]. Within this range, for every 10°C increase in temperature, the growth rate of *C. elegans* roughly doubles. The ability to control the temperature and rate of animal development allows researchers to isolate temperature-sensitive mutants and study the effects of temperature on biological processes. Continual growth above 25°C is not possible because it results in sterility.

C. elegans is known for its unique sexual characteristics. Wild-type *C. elegans* can exist in two distinct sexual forms: self-fertilizing hermaphrodites and males (Figure.1.1). The males show a distinct fan tail structure compared to the hermaphrodites.

(a) (b)

Figure. 1. 1 *C. elegans* hermaphrodite and male

(a) Representative hermaphrodite *C. elegans*. Note that there is a larva on top of the hermaphrodite. (b) Representative male *C. elegans*. The tail is on the left, and the head is on the right. Scale bar: 50 µm.

Hermaphrodites have two X chromosomes, their genotype is referred to as XX [3]. In nature, the majority of offspring produced by self-fertilization are hermaphrodites. This is due to the rarity of spontaneous non-disjunction of the X chromosome during meiosis, which causes a male progeny. Only 0.1-0.2% of progeny are male in the wild. However, researchers can induce a short-term increase in male production by exposing *C. elegans* to higher temperatures. The males have a single X chromosome, and their genotype is referred to as XO. The absence of a Y chromosome in *C. elegans* number of X chromosomes determines the organism's sex [3]. Both sexes of *C. elegans* are diploid for five autosomal chromosomes. Notably, when hermaphrodites mate with males, they can produce over 1000 offspring, indicating that sperm production is a limiting factor in self-fertilization [4-6]. The unique sexual characteristics of *C. elegans* have made it an ideal model organism for studying fundamental questions in genetics and developmental biology.

The structure of *C. elegans* is characterized by its cylindrical shape, which is divided

into three distinct regions: the head, midbody, and tail. The head contains sensory organs, such as the amphid and phasmid neurons, which are responsible for detecting chemical and mechanical stimuli [7]. The midbody contains the pharynx, which functions in feeding and digestion, and the gonad, which produces gametes. The tail contains the anus and some motor neurons that participate in locomotion.

During its development, *C. elegans* generates a specific number of somatic cells, with a certain proportion undergoing programmed cell death at specific time points. As a result, the adult hermaphrodite *C. elegans* has a precisely defined number of somatic cells (959 somatic cells) that include various cell types, like neurons, body wall muscle cells, and various epithelial, reproductive, and supporting cells [8, 9]. Notably, the hermaphrodite *C. elegans* has two gonad arms, while the male' gonad has only one arm, highlighting the sexual dimorphism present in this organism. This leads to differences in the arrangement of reproductive and supporting tissues, which contribute to the overall shape of the worm.

In addition, one of the most striking features of *C. elegans* is the precise cell lineage of its development. The entire development of *C. elegans*, from a single-celled zygote to a mature adult, has been mapped at the single-cell level. This provides an unparalleled level of understanding of how the different tissues and organs of *C. elegans* develop and function [9-11]. In our study, we investigate the relationship between GSC proliferation and oocyte generation, as well as ovulation, using the animal model *C. elegans*.

1.2 *C. elegans'* life cycle

After hatching, *C. elegans* develop through L1, L2, L3, L4, and adult stages [12]. However, *C. elegans* may enter the dauer stage in response to environmental cues such as high population density, limited food availability, and high temperatures. The exact timing of when *C. elegans* enters dauer depends on the specific environmental

conditions it experiences. In general, when faced with unfavourable conditions, *C. elegans* will enter dauer after the L2 stage or enter L1 arrest after hatching (Figure. 1.2) [13] [14].

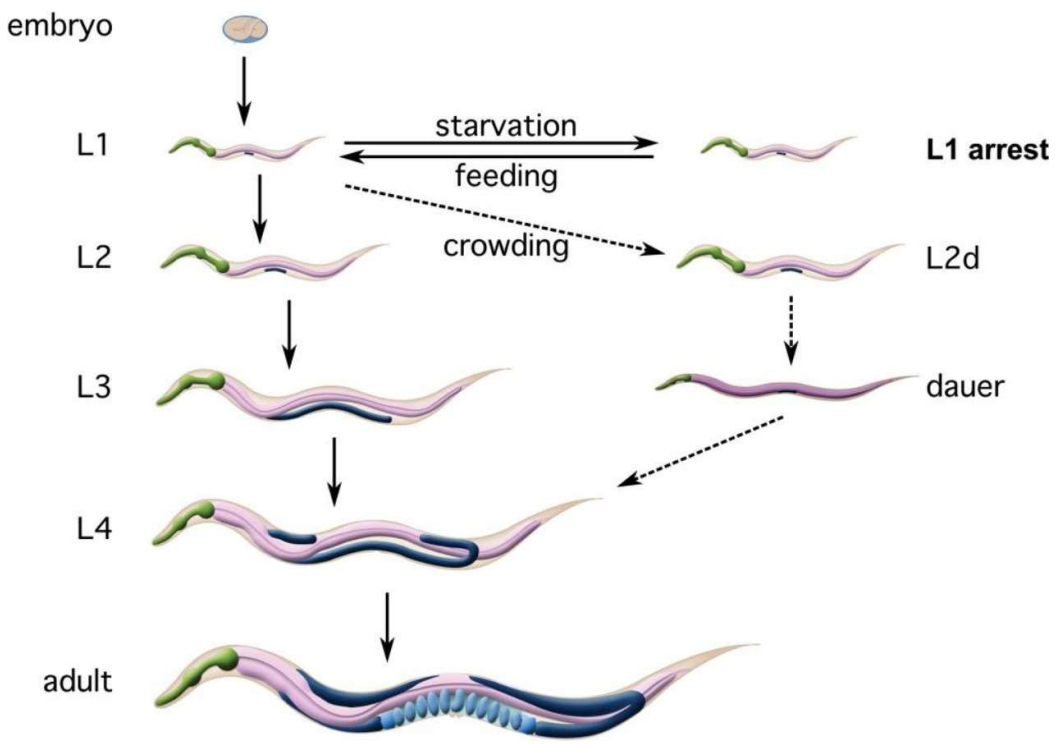

Figure. 1. 2 C. elegans' life cycle [12]

After hatching, *C. elegans* develop through L1, L2, L3, L4, and adult stages. And when faced with unfavourable conditions, *C. elegans* will enter L1 arrest after L1 stage or enter dauer after the L2 stage.

During dauer, the worm undergoes significant physiological and metabolic changes to increase its chances of survival until more favourable conditions are encountered [15]. The dauer stage can last for up to several months. Once the environmental conditions become favourable again, such as the availability of food and optimal temperature, the dauer larvae can recover and resume normal development.

1.3 History of the use of *C. elegans* as a research model

C. elegans was used as an animal model *potentially since* the 17th century. Table. 1. 2 illustrates the historical use of *C. elegans* as a model

Table. 1. 1 *C. elegans* was used as model history

First phase	
17th Century	Researchers aimed to describe and classify various nematode species.
In 1866	Schneider conducted a comparative analysis of multiple species [16].
Second phase	
The end of the 19th century	Nematodes began to be employed as model organisms for investigating broader biological mechanisms
In 1900	Maupas formally described the *C. elegans* species via a publication [17].
Third phase	
In the 1940s	Research teams started utilizing free-living nematodes as model organisms
In 1952	Nigon employed cytological studies of meiosis and a tetraploid line to uncover the chromosomal basis of *C. elegans'* sex determination [18].
Fourth phase	
In 1974	The influential work from Sydney Brenner and his colleagues focused specifically on *C. elegans*, marking a significant milestone in establishing this species as a premier model organism. [8].
Nowadays	

C. elegans is being extensively employed to explore a vast array of biological processes and mechanisms.

In the 17th century, the study of free-living nematodes focused primarily on collecting and observing their morphology, marking the initial phase of research in this field. During this period, researchers aimed to describe and classify various nematode species while also gaining insights into their natural habitats. Noteworthy works, including Schneider's monograph in 1866, involved the comparative analysis of multiple species [16].

A significant turning point occurred at the end of the 19th century, marking the onset of the second phase, where nematodes began to be employed as model organisms for investigating broader biological mechanisms. It was during this phase that the attention turned towards *C. elegans*. Maupas formally described the *C. elegans* species in 1900 via a publication [17]. Maupas also conducted pioneering experiments involving crosses to explore the mechanisms of sex determination, showcasing the species' potential as a model organism [17].

The third historical phase in free-living nematode research emerged in the 1940s when research teams started utilizing free-living nematodes as model organisms. This phase saw advancements in techniques for crossing selfing species like *C. elegans*. Notably, Nigon employed cytological studies of meiosis and a tetraploid line to uncover the chromosomal basis of *C. elegans'* sex determination [18].

The final and transformative phase in the development of free-living nematodes as model organisms commenced in 1974 with the ground-breaking publications by Sydney Brenner and his colleagues. Their influential work focused specifically on *C. elegans*, marking a significant milestone in establishing this species as a premier model organism [8]. These publications laid a solid foundation for future research and set the

stage for the widespread adoption of *C. elegans* as a powerful tool in scientific inquiry.

Nowadays, *C. elegans* has been extensively employed to explore a vast array of intricate biological processes and mechanisms, such as developmental biology [2], evolutionary biology [19], epigenetics [20], neurodegenerative diseases [21], cancer research [22], stem cell biology [23], metabolism and aging [24], drug discovery [25]. In our lab, we employ *C. elegans* as a powerful model organism to delve into the mechanisms underlying GSC proliferation and its interplay with oocyte formation and ovulation. Additionally, we aim to unravel the mechanisms driving tumour formation, shedding light on the processes that govern this complex phenomenon.

1.4 *C. elegans* advantages and traits

1.4.1 General *C. elegans* advantages and traits

As mentioned earlier, *C. elegans* is a highly valuable model organism that has been widely utilized to investigate a diverse range of biological phenomena [8]. It is chosen for its numerous unique advantages, such as transparency, well-defined lineage and cell fate, short lifespan, and genetic manipulability, making it an exceptional tool for exploring developmental processes, aging, drug discovery, and disease.

1.4.2 The utility of *C. elegans* advantages in scientific research

The transparency of *C. elegans* enables researchers to easily label proteins and examine patterns of gene expression and interactions. With its well-defined lineage and cell fate, every cell in the worm's body can be traced back to a specific ancestor cell, which makes it an ideal model for examining the fundamental mechanisms of tissue development [9]. The relatively short lifespan and rapid life cycle of *C. elegans* makes it an ideal model organism, particularly in the field of aging research. With its unique advantages and traits, *C. elegans* has become widely recognized and extensively utilized in scientific research [26]. In the field of drug discovery, *C. elegans* has numerous biological

pathways that are conserved in humans, making it a useful model for exploring the effects of drugs on specific pathways [27]. Due to its relatively simple nervous system, *C. elegans* is also employed in drug toxicity studies, enabling researchers to examine the effects of drugs on behaviour and neural function [28, 29]. When investigating disease, most of *C. elegans* genes are highly conserved in humans and can be examined in order to gain a better understanding of gene function. Moreover, it is easily genetically manipulated, allowing for the creation of disease models and investigation of specific genetic mutations that cause or contribute to disease [30]. This can further elucidate the pathogenesis and mechanism of disease at a cellular and molecular level.

1.4.3 *C. elegans* advantages compared with other animal models

In the field of scientific research, studying human subjects has always presented significant challenges due to ethical considerations and practical limitations [31]. Other mammalian model organisms, such as mice [32, 33], rabbits [34, 35], dogs [36, 37], and pigs [38, 39], have played crucial roles in investigating certain human diseases through genetic manipulation. When it comes to modelling certain diseases and conducting rapid studies, other mammals, have their limitations. For example, studying genes that result in homozygotic mutants leading to embryonic lethality has its limits. Additionally, effective rescue experiments still pose a significant challenge [40, 41].

Despite the availability of advanced tools such as RNA interference (RNAi) and CRISPR/Cas9 genome editing, as well as classical biochemical techniques, investigations conducted on cell lines have proven to be valuable in uncovering signalling pathways. Nevertheless, it's worth noting that these studies are constrained by the absence of the complete organismal physiology within cell culture environments [30].

A remarkable alternative has emerged in the form of *C. elegans*, which offers a unique set of advantages that bypass these ethical and practical concerns. In humans,

maintaining ethical standards is a major concern in scientific and medical research. *C. elegans* provides an ethically favourable platform for scientific inquiry as it eliminates the need for invasive studies involving human subjects. *C. elegans* allows for ease of study while still having the physiology present in a whole animal and the ability to recapitulate at least some aspects of human disease. Furthermore, the high costs and extended lifespans associated with larger mammals often impede research progress.

1.5 Genetic Manipulation in *C. elegans*

In our lab, *C. elegans* is also employed for tumour gene screening following random mutagenesis treatment, capitalizing on its transparency and capacity to produce numerous offspring for efficient screening. Subsequently, we can manipulate the tumour gene in *C. elegans* to delve deeper into its functions. Nowadays, there are numerous methods available to manipulate *C. elegans* genes. However, it's important to note that the complete genome sequence of *C. elegans* was only published in 1998. Since then, extensive studies and annotations have illuminated its structure, function, and evolution [42].

1.5.1 *C. elegans* genetic traits

The *C. elegans* genome consists of approximately 100 million base pairs, encoding around 19500 protein-coding genes [43]. *C. elegans* is a powerful animal model due to its smaller and simpler genome structure with fewer repetitive sequences and genetic redundancy, which makes it easier for researchers to perform simple experiments like polymerase chain reaction (PCR), reverse transcription-polymerase chain reaction (RT-PCR), quantitative real-time polymerase chain reaction (qRT-PCR) [44]. Despite these differences, both *C. elegans* and humans share a significant number of conserved genes involved in basic biological processes, including metabolism, cell division, and signalling pathways [26]. Furthermore, many genes associated with human diseases, such as Alzheimer's and cancer, have counterparts in *C. elegans* that can be studied to gain insights into disease mechanisms [45].

Our study focused on the use of *C. elegans* as a model to investigate Cowden's syndrome, a rare genetic disorder characterized by the development of multiple hamartomas in different tissues of the body, such as the skin, mucous membranes, gastrointestinal tract, thyroid gland, and breast tissue [46]. By studying this model, we hope to gain a deeper understanding of the genetic mechanisms underlying the development of this condition and potentially identify new therapeutic targets.

The genetic traits of *C. elegans* make it an ideal model organism for gene editing studies, and it can be easily manipulated using a variety of genetic tools such as RNAi, CRISPR-Cas9, and extrachromosomal array systems, allowing for precise and efficient modifications of gene expression and function.

1.5.2 The methods used for *C. elegans* genetic manipulation

1.5.2.1 RNA interference (RNAi)

C. elegans is an excellent animal model for gene expression studies, with a wide range of techniques available for both gene suppression and stimulation. One such technique is RNAi, a popular method for suppressing gene expression in *C. elegans* [47]. By simply feeding the nematodes with bacteria that have been transformed with a plasmid designed to produce double-stranded RNA against a gene of interest and spreading the bacterial culture on nematode growth media (NGM), targeted knockdown of gene expression can be achieved efficiently and specifically [48]. Additionally, the availability of a well-annotated genome sequence and a large collection of RNAi clones and reagents makes *C. elegans* an extremely convenient and cost-effective system for RNAi experiments [47].

1.5.2.2 CRISPR/Cas9

Undoubtedly, CRISPR/Cas9 has become a widely adopted tool for modifying gene expression in *C. elegans* [49, 50]. To achieve successful genome editing, it is imperative to ensure the proper localization of the Cas9 protein and sgRNA within the nucleus, where they can form a complex with the DNA. To achieve permanent and heritable

changes, such as the generation of heritable mutations, it is crucial to ensure the expression of Cas9 and sgRNA within the germline. Conversely, if the objective is to generate somatic mutations that are not passed down to future generations, then expression within somatic tissues is required [51].

Eukaryotic cells possess inherent mechanisms for repairing DNA double-strand breaks (DSBs), and these breaks can be mended through either the error-prone non-homologous end-joining (NHEJ) repair pathway or the homology-directed repair (HDR) pathway [52]. To introduce specific point mutations or insertions/deletions of a desired sequence, we manually provide a template that can be utilized by the HDR pathway. However, the HDR pathway is less likely to repair DSBs in most eukaryotic cells. In our lab, to enhance the chances of successful repair, we employ RNA interference (RNAi) targeting *cku-80* while feeding it to *C. elegans* [53]. Additionally, we employ the *dpy-10* co-CRISPR strategy with the *Paix et al.* protocol to assess the efficiency of targeted gene editing [54, 55]. Subsequently, we use micro-injection to deliver the complex, which includes (CRISPR/CAS9 + targeted gene sgRNA, desired template for targeted gene, CRISPR/CAS9 + targeted *dpy-10* sgRNA, and desired template for *dpy-10*), into the core of the distal germline [56]. This region contains a central core of cytoplasm that is shared by many germ cell nuclei. Finally, we can obtain heritable mutations to advance our research.

1.5.2.3 Extrachromosomal arrays (ECs)

In addition, high levels of transgene expression in *C. elegans* can be achieved using ECs [57]. These are extrachromosomal DNA molecules that replicate autonomously and are inherited independently of chromosomes. In our study, we used ECs to rescue the target gene in different tissues of *C. elegans* with loss-of-function mutations, allowing us to determine which tissues require the gene.

1.6 Understanding Germline development

In our research, we have specifically selected the *fog-1(q253)* strain as our background

strain. The decision to use this strain is driven by its unique characteristics, as it represents a feminized variant of *C. elegans* that is incapable of sperm generation and therefore exhibits oocyte accumulation [58, 59]. This phenotype offers an excellent opportunity to delve deeper into the mechanisms underlying oocyte arrest and accumulation mechanisms in the absence of sperm.

1.6.1 germline proliferation (Figure. 1.3)

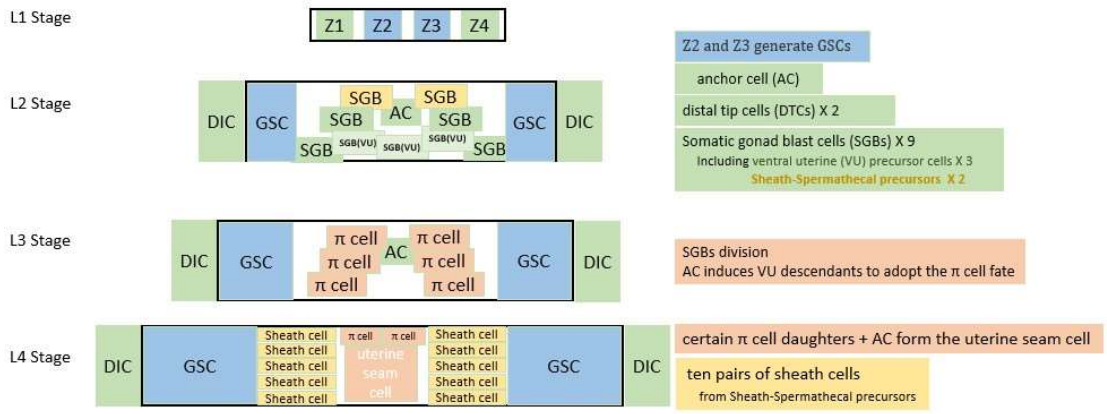

Figure. 1. 3 germline proliferation

Hermaphrodites of the model organism *C. elegans* possess two prominent gonad arms that undergo development from specific cells during early stages of the organism's life cycle. The gonad primordium is formed by four cells, namely Z1, Z2, Z3, and Z4, at the L1 stage. Among these cells, Z1 and Z4 are referred to as somatic gonad precursors. Progressing to the L2 stage, Z1 and Z4 proliferate and give rise to twelve cells, which include the terminally differentiated anchor cell (AC), two distal tip cells (DTCs), and nine somatic gonad blast cells (SGBs), including three ventrals uterine (VU) precursor cells and two Sheath-Spermathecal precursors. During continuous development in the L3 stage, the SGBs undergo division, and following two rounds of VU cell division, the AC induces specific VU descendants to adopt the π cell fate. Subsequently, in the L4 stage, certain π cell daughters merge with the AC, forming the multinucleate uterine seam cell, while ten pairs of sheath cells are also established [60].

The two distal tip cells (DTCs) play a crucial role in the proliferation of the germ line. Ultimately, the somatic gonad blast cells (SGBs) undergo division and contribute to the structural cells of the gonad, the anchor cell (AC) orchestrates the development of the uterus and vulva, and the DTCs facilitate GSC proliferation and the outward extension of the gonad arms [61]. Another set of cells, Z2 and Z3, known as primordial germ cells, have a significant role in germline survival. Z2 and Z3 cells generate GSCs that become

segregated into the gonad arms during somatic primordium formation [60]. The proliferation of Z2 and Z3 cells is influenced by nutritional and cell-cell signals. In the adult stage, the *C. elegans* germ line proliferates from Z2 and Z3 cells, resulting in the generation of over a thousand cells. The germline proliferation is controlled by the DTCs, which provide a stem cell niche at the distal end of the adult gonad. Signalling between the distal tip cells and the germline is mediated through the *Notch* signalling pathway [62]. This network of cellular interactions and signaling pathways plays a crucial role in the development and maintenance of the germ line in *C. elegans*.

1.6.2 *Notch* signaling

The discovery of the *NOTCH* gene can be traced back to the early 1910s when it was first described in studies involving *Drosophila melanogaster* mutants with notched wings [63-65]. Further investigations in *D. melanogaster* revealed that the NOTCH protein spans the cell membrane and consists of multiple epidermal growth factor (EGF)-like repeats [66]. In the late 1980s and early 1990s, homologs of *NOTCH*, namely *lin-12* and *glp-1*, were identified in the nematode *C. elegans*, suggesting their involvement in *C. elegans* development [67-69]. *Lin-12* and *glp-1* encode Notch receptor proteins, and their identification was achieved through genetic screens aimed at identifying developmental mutants. Genetic analysis has since revealed both unique and overlapping roles for these two genes in specifying cell fates. Mutations in *lin-12* have been found to cause various cell fate transformations, including those related to early gonad genesis, vulval precursor cell fate specification, sex mesoblast specification, and π cell specification during hermaphrodite gonad genesis [69-73]. In the case of *glp-1*, loss of "zygotic" *glp-1* activity limits germline proliferation and leads to premature entry of germ cells into meiosis [68]. Subsequent studies led to the discovery of dominant alleles of *glp-1* that unveiled an intriguing phenomenon. These alleles manifested as a remarkable proliferation of the germline through continuous mitotic activity, but at the expense of diminished gamete production [74, 75]. Furthermore, when examining double mutants lacking both *lin-12* and *glp-1*, a striking absence of the rectum, anus, and excretory cell became apparent. These observations underscore

the critical role of cell fate decisions during embryogenesis and highlight the interplay between *lin-12* and *glp-1* in orchestrating developmental processes [76]. These findings highlight the crucial roles of the *lin-12* and *glp-1* genes in *C. elegans* development and provide valuable insights into the complex mechanisms governing cell fate determination.

The germline proliferation relies on the *Notch* signalling pathway, which guides developmental processes during both larval stages and adult maintenance [77-79]. At the heart of this pathway lie the essential players: the signalling ligand LAG-2, the receptor GLP-1, and the dedicated transcription factors LAG-1 and LAG-3/SEL-8. The depletion of any of these core components prompts germ cells to exit the mitotic cell cycle, transitioning into meiosis [68, 76, 80]. Conversely, hyperactivated LAG-2 ligand or GLP-1 receptor results in uncontrolled germline mitoses and the formation of germline tumours. DTCs express the signalling ligand LAG-2 [81]. The GLP-1 receptor is expressed in the germ line, where it receives the LAG-2 signal and promotes mitosis over meiosis [82, 83]. While *glp-1* mRNA is present throughout the germ line, the GLP-1 protein is restricted to the mitotic region [84]. This restriction is mediated, at least in part, by the translational repression of *glp-1* mRNA by the GLD-1 protein as germ cells enter meiosis. Notably, GLD-1 directly binds to the *glp-1* 3'UTR and represses its translation in the embryo and meiotic region of the germ line [85-87]. These complex regulatory mechanisms underline the significance of *Notch* signalling in controlling germline proliferation and differentiation, and provide valuable insights into the spatial and temporal coordination of cell fate decisions in the *C. elegans* germ line.

The balance between continued mitotic division and entry into the meiotic cell cycle is regulated by a complex network of RNA regulatory proteins. Among these regulators, the FBF RNA-binding protein plays a crucial role by repressing the expression of specific mRNAs associated with downstream control pathways. Notably, the involvement of *Notch* signalling in this network has been established through the transcriptional regulation of *fbf-1* (fem-3 mRNA binding factor-1) and *fbf-2* (fem-3

mRNA binding factor-2). However, it is important to note that this simplified perspective does not capture the full complexity of the regulatory mechanisms involved. *Notch* signalling likely controls additional regulators beyond FBF, and the RNA regulatory network itself is unable to fully govern the decision between mitosis and meiosis [62]. Four key regulators, namely GLD-1, GLD-2, GLD-3, and NOS-3, have been identified as crucial players in controlling the entry into meiosis [88-91]. These findings underscore the complex nature of the regulatory pathways governing the mitosis/meiosis decision and shed light on the multifaceted mechanisms involved in *C. elegans* germ line development.

1.6.3 FBF promotes mitosis

In the nematode *C. elegans*, the regulation of germline development and stem cell maintenance involves the interplay of two key genes: *fbf-1* and *fbf-2*, which give rise to the FBF-1 and FBF-2 proteins. These proteins play essential roles in facilitating continued mitotic divisions during the late larval and adult stages, including the maintenance of adult germline stem cells [92]. Interestingly, single mutants of *fbf-1* and *fbf-2* exhibit normal germline organization, resembling the wild type, and retain self-fertility [93]. However, in *fbf-1 fbf-2* double mutants, a distinct phenotype emerges. Germ cells proceed through normal mitotic divisions until the L4 stage, after which they exit the mitotic cell cycle, initiate meiosis, and undergo spermatogenesis [92]. Consequently, FBF emerges as a crucial regulator of adult germline stem cells.

The control of germline fate by FBF is accomplished through the posttranscriptional repression of numerous target mRNAs [94]. These target mRNAs contain FBF-binding elements (FBEs) within their 3' untranslated regions (3'UTRs) and exhibit elevated protein production in germ lines lacking or having reduced FBF activity Among the known FBF target mRNAs, *gld-1* and *gld-3* encode regulators that promote meiosis. Additionally, the FBF protein activity is antagonized by GLD-3, a homolog of Bicaudal-C that interacts with FBFs. Notably, the *fbf-1* and *fbf-2* mRNAs themselves

are also subject to FBF-mediated repression, representing a self-regulatory mechanism to maintain appropriate FBF levels. Through *fbf* mRNA auto-regulation and the antagonistic role of GLD-1, FBF-1 and FBF-2 are regulated. In contrast, *fbf-1* lacks the expected consensus LAG-1-binding sites and remains unresponsive to signaling changes, aligning with its distinctive expression pattern. Notably, *fbf-2* mRNA and FBF-2 protein are specifically localized in the distal-most germ line, where FBF-2 expression becomes responsive to *Notch* signalling. This response is likely facilitated by the presence of four LAG-1 binding sites in the 5' flanking region of the *fbf-2* gene. However, while this direct link sheds light on the role of *Notch* in *fbf-2* expression, it alone falls short of explaining the comprehensive control exerted by *Notch* signaling on germline proliferation, suggesting the involvement of additional *Notch* target genes [62]. These intricate regulatory mechanisms highlight the complex interplay between FBF, *Notch* signaling, and downstream effectors in governing germline proliferation and cell fate decisions in *C. elegans*.

1.6.4 GLD-1, GLD-2, GLD-3 and NOS-3 control entry into meiosis

The transition from mitosis to meiosis, a crucial process in germ line development, is tightly regulated by four key regulators: GLD-1, GLD-2, GLD-3, and NOS-3. These regulators play pivotal roles in orchestrating meiotic entry. It has been observed that GLD-1, GLD-2, and NOS-3 act downstream of FBF genetically, with *gld-1* mRNA being a direct target of FBF repression [88, 90, 92]. Meiotic entry is controlled through a two-pronged regulatory pathway, with GLD-1 and NOS-3 forming one branch and GLD-2 and GLD-3 constituting the other. Notably, GLD-1 and GLD-2 emerge as the primary regulators among the GLD/NOS proteins. GLD-1, a sequence-specific RNA-binding protein of the STAR/quaking family, functions as a translational repressor [95]. In contrast, GLD-2, a cytoplasmic poly(A) polymerase and translational activator [96, 97] is believed to drive germ cells from mitosis to meiosis by simultaneously repressing mitosis-promoting mRNAs and activating meiosis-promoting mRNAs. Supporting this hypothesis, GLD-1 directly represses *glp-1* mRNA [85] and regulates the expression of both FBF-1 and FBF-2. Thus, GLD-1 appears to promote meiosis, at least partially,

through negative feedback on mitosis-promoting regulators. On the other hand, the only known target of activation by the GLD-2 poly(A) polymerase is *gld-1* mRNA [97], which provides a positive feed-forward mechanism to robustly drive germ cells into meiosis. However, it is important to note that GLD-2 likely controls other target mRNAs as well, as evidenced by its ability to induce meiotic entry in *gld-1* null mutants.

GLD-3 and NOS-3 appear to regulate meiotic entry by modulating the activities of GLD-2 and GLD-1, respectively. GLD-3, a member of the Bicaudal-C family of RNA-binding proteins, enhances the poly(A) polymerase activity of GLD-2 [88, 96]. In contrast, NOS-3, belonging to the Nanos family of RNA-binding proteins, affects the accumulation of GLD-1 through an unknown mechanism [89]. The interplay between these regulators adds another layer of complexity to the control of meiotic entry. By shedding light on the roles of GLD-1, GLD-2, GLD-3, and NOS-3 in governing meiotic entry, we gain valuable insights into the molecular mechanisms underlying germ line development in *C. elegans*.

1.6.5 Other RNA regulators

The control of germline proliferation involved a complex interplay of various RNA regulators. While our understanding of this process is expanding, it is essential to highlight the significant contributions of other RNA regulators, such as *fog-1* and *fog-3*. FOG-1 and FOG-3 are distinct RNA regulators that exhibit remarkable similarities in their biological roles. They exert significant influence not only on the mitosis/meiosis decision but also on the determination of sperm and oocyte fates. These regulators operate in a dose-dependent manner, where the levels of FOG-1 dictate germ cell fates. High levels of FOG-1 promote sperm specification, while low levels of FOG-1 maintain germ cells in the mitotic state, particularly in the absence of FBF. On the other hand, the absence of FOG-1 results in the initiation of oogenesis [98]. Similarly, FOG-3 also affects both the mitosis/meiosis decision and the determination of sperm and oocyte fates, although the specific dose dependency of FOG-3 remains to be thoroughly

investigated. Notably, the loss of function of both *fog-1* and *fog-3* leads to a transformation from spermatogenesis to oogenesis, indicating their pivotal roles in governing germ cell fate. Furthermore, FOG-1 and FOG-3 function at the end of the sex determination pathway in the germ line, along with *fem-1*, *fem-2,* and *fem-3,* suggesting that these five genes may collectively act as terminal regulators of germ cell fate, specifically specifying spermatogenesis [99-101].

In our study, we capitalized on the absence of *fog-1*, which leads to oogenesis, as a foundation for investigating the complex processes of oocyte arrest and accumulation in the absence of sperm. By delving into the underlying mechanisms of *fog-1*-deficient oogenesis, we aim to gain valuable insights into the complex regulatory networks governing these critical aspects of germ line development.

1.7 Spermatogenesis and Oogenesis

Hermaphrodites first produce haploid amoeboid sperm during the L4 stage. As they near adulthood, they switch to produce larger oocytes [102]. Spermatogenesis and oogenesis are vital processes in the reproductive biology of organisms, including the model organism *C. elegans* [8]. In *C. elegans* hermaphrodites, spermatogenesis occurs during the L4 stage, where germ cells undergo differentiation to produce functional sperm [103]. On the other hand, oogenesis, the development of oocytes, takes place after the L4 stage. The timing and regulation of these distinct processes in *C. elegans* present intriguing questions that have yet to be fully answered. Understanding the mechanisms underlying spermatogenesis and oogenesis in *C. elegans* is essential for unravelling the complicated dynamics of germ cell development. During spermatogenesis, a series of events occur to generate mature sperm. The germline stem cells undergo mitotic divisions, followed by meiosis, leading to the production of haploid spermatocytes. These spermatocytes further differentiate and undergo a dramatic morphological transformation to develop into spermatozoa. Various factors and regulatory pathways orchestrate the precise timing and coordination of these developmental events, ensuring the production of functional sperm [104]. Oogenesis,

in contrast, involves the formation of oocytes from germ cells. The oocyte development in *C. elegans* is a complex and highly regulated process. It includes cellular events such as meiotic divisions, cytoplasmic rearrangements, and the assembly of specialized structures within the oocyte. The oocytes then undergo maturation, acquiring the ability to be fertilized and develop into viable embryos. By studying the processes of spermatogenesis and oogenesis in *C. elegans*, researchers aim to unravel the underlying molecular mechanisms and regulatory networks involved [62, 105].

In addition, *C. elegans* typically lays around 300 eggs, which is known as the brood size. Researchers can use brood size as an indicator to assess the status of spermatogenesis and oogenesis in *C. elegans* [9]. A decrease in brood size suggests that there may be a disruption in the reproductive process, while an increase in brood size indicates that the process is being stimulated. Understanding the optimal growth conditions and reproductive behavior of *C. elegans* is crucial for designing effective experiments and interpreting research results accurately.

1.7.1 Spermatogenesis and major sperm protein

Spermatogenesis, the process by which sperm is produced from undifferentiated germ cells, is a fundamental aspect of reproductive biology in many organisms. In dioecious animals, this process is exclusive to males. However, in the nematode *C. elegans*, spermatogenesis occurs during a specific stage of germline development in hermaphrodites, preceding the onset of oogenesis [106]. The formation of spermatozoa in *C. elegans* involves a series of detailed steps and regulatory mechanisms.

The journey begins with the formation of primary spermatocytes, which initially exist as syncytia with a cytoplasmic core known as the rachis. These primary spermatocytes originate from germline stem cells [107]. During their differentiation, the first meiotic division yields two secondary spermatocytes, and the second meiotic division results in the production of four haploid spermatids. These round, non-motile spermatids bud

from a residual body that contains components unnecessary for further development or sperm function. The subsequent process of activation, also known as spermiogenesis, is triggered by an extracellular signal, leading to pseudopod extension and the acquisition of motility, which are characteristic features of mature spermatozoa [108].

During spermatogenesis, a critical component called major sperm protein (MSP) plays a significant role. MSP assembles as para crystalline arrays in fibrous bodies associated with membranous organelles, starting from primary spermatocytes and continuing through the secondary spermatocyte stage. These fibrous body-membranous organelle complexes segregate into spermatids, and upon separation from the residual body, MSP dissociates into the cytosol. Upon activation, MSP undergoes reassembly into filamentous fibres within the pseudopod, reflecting the various stages of spermatogenesis [108].

One compelling question that has fascinated researchers is the nature of the signal from sperm that triggers oocyte meiotic maturation. There is a ground breaking study by McCarter et al., it was revealed that a signal associated with sperm promotes oocyte meiotic maturation independently of fertilization [105]. Their experiments using genetically altered XX animals that do not produce sperm, the rates of oocyte maturation and ovulation were significantly low. However, when these females were mated with wild-type males or sperm-defective mutants, the normal rate of oocyte maturation was restored, suggesting the crucial role of sperm in this process. Recent studies by Miller et al. shed light on this topic by revealing the dual role of MSP in *C. elegans* reproduction. MSP, which is crucial for the actin-independent motility of nematode spermatozoa, also acts as a hormone that induces oocyte meiotic maturation and contraction of the gonadal sheath cells [109]. This ground-breaking discovery highlights the multifaceted nature of MSP and its involvement in crucial reproductive processes in *C. elegans*.

1.7.2 Oogenesis

In the context of *C. elegans*, GSC proliferation serves the purpose of self-renewal and maintaining a specific GSC population size. On the other hand, GSC differentiation is responsible for generating gametes (Figure. 1.4).

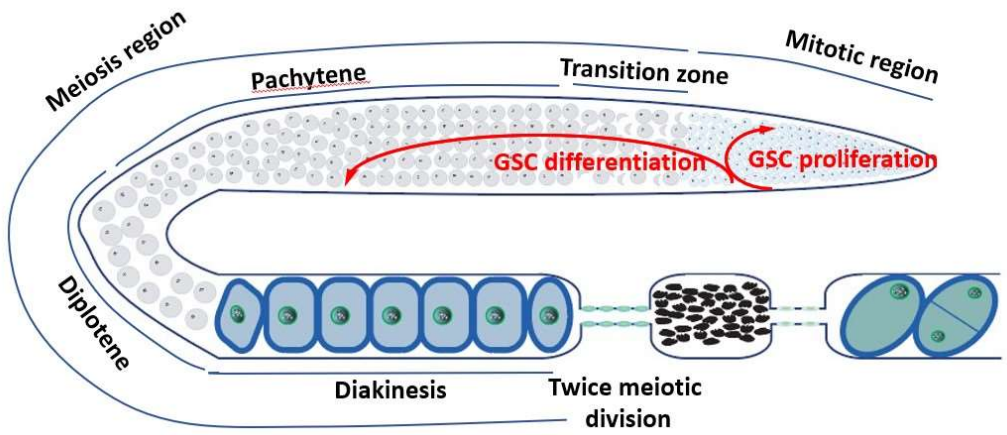

Figure. 1. 4 Germline proliferation and differentiation

At the distal region of the gonad arms, GSCs undergo proliferation, creating a pool of these cells. As the GSCs progress through different stages, including the transition zone, pachytene, diplotene, diakinesis, and the first and second meiotic divisions, they undergo crucial events necessary for gamete formation [110].

Sexual reproduction in organisms involves the production of haploid gametes, such as sperm and eggs, each containing a single copy of each chromosome. In the nematode *C. elegans*, the process of gamete production occurs in the two large gonad arms present in the organism. During meiotic prophase in organisms, a series of events occur to ensure the proper alignment, pairing, and separation of chromosomes. In the early stages of meiotic prophase, specifically the zone encompassing leptotene and zygotene, homolog pairing is established, and DNA DSBs are formed [111, 112]. This sets the stage for subsequent processes that are essential for successful meiosis.

As meiotic prophase progresses into early pachytene, the synaptonemal complex (SC) assembles, serving as a physical scaffold that holds aligned homologous chromosomes

together. This complex plays a crucial role in ensuring the accurate alignment and cohesion of homologs during meiosis. By late pachytene, homologous recombination takes place, leading to the formation of inter-homolog crossovers (COs). These CO events facilitate genetic exchange between homologous chromosomes and contribute to the generation of genetic diversity. Following the disassembly of the synaptonemal complex during late prophase, physical attachments called chiasmata persist between homologous chromosomes [111]. These chiasmata are formed by a combination of crossovers and sister chromatid cohesion. They play a vital role in holding homologous chromosomes together until the first meiotic division, where parental homologs are separated, reducing the ploidy to the haploid state. In the second meiotic division, sister chromatids are separated, ensuring that each resulting gamete receives a single copy of each chromosome [110, 113]. Recombination and crossovers during meiosis not only enable proper chromosome segregation but also introduce genetic exchange between homologous chromosomes.

1.8 Oocyte maturation, fertilization and ovulation

Sexual reproduction is a fundamental biological process that relies on meiosis to generate haploid gamete nuclei, which subsequently fuse during fertilization to form a diploid zygote. This process is essential for the perpetuation of species and the maintenance of genetic diversity. In the nematode *C. elegans*, an aspect of sexual reproduction is the tight temporal coupling of meiotic maturation, fertilization and ovulation. These coordinated events ensure the successful fusion of gametes and the continuation of the species.

1.8.1 Oocyte maturation

The interaction between MSP and oocytes involved the VAB-1 *Eph* receptor expressed on the oocyte surface, as well as MSP receptors expressed on the sheath cells. The VAB-1 *Eph* receptor (EphR) tyrosine kinase was identified as the sole known MSP receptor to date. Upon MSP binding, VAB-1 underwent trafficking from the cell surface

to recycling endosomes, potentially involving the downstream participation of the inositol triphosphate receptor ITR-1 [114]. Genetic studies have indicated that VAB-1 plays multiple roles in regulating oocyte maturation, including the activation of the ERK/MAPK MPK-1 [115].

Another fascinating aspect is the stimulation of a sheath $G_{\alpha s}$-adenylate cyclase cascade by MSP binding to MSP receptors, which antagonizes sheath/oocyte gap junctional signalling. At the sheath/oocyte interface, innexins, specifically INX-14 and INX-22, were found to localize to plaque-like structures, potentially forming gap junction channels [116-118]. However, the precise molecular mechanism by which INX-14 and INX-22 negatively regulate MPK-1 remains poorly understood. It is noteworthy that MPK-1 activity is primarily regulated through phosphorylation, and temperature-sensitive *mpk-1(ga111)* mutant studies have revealed delayed oocyte maturation, resembling diakinesis-arrested oocytes in unmated females [119]. These findings provide compelling evidence for the critical involvement of oocyte MPK-1 phosphorylation in MSP-induced oocyte maturation. Additionally, VAB-1, along with potentially other MSP receptors in oocytes, was found to regulate the activity of an NMDA-subtype glutamate receptor containing the NMR-1 subunit. Calcium (Ca^{2+}) ion influx through this glutamate receptor is believed to modulate the activity of UNC-43 CaMKII. While UNC-43 redundantly functions in promoting oocyte maturation, the underlying mechanism remains poorly understood [120].

1.8.2 Fertilization

Fertilization, the process by which two haploid gametes merge to form a diploid embryo, represents a reproductive system of organisms. Among these organisms, the microscopic roundworm *C. elegans* offers an attractive insight into this process. During oogenesis, the developing oocyte initiates the first meiotic division but subsequently halts at diakinesis, the final stage of prophase [121]. The resumption of meiosis and the contraction of the gonadal sheath are triggered by a secreted sperm

protein hormone known as MSP [109]. This process results in the ovulation of the maturing oocyte into the spermatheca, where sperm storage and fertilization take place [122, 123]. The initial interaction between the amoeboid *C. elegans* sperm and the oocyte occurs through the pseudopod of the sperm, ultimately leading to their fusion [124] .

A specialized structure within the hermaphrodite's reproductive tract is dedicated to the storage and fertilization of mature oocytes. The presence of the oocyte serves as the vital trigger for the rapid activation of the non-motile spermatids. This process, although not completely understood, is thought to involve changes in intracellular calcium levels and signalling pathways [120, 122, 125]. Consequently, these activated spermatids transition into motile spermatozoa, primed for their indispensable role in fertilization. However, for the spermatozoa that fertilized the oocyte, their journey ends there as spermatozoa. They become pro-nuclei that will serve in the development of the zygote. The fertilized egg departs from the spermatheca and enters the uterus. However, the journey of the other spermatozoa doesn't end there; they must undertake a remarkable challenge: swimming back to the spermatheca to successfully fertilize the subsequent maturing oocyte. [6, 104].

1.8.3 Ovulation process

Ovulation, a critical process essential for fertility, relies on the interplay of multiple cellular components, including sperm, oocytes, proximal sheath cells, and the spermatheca. The spermatheca, which serves as the site for fertilization, is composed of distinct cellular structures: an 8-cell distal neck, a 16-cell central bag, and a syncytial 4-cell spermatheca-uterine valve (sp-ut valve).

1.8.3.1 Oocyte transport to the spermatheca (Figure. 1.5)

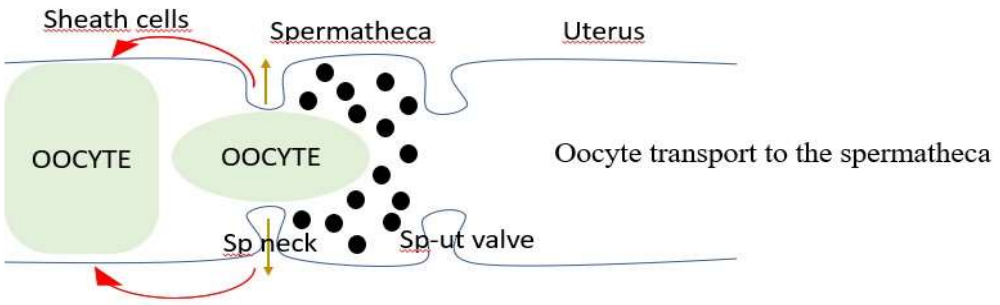

Figure. 1. 5 Oocyte transport to the spermatheca from sheath cells

Schematic of the initiation of ovulation, characterized by robust contractions of the sheath cells and the dilation of the distal spermatheca.

The initiation of ovulation involves powerful contractions of the sheath cells accompanied by the dilation of the distal spermatheca. This coordinated action allows the distal spermatheca to enclose the proximal oocyte, enabling its passage through a constriction and entry into the spermatheca, where fertilization promptly takes place.

Let us delve into the sheath cell contractions first (Figure. 1.4). The gonadal sheath cells establish gap junction connections with oocytes and respond to signals from sperm, particularly MSP [109, 126]. Binding of MSP to the VAB-1/EphR on the sheath cells triggers precise contractions and relaxation during ovulation [115]. Another significant contributor to ovulation is LIN-3/EGF, a substance believed to be secreted by maturing oocytes. The neighbouring gonad sheath cells likely perceive LIN-3 signals through LET-23/EGF receptor (EGFR). Genetic investigations into the gonad-specific LIN-3 pathway have uncovered the involvement of key genes associated with inositol-(1,4,5)-trisphosphate (IP_3) signalling, including *plc-3*, an enzyme critical for IP_3 production, and ITR-1/IP_3 receptor (IP_3R), a receptor implicated in IP_3-mediated calcium signalling [127]. *Plc-3* functions by cleaving phosphatidylinositol-(4,5)-bisphosphate (PIP_2) into IP_3 and diacyl glycerol (DAG). The resulting IP_3 molecules bind to ITR-1/IP_3R, an intracellular Ca^{2+}-gated channel located on the surface of the endoplasmic reticulum (ER), thereby releasing Ca^{2+} from the ER into the cytoplasm [128]. The increase in

cytosolic Ca^{2+} levels activates MLCK-1 (myosin light chain kinase), which phosphorylates and activates myosin, contributing to the process of sheath cell contractions [129]. This orchestrated interplay of signalling molecules, involving MSP, VAB-1/EphR, LIN-3/EGF, LET-23/EGFR, PLC-3, and ITR/IP_3R, governs the precise contractions of sheath cells during ovulation.

The process of oocyte from the sheath cells into the spermatheca requires more than just sheath cell contractions; it also necessitates simultaneous dilation of the distal spermatheca. However, there is a notable absence of concrete evidence to elucidate the mechanism behind spermatheca dilation. In 1998, Clandinin proposed that spermatheca dilation might be regulated through the LIN-3/LET-23/phospholipase C (PLC)/ITR-1 pathway, similar to the one governing sheath cell contractions. Nevertheless, this paper highlights several critical gaps in our understanding. These gaps include the absence of direct evidence regarding whether the maturing oocyte secretes LIN-3, whether LET-23 is indeed expressed on the spermatheca, which specific PLC protein is involved in this cascade, and the precise mechanism by which an increased concentration of intracellular calcium triggers spermatheca dilation. Consequently, the current understanding of spermatheca dilation remains incomplete, and further extensive research is required to shed light on this process [127].

1.8.3.2 Embryo exit from spermatheca (Figure. 1.6)

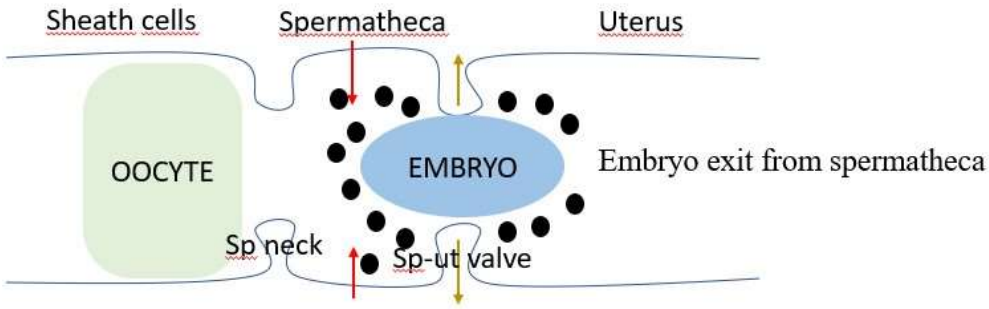

Figure. 1. 6 Embryo exit from spermatheca into the uterus

Schematic of the embryo into the uterus from the spermatheca, characterized by robust contractions of the spermatheca and the dilation of the sp-ut valve.

After the oocyte gets into the spermatheca, pushing the embryo into the uterus also requires the coordinated contraction of the spermatheca and dilation of the sp-ut valve. The signalling pathways responsible for regulated contraction in the spermatheca resemble those found in smooth muscle and non-muscle cells. [130-132]. Two essential pathways, one dependent on Ca^{2+} and the other on Rho GTPase, are both necessary for spermathecal contractility. It has been reported that LIN-3 can bind to LET-23/EGFR on the spermatheca, triggering Ca^{2+} release from the ER through the phospholipase PLC-1 [127]. The Rho-dependent pathway is activated by oocyte entry, displacing a mechanosensitive Rho GTPase activating protein (Rho GAP), a sperm-specific Protein with VWFA and Cache Domains 1 (SPV-1), from the membrane. This displacement leads to the activation of RHO-1 [133]. GTP-bound RHO-1 then activates LET-502/ROCK, which phosphorylates myosin and inhibits myosin phosphatase, resulting in increased levels of phosphorylated myosin [134].

Furthermore, cyclic adenosine monophosphate (cAMP), an important second messenger, plays a crucial role in various biological processes. The levels of cAMP are partially regulated by phosphodiesterase (PDE), enzymes that convert cAMP into AMP. Protein kinase A (PKA) consists of two catalytic subunits (KIN-1/PKA-C) and two regulatory subunits (KIN-2/PKA-R). When cAMP binds to the KIN-2/PKA-R subunits,

PKA is activated, leading to the release of the KIN-1/PKA-C subunits. In the absence of cAMP, PKA-R acts as an inhibitor of KIN-1/PKA-C. Once released, KIN-1/PKA-C can promote PLC-1 to initiate the ITR-1/Ca^{2+} cascade, leading to spermatheca contraction, while also inhibiting RHO-1 to inactivate the LET-502/MEL-11 cascade, which also contributes to spermatheca contraction [135].

The syncytial 4-cell sp-ut valve serves as a barrier preventing premature release of oocytes into the uterus upon entry into the spermatheca. This allows sufficient time for the oocyte to be fertilized and develop an eggshell. However, little is currently known about the signalling networks that regulate contractility in the sp-ut valve. Additionally, PLC-1 is not expressed in the sp-ut valve, suggesting the presence of a distinct mechanism for Ca^{2+} regulation compared to the spermathecal bag [136]. Future studies may uncover the details of how PKA regulates Ca^{2+} Signalling in the sp-ut valve. Understanding the coordination of signalling mechanisms among sperm, oocytes, sheath cells, and the distal spermatheca remains an ongoing challenge.

1.9 GSC proliferation regulatory mechanisms

As mentioned, niche signalling plays a critical role in germline proliferation, providing instructions for GSC fate determination. However, the factors controlling the rate of GSC proliferation remained elusive until the discovery that the nutritional status of an organism influences GSC proliferation. In *Drosophila*, it was observed that following nutrition, insulin-like peptides are secreted from the nervous system, stimulating GSC proliferation [137]. Notably, nutrition and systemically released insulin-like peptides also support the proliferation of other stem cell populations, such as intestinal stem cells, neuroblasts, and hematopoietic progenitors in *Drosophila* [138]. Similarly, in *C. elegans*, the insulin-like/IGF-1 signalling (IIS) pathway is activated in response to nutrition and plays a systemic role in promoting the proliferation of their only stem cell type, GSCs [59, 139-142]. While an animal's nutritional status partially explains the proliferative behaviour of its stem cell populations, variations in proliferation rates exist

both among different tissue-specific stem cells and within separate populations of the same stem cell type [143]. For instance, in the *C. elegans* adult hermaphrodite, GSC proliferation rates are influenced not only by nutrition and IIS but also by the demand for their terminally differentiated progenies, the oocytes [142].

This phenomenon is apparent in *fog-1* mutants lacking sperm, in which mature oocytes are no longer fertilized and accumulate in the proximal gonad. This accumulation triggers a feedback signal that suppresses GSC proliferation at the distal end, effectively halting the production of new oocytes [59, 144, 145]. Thus, the insulin-like/IGF-1 signalling pathway, known as IIS, promotes GSC proliferation, while oocyte accumulation suppresses GSC proliferation at the distal end. The interplay between niche signalling, nutritional status, IIS, and the demand for specific cell types highlights the intricate mechanisms governing germline proliferation and fate determination.

1.9.1 IIS pathway

The IIS pathway in *C. elegans* serves as a crucial link between nutrient levels and various biological processes, including metabolism, growth, development, longevity, and behaviour. Remarkably, the insulin signalling pathway exhibits a high degree of conservation between humans and *C. elegans*, with the major components in human insulin signalling having corresponding homologs in *C. elegans* that functionally resemble their human counterparts [146]. At the core of the *C. elegans* IIS pathway are insulin-like peptides (ILPs), some of which can bind to and activate the human insulin receptor (Figure. 1.7) [147-149]. Activation of the DAF-2/IGFR in *C. elegans* leads to the recruitment and activation of the phosphoinositide 3-kinase AGE-1/PI_3K. AGE-1/PI_3K phosphorylates the membrane lipid PIP_2 to generate phosphatidylinositol-3,4,5-triphosphate (PIP_3), a crucial secondary messenger. PIP_3, in turn, recruit's serine/threonine kinases PDK1, which activates AKT-1 and AKT-2 kinases. This cascade culminates in the phosphorylation of the *DAF-16/FoxO* transcription factor. Phosphorylation of *DAF-16/FoxO* governs its interactions with the 14-3-3 proteins PAR-5 and FTT-2, thereby influencing the nuclear/cytoplasmic distribution of *DAF-*

16/FoxO [146, 150]. When *DAF-16* enters the nucleus, it initiates the activation of its target genes.

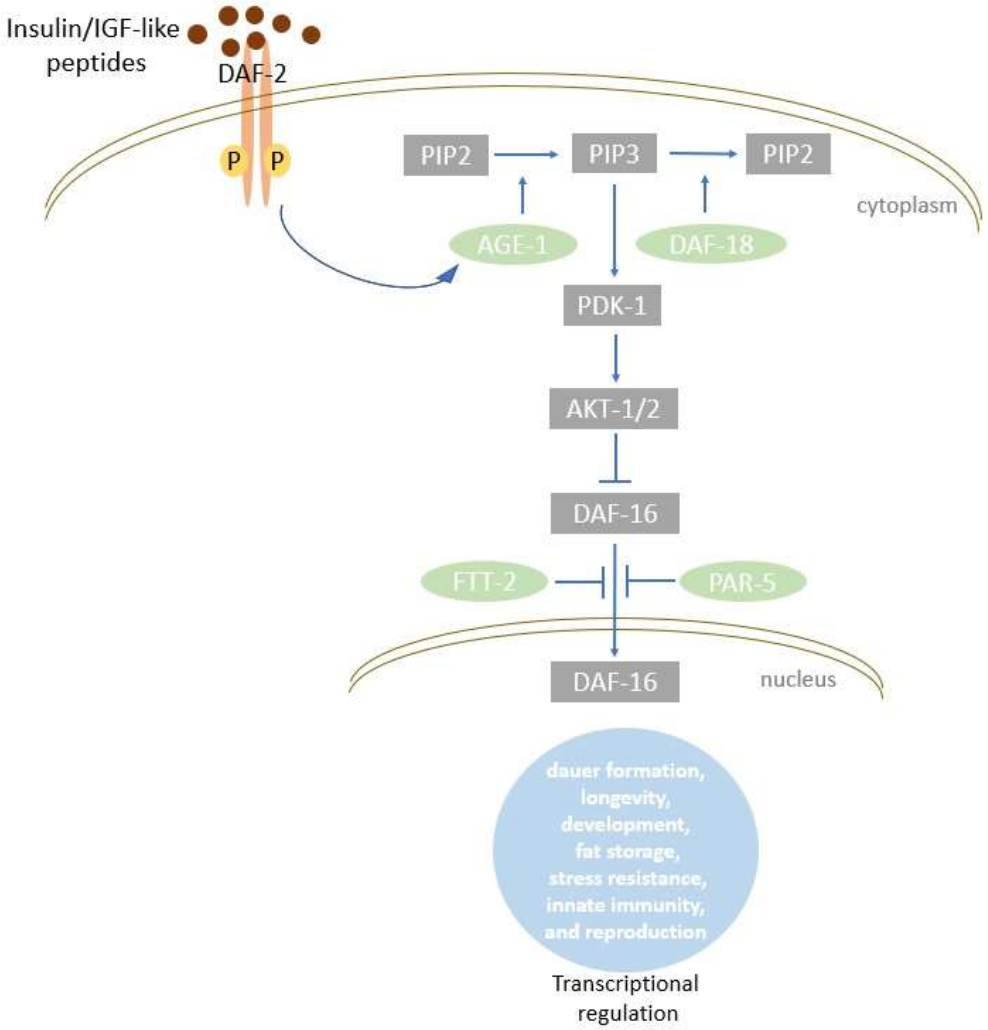

Figure. 1. 7 IIS pathway

DAF-16 functions as a central regulator for signalling the IIS pathway. DAF-16 integrates signals perceived by the DAF-2 receptor and binds to thousands of targets genes, thereby transducing these upstream signals to regulate distinct biological processes, such as dauer formation, longevity, development, fat storage, stress resistance, innate immunity, and reproduction [151, 152]. Interestingly, in relation to GSC proliferation, recent studies have revealed the involvement of a novel cell non-autonomous DAF-16/FOXO activity, which is required for maintaining adult germline progenitors [153].

The *daf-18* gene also plays a significant role in the IIS pathway. DAF-18 acts as an antagonist of insulin signalling through two mechanisms. First, it dephosphorylates PIP_3 to convert it back to PIP_2. Second, it directly dephosphorylates the insulin receptor substrate-1 (IRS-1). Conversely, when the IR is activated by insulin, it can operate through two distinct modes of activation. One mode involves activating PI_3K to produce more PIP_3, while the other mode entails phosphorylating PTEN for degradation.

1.9.2 Tissue need pathway

In our study, we utilized the *fog-1* mutation as a background to investigate the regulatory mechanisms underlying GSC proliferation. The *fog-1* mutation results in the absence of sperm, leading to the accumulation of mature oocytes in the proximal gonad. This oocyte accumulation phenomenon triggers a feedback signal that exerts inhibitory effects on GSC proliferation at the distal end of the gonad, effectively halting the production of new oocytes [59, 144, 145]. We refer to this feedback mechanism as homeostatic signalling.

Interestingly, despite the presence of high systemic IIS activation, the accumulation of mature oocytes in the *C. elegans* germline has been shown to inhibit adult GSC proliferation through the involvement of DAF-18/PTEN [59]. This feedback mechanism operates through a cryptic signalling pathway that requires the participation of PAR-4/LKB1, AAK-1/AMPK, and PAR-5/14-3-3. These factors collaborate to inhibit the activity of MPK-1/MAPK, antagonize IIS signalling, and suppress both GSC proliferation and the production of additional oocytes [154]. The inhibitory effect of oocyte accumulation on GSC proliferation, mediated by the *daf-18/par-4/aak-1/par-5* pathway, acts in parallel with the IIS signalling pathway, which promotes GSC proliferation. By elucidating the interplay between oocyte accumulation and GSC proliferation regulation, our study sheds light on the balance maintained within the germline and provides insights into the coordination of feedback mechanisms that ensure proper reproductive processes in *C. elegans.*

1.9.3 Homeostatic signalling prevents benign tumours

Tumours differ from tissue hyperplasia, which is reversible and arises due to developmental or environmental triggers, and in this condition, the additional cells are usually well-organized within the tissue. Conversely, tumours exhibit disorganization and continue to grow. Initially, tumours can be benign, composed of disorganized cells without the capacity to invade neighbouring tissues or metastasize. Therefore, benign tumours are non-cancerous and typically not an immediate life-threatening concern depending on their location. However, benign tumours possess the potential to transform into malignant ones [155-158]. Thus, their development can be regarded as a crucial early stage in carcinogenesis. [142].

In wild-type *C. elegans*, the sperm constitutively secrete MSPs that activate cAMP signalling in the proximal somatic gonad. This cAMP signalling pathway leads to the activation of OMA-1 and OMA-2 in the proximal-most oocyte, triggering oocyte maturation. However, in the absence of OMA-1 and OMA-2, despite normal sperm production and MSP signalling activation in the somatic gonad, oocytes fail to mature and accumulate. Consequently, the accumulation of oocytes triggers the activation of the *daf-18/par-4/aak-1/par-5* pathway, inhibiting GSC proliferation and maintaining tissue homeostasis [154].

However, when homeostatic signalling is disrupted, as seen in mutants that lack functional AAK-1, the production of oocytes continues unabated, leading to the development of differentiated benign tumours (Figure. 1.8) [142]. These tumours arise due to the uncontrolled proliferation of GSCs in response to the absence of the inhibitory feedback from accumulated oocytes. The inability to halt GSC proliferation in the presence of excessive terminal cells (oocytes) highlights the critical role of homeostatic signalling in preventing the formation of benign tumours.

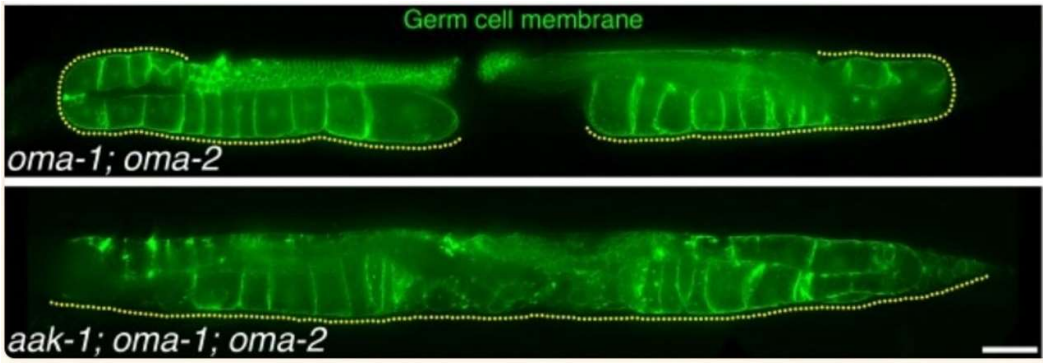

Figure. 1. 8 Benign tumours are generated in *aak-1; oma-1; oma-2* mutant

mex-5p::mNeonGreen::PLCδ-PH (green) labelling the germ cell membrane. The region containing oocytes is indicated by a yellow dashed line.

1.10 *DAF-18/PTEN* in homeostatic signalling

In our current understanding, the *fog-1* mutation in *C. elegans,* which leads to the absence of sperm and to the accumulation of mature oocytes in the proximal gonad has revealed the existence of a remarkable homeostatic signal that effectively inhibits GSC proliferation at the distal end of the gonad. Among the key players involved in this regulatory mechanism is the gene *daf-18*. Interestingly, the *fog-1, daf-18* double mutant does not show any oocyte accumulation in the proximal gonad. To fully comprehend the implications of mutating *daf-18* in the *fog-1* background, it is essential to explore the nature of *daf-18* and consider the findings from previous studies that shed light on its function.

1.10.1 Introducing *daf-18/PTEN*

In 1997, the discovery of *PTEN*, also known as *MMAC1* or *TEP1,* marked a significant milestone in cancer research, as it became recognized as the second most frequently mutated tumour suppressor gene in human cancer, following only *P53* [159-161]. It was soon found that germline mutations in *PTEN* were responsible for Cowden's disease, an autosomal dominant condition characterized by the development of benign

and malignant neoplasms in multiple organs, most commonly the breast, thyroid, and skin [162, 163]. The clinical recognition of CS dates back to 1963, and its association with *PTEN* mutations was established in 1997 [164]. Approximately 80% of CS patients exhibit identifiable mutations in the *PTEN* gene, situated on chromosome 10 q23.3 [165]. The *PTEN* gene plays a crucial role in regulating apoptosis and the cell cycle by influencing the phosphatidylinositol 3-kinase (PI3K)/AKT/mammalian target of rapamycin (mTOR) pathways. The PI3K/AKT/mTOR pathway is a vital intracellular signalling pathway that governs the cell cycle [164]. The pathway initiates with the phosphorylation of PI3K enzymes, resulting in the formation of phosphatidylinositol diphosphate (PIP2) and triphosphate (PIP3). PIP3 activates AKT, subsequently activating mTOR, which plays a central role in protein synthesis, cell growth, proliferation, and inhibition of apoptosis. The *PTEN* gene modulates the cell cycle by suppressing the PI3K/AKT/mTOR pathway, leading to reduced proliferation and cell survival, ultimately preventing tumour formation. Consequently, PTEN mutations are associated with various cancers and tumour development [166].

In *C. elegans*, the ortholog of *PTEN* is known as *daf-18* [149]. The genomic position of *daf-18* is IV:420011.425177. Expression of *daf-18* is observed throughout the entire *C. elegans* organism [167]. Notably, human PTEN can functionally replace DAF-18 and rescue the phenotype defects observed in *daf-18* loss-of-function mutants, indicating a remarkable conservation of function between the two [168]. This suggests that the regulators of DAF-18/PTEN in *C. elegans* are likely highly conserved as well, making *C. elegans* an excellent model organism for exploring PTEN function.

The structure of DAF-18 reveals key domains, including a phosphatase domain, a C2 domain, and a PDZ binding domain. DAF-18 exhibits dual phosphatase activity, targeting both lipids and proteins. Its lipid phosphatase activity is well characterized and acts as an antagonist to the PI_3K signalling pathway by converting PIP_3 to PIP_2 [169]. Furthermore, DAF-18 can dephosphorylate protein substrates such as the insulin receptor substrate-1 (IRS1), FAK, and Src kinase, thereby exerting regulatory control

over various signalling pathways [170-173]. Mutations in *daf-18* that alter its function have been identified in *C. elegans*, including the phosphatase inactive mutant C169S, the lipid phosphatase inactive mutant G174E, and the protein phosphatase inactive mutant D137A [168, 174, 175]. Interestingly, two recent studies aimed to assess whether the D137A and G174E alleles exhibit overlapping effects on DAF-18 function or if they are specifically associated with each enzymatic activity. This assessment was conducted by analysing D137A/G174E trans-heterozygotes. If these alleles are truly specific, they should complement each other, resulting in trans-heterozygotes displaying a wild-type-like phenotype. However, the D137A/G174E trans-heterozygotes appear unable to maintain quiescence of the somatic gonad or germ line of dauer larvae and are also unable to promote starvation resistance during L1 arrest. These findings offer a cautionary tale for their use in associating a specific mutant phenotype caused by loss of *daf-18* activity to a specific enzymatic activity of DAF-18/PTEN[176, 177].

1.10.2 *daf-18* previous studies

As previously mentioned, *daf-18* emerges as a key player in the IIS pathway, counteracting the activity of PI_3 kinase/AGE-1. Numerous studies have explored the regulatory functions of DAF-18 within this pathway, particularly regarding dauer formation. While *daf-16* serves as a central regulator controlling dauer development in the IIS pathway, evidence suggests that *daf-18* also plays a role in dauer control. Moreover, PIP_3, a critical lipid second messenger, has been implicated in dauer development [168]. Research has demonstrated that dauer formation requires *daf-18* expression in multiple tissues [167].

Interestingly, investigations into a null *daf-16(mu86)* mutation have revealed divergent pathways governing the initiation of postembryonic germline proliferation upstream of *daf-16*. While the mitotic quiescence of Z2 and Z3 during L1 diapause remains unaffected by the loss of *daf-16* [178], germ cell growth and division occur in *daf-18* loss-of-function (LF) L1 larvae [179]. This suggests that *daf-18* mediates L1 mitotic

arrest in the germline through distinct downstream effector genes, separate from *daf-16*. Additionally, reports indicate that *daf-18/PTEN* acts non-autonomously within the somatic gonad to maintain the developmental quiescence of SGBs and GSCs. Remarkably, *daf-18* activity in the distal tip cells (DTCs) alone is sufficient to sustain non-autonomous quiescence in both SGBs and GSCs [60].

1.11 Problem statement

In our lab, we are exploring the role of *daf-18* in controlling GSC proliferation. Indeed, a captivating mechanism was uncovered wherein the accumulation of oocytes, the terminally-differentiated GSC progeny, in sperm-less hermaphrodites is associated with the downregulation of GSC proliferation. It was further shown that *daf-18* was indispensable for the accumulation of oocytes within the *C. elegans* germ line and the associated homeostatic influence signalling on GSC proliferation [59]. Interestingly, *DAF-18* does not impede GSC proliferation by directly inhibiting IIS through its antagonism of AGE-1/PI_3K activity. This revelation stems from the observation that DAF-16 the transcription factor eventually suppressed by AGE-1, remains inactive in sperm-less animals and is dispensable for the feedback regulation of GSCs [154]. Instead, it was found that DAF-18 must inhibit MPK-1, through a partially unknown pathway implicating multiple tissues (Figure. 1.9), to suppress GSC proliferation.

Here we asked the specific question of how DAF-18 acts to block oocyte activation and ovulation in the absence of sperm, which precludes the downregulation of GSC proliferation. This question is of high importance also because oocytes are very precious cells, typically requiring the sacrifice of many other cell's cytoplasm to expand in size, and uniquely possessing the capacity to propagate the species, yet *fog-1; daf-18(ø)* mutants sadly waste them all, ovulating them one after another. As such, unlike *fog-1* single mutants, *fog-1; daf-18(ø)* doubles do not accumulate oocytes and their GSCs keep proliferating as in wild-type to sustain a useless full blown oogenic program. In a genetic background preventing oocyte activation and laying, lack of homeostatic

signalling causes oocytes to hyperaccumulate to form a benign tumour [154]. This defect is reminiscent of Cowden's syndrome in humans and suggests that hamartomas may potentially arise in patients hemizygous for PTEN because of defective homeostatic signalling [142].

Given these observations, our research aims to untangle the complex relationship between *daf-18,* oocyte accumulation, and GSC proliferation (Figure. 1.9). Through careful investigation and analysis, we hope to shed light on the underlying mechanisms that govern these processes, advancing our understanding of how cells coordinate their growth and development in this fascinating biological system.

As we delve into our main thesis, the following aims guide our research, outlining the specific areas we aim to explore.

Aim 1: Investigate the mechanism by which DAF-18 prevents oocyte activation and ovulation in the absence of sperm, consequently influencing the downregulation of GSC proliferation.

Aim 2: Clarify the complex relationship among *daf-18*, oocyte accumulation, and GSC proliferation.

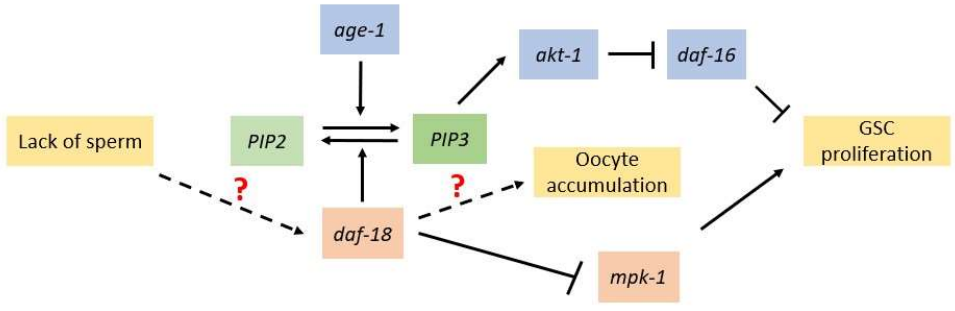

Figure. 1. 9 The complex relationship between *daf-18*, oocyte accumulation, and GSC proliferation

CHAPTER Ⅱ

MATERIALS AND METHODS

2.1 *C. elegans* genetics

Animals were maintained at 15℃ on standard NGM plates and fed *E. coli* bacteria of the strain OP50, unless otherwise indicated [8]. The Bristol isolate (N2) was used as wild-type throughout. All alleles, deficiencies and transgenes used are shown in Table .2.1.

Table. 2. 1 Strains, alleles, transgenes and rearrangements used in this work

Ø means null

Name in text	Genotype of animal assayed or of parent with marker for identification of animal assayed among progeny	Strain name and note
wild-type	wild-type	N2
fog-1	*fog-1(q253)I*	JK560
fog-1; daf-18(ø)	*fog-1(q253)I; daf-18(ok480)IV*	UTR26
fog-1; daf-18(ø); germline::daf-18(+)	*fog-1(q253)I; narSi5[Pmex-5::GFPo::DAF-18(+) + unc-119(+)]II; daf-18(ok480)IV*	UTR248
fog-1; daf-18(ø); seam cell::daf-18(+)	*fog-1(q253)I; daf-18(ok480)IV; narEx76[Pnhr-72::DAF-18(+); Pmyo-3::mCherry]*	UTR199
fog-1; daf-18(ø); intestine::daf-18(+)	*fog-1(q253)I; daf-18(ok480)IV; narEx64[Pelt-7::DAF-18(+); Pmyo-3::mCherry]*	UTR185
fog-1; daf-18(ø); neurones::daf-18(+)	*fog-1(q253)I; daf-18(ok480)IV; narEx85[Punc-119::DAF-18(+); Pmyo-3::mCherry]*	UTR223
fog-1; daf-18(ø); muscle::daf-18(+)	*fog-1(q253)I; daf-18(ok480)IV; narEx100[Peunc-54::DAF-18(+), Peunc-54::GPF]*	UTR294

	fog-1(q253)I; daf-18(ok480)IV; narEx93[Pmyo-3::RFP::DAF-18]	UTR285
fog-1; daf-18(ø); sheath cells::daf-18(+)	*fog-1(q253)I;daf-18(ok480)IV; narEx99[Plim-7::RFP::DAF-18; Pmyo-2::GFP]*	UTR315
fog-1; daf-18(ø); Sp+Ut::daf-18(+)	*fog-1(q253)I; daf-18(ok480)IV; narEx2[Pfos-1a::GFP::DAF-18; Pmyo-3::mCherry]*	UTR34
fog-1; daf-18(ø); Sp-Ut Valve::daf-18(+)	*fog-1(q253)I; daf-18(ok480)IV; narEx105[Ptag312::GFP::daf-18;Pmyo-2::GFP]*	UTR336
fog-1; daf-18(ø); Sp Neck::daf-18(+)	*fog-1(q253)I; daf-18(ok480)IV; narEx107[Pipp5::GFP::daf-18;Pmyo-2::GFP]*	UTR338
GCaMP	*xbIs1101[Pfln-1::GCaMP + rol-6(su1006)gf]II*	UN1108
fog-1; GCaMP	*fog-1(q253)I; xbIs1101[Pfln-1::GCaMP + rol-6(su1006)gf]II*	UTR334
fog-1; GCaMP; daf-18(ø)	*fog-1(q253)I; xbIs1101[Pfln-1::GCaMP + rol-6(su1006)gf]II; daf-18(ok480)IV*	UTR333
fog-1; daf-18(G174E)	*fog-1(q253)I; daf-18(nar57 [G174E])*	UTR390
fog-1; plc-1(ø); somatic cells::plc-1(+)	*fog-1(q253)I;* plc-1(ø) X; kfEx2[Psur-5::plc-1::GFP]	UTR456
fog-1; GCaMP; plc-1(ø); somatic cells::plc-1(+)	*fog-1(q253)I; xbIs1101[Pfln-1::GCaMP + rol-6(su1006)gf]II;* plc-1(ø) X; kfEx2[Psur-5::plc-1::GFP]	UTR412
fog-1; daf-18(ø); plc-1(ø); somatic cells::plc-1(+)	*fog-1(q253)I; daf-18(ok480)IV;* plc-1(ø) X; kfEx2[Psur-5::plc-1::GFP]	UTR316
fog-1; GCaMP; daf-18(ø); plc-1(ø); somatic cells::plc-1(+)	*fog-1(q253)I; xbIs1101[Pfln-1::GCaMP + rol-6(su1006)gf]II; daf-18(ok480)IV;* plc-1(ø) X; kfEx2[Psur-5::plc-1::GFP]	UTR416
daf-2	*daf-2(e1370)III*	CB1370
daf-2; daf-18(ø)	*daf-2(e1370)III; daf-18(nr2037)IV*	UTR175

daf-2; daf-18(ø); germline::DAF-18(+)	*narSi5[Pmex-5::GFPo::DAF-18(+) + unc-119(+)]II; daf-2(e1370)III; daf-18(nr2037)IV;*	UTR179
oma-1; oma-2	*cpSi42[Pmex-5::mNeonGreen::PLCδ-PH::tbb-2 3'UTR + unc-119(+)]II; oma-1(zu405te33)/nT1 [qIs51] IV; oma-2(te51)/nT1 V*	UTR19
daf-18(ø);oma-1;oma-2	*cpSi42[Pmex-5::mNeonGreen::PLCδ-PH::tbb-2 3'UTR + unc-119(+)]II; daf-18(ok480) IV; oma-1(zu405te33)/nT1 [qIs51] IV; oma-2(te51)/nT1 V*	UTR29
lin-3::mNG	*lin-3(zh112[mNG::LoxP::3xFLAG])IV*	AH4511 Ref Alex Hajnal paper[180]
let-23::gfp	*zhIs35[let-23p::LET-23::GFP; unc-119(+)] I; unc-119(ed3) III*	AH1747 from Caenorhabditis Genetics Center (CGC)
akt-1	*akt-1(ok525) V*	RB759 from Caenorhabditis Genetics Center (CGC)
fog-1; daf-18; akt-1	*fog-1(q253)I; daf-18(ok480)IV; akt-1(ok525) V*	UTR461

2.2 Plasmids and transgenics

We used the Gibson[181] method for assembling all plasmids. The source DNA and primers that were used to generate all plasmids, as well as their microinjection concentrations, are found in Table. 2.2.

Table. 2. 2 plasmid design

Plasmid name	Description	Injection concentration	Reference
pKSII	Empty vector	100ng/µL	N/A
pPOM4	*Pmex-5::GFP::DAF-18(+)* for single-copy insertion on LGII	50ng/µL	N/A
pFS2	*Pelt-7::DAF-18(+)*	50ng/µL	(Ref F. Solari paper [167])
pFS4	*Punc-119::DAF-18(+)*	50ng/µL	(Ref F. Solari paper [167])
pFS5	*Peunc-54::DAF-18(+)*	50ng/µL	(Ref F. Solari paper [167])
pFS6	*Pnhr-72::DAF-18(+)*	50ng/µL	(Ref F. Solari paper [167])
pJC3	*Pmyo-3::RFP::DAF-18(+)*	50ng/µL	N/A
pFS9	*Peunc-54::GFP*	50ng/µL	(Ref F. Solari paper [167])
pOG1	*Pfos-1a::GFP::daf-18(+)*	50ng/µL	N/A
pJC4	*Plim-7::RFP::DAF-18(+)*	50ng/µL	N/A
pJC10	*Pipp-5::GFP::DAF-18(+)*	50ng/µL	N/A
pJC14	*Ptag-312::GFP::DAF-18*	50ng/µL	N/A

Extra-chromosomal arrays were generated by standard germline microinjections at a total concentration of 200 ng/µL, using pKSII as a filler DNA and pCFJ104[*Pmyo-3::mCherry*] (5 ng/µL) or pMR352[*Pmyo-2::GFP*] (50 ng/µL) as a co-injection markers [56, 182]. To rescue DAF-18 specifically in the germline, we used CRISPR/Cas9 to insert a single copy of a *Pmex-5::GFP::DAF-18(+) + unc-119(+)* fragment at ttTi5605 (LG II, +0.77 M.U.) into *unc-119(ed3)* mutants, using pPOM4 (Table S2) and pDD122 [183]. A single line (*narSi5*) was obtained after injecting > 80 animals. To generate the *daf-18(G174E)* variant, we used the *dpy-10* co-CRISPR strategy with the *Paix et al.* protocol to modify *fog-1(q253)* [54, 55]. The sgRNAs and repair templates sequences used for both CRISPRs are shown in Table. 2.3 CRISPR design

Table. 2. 3 CRISPR design

Name	Source material	Primers (5'->3')	Injection concentration
pJC15	PDD162	*F: 5'-ACA TAT CAT CAC TCC GGT AGT TTT AGA GCT AGA AAT AGC AAG-3'* *R:* 5'-CAA GAC ATC TCG CAA TAG G-3'	16.66 ng/µl
pJC16	PDD162	*F: 5'-AAG CTG GAA AAG GCC GTA CGT TTT AGA GCT AGA AAT AGC AAG-3'* *R:* 5'-CAA GAC ATC TCG CAA TAG G-3'	16.66
pJC17	PDD162	*F: 5'-TAC ACT GTA AAG CTG GAA AGT TTT AGA GCT AGA AAT AGC AAG-3'* *R:* 5'-CAA GAC ATC TCG CAA TAG G-3'	16.66
Repair Template for G174E	N/A	*5'-GAT AAA CAT GTA ATA GCT GTA CAC TGT AAA GCT GGA AAA G**AG CGC ACT** GGA GTG ATG ATA TGT GCT CTT CTC ATC TAC ATC AAC*-3'	1µg/µl
pµMP27	*PDD162*	*F:*5'GCT ACC ATA GGC ACC ACG AGG TTT TAG AGC TAT GCT GTT TTG-3' *R:* 5'-CAA GAC ATC TCG CAA TAG G-3'	25 ng/µl
Repair Template for DYP-10	N/A	*5'*-CAC TTG AAC TTC AAT ACG GCA AGA TGA GAA TGA CTG GAA ACC GTA CCG CAT GCG GTG CCT ATG GTA GCG	1µg/µl

		GAG CTT CAC ATG GCT TCA GAC CAA CAG CCT AT-3’	

2.3 Oocyte counts

Late-L4 stage animals were transferred from 15°C to a new plate at 25°C and after 3 days, F1 late-L4s, synchronized based on vulva development [184] were picked to a new plate at 25°C, and grown for an additional 24 hours [59]. This procedure allowed to inactivate the temperature sensitive *fog-1(q253)* throughout larval development to prevent sperm formation [58]. Resulting day 1 adults (A1) were harvested, paralysed with 4.15 mM (0.1%) Tetramisole and mounted onto M9 + 3% agarose pads. The number of oocytes per gonad arm, and degree of their compaction, were determined by differential interference contrast (DIC) examination.

2.4 Germline mitotic index

Progenitor zone mitotic indexes were evaluated as previously described [23, 59, 154, 185, 186], by transferring late-L4 stage animals from 15°C to a new plate at 25°C and after 3 days picked the F1 late-L4 stage animals [184], to a new plate at 25°C, and allowed them to grow for an additional 24 hours [59]. Resulting A1 animals were harvested and their gonads were dissected and stained as previously described [186]. Briefly, worms were transferred into an 8 µL drop of 1X PBS on a microscope slide cover glass and quickly dissected using a 25G surgical needle tip. The cover glass was then flipped onto a poly-L-lysine coated slide and submitted to a freeze-crack procedure. Samples were then fixed in -20°C methanol for 1 minute and post fixed in a 3.7% paraformaldehyde solution (3.7% paraformaldehyde (PFA), 1X PBS, 0.08 M HEPES, 1,6 mM $MgSO_4$ et 0,8 mM EGTA) for 30 minutes. Using 1ml PBST (PBS + 0.1% Tween 20) slides were rinsed twice and incubated 10 minutes in PBST each time. Samples were then blocked in 300 µL blocking solution (PBST + 3% BSA) for 1h at room temperature. Samples were stained using primary rabbit anti-WAPL-1 (1:500, Sdix #4930.00.02) to mark GSCs along with their proliferating progeny [187], and

mouse anti-phospho[ser10]-histone H3 antibodies (1:250, Cell Signalling #9706) were used to mark G2/M-phase nuclei, and counter-stained with 0.7 μg/mL 4'6-diamidino-2-phenylindole (DAPI) to highlight all nuclei. Undifferentiated germ nuclei counting in 3 dimensions was partially automated using an ImageJ plugin developed by Dr Jane Hubbard's laboratory [188].

2.5 Dauer formation assays

Dauer formation was scored as described in previous reports [189]. Briefly, for Figure. 4, synchronized batches of eggs were allowed to hatch at 15℃ for 36 hours, and were upshifted to 25°C as L1s to induce dauer entry. Dauer formation rate was evaluated by the number of dauer 96 hours later divided by the number of all *C. elegans*. For Fig. 5 and 6, hermaphrodites were picked together with males at the L4 stage and allowed to mate for 24 hours. Hermaphrodites were then singled onto new plates at 25°C. Dauer formation rate was evaluated by the number of dauer 96 hours later divided by the number of L4 and adult.

2.6 Whole-worm DAPI Staining

Whole-worm DAPI staining was done as previously described [190]. Briefly, animals were washed off plates and soaked in Carnoy's solution (60% ethanol, 30% acetic acid, 10% chloroform) on a shaker overnight. Animals were then washed three times (10 minutes each) in PBST and stained in 1 μg/ml DAPI solution for 30 minutes. Finally, larvae were washed three more times (10 minutes each) in PBST and mounted in Duolink mounting medium (Sigma #1003264403).

2.7 Antibody staining

A1 animals were harvested, and their gonads were dissected and stained as described in the Germline mitotic index section above [186]. Primary mouse monoclonal anti-PIP_3 antibodies (1:100, Echelon Z-P345) and rabbit anti-HIM-3 (kind gift from M.

Zetka), and secondary A488-conjugated goat anti-mouse or A546-conjugated goat anti-rabbit antibodies (both at 1:500, Invitrogen Cat# A32731; RRID: AB_2633280 and Cat# A-11035; RRID: AB_143051) were used. DAPI was used as a counterstain.

2.8 Ca^{2+} imaging

Spermatheca Ca^{2+} imaging was evaluated in A1 animals using the *Pfln-1::GCaMP3* sensor (kind gift from Erin J. Cram) as previously described [134]. Late-L4 stage animals were transferred from 15°C to a new plate at 25°C and after 3 days picked the F1 L4 stage animals, then transferred the F1 L4 stage animals to a new plate at 25°C grown for an additional 24 hours and filmed at A1.

2.9 Image acquisition and processing

For figures 2a, 7a, 9, 10b, 14b, 17, 19, three-dimensional DIC and epifluorescence images were acquired every micron using a Plan-Apochromat 20x dry objective (NA 0.8) mounted on an inverted Zeiss Axio Observer.Z1. For figure 18 three-dimensional DIC and epifluorescence images were acquired every micron using a Plan-Apochromat 40x oil objective (NA 0.8) mounted on aninverted Zeiss Axio Observer.Z1. Images were stitched using the Zen software (2.6 Blue Edition). Epifluorescence signals were overlaid to the DIC images using Fiji, and animals were straightened using ImageJ.

For figure 3a, 8a, 11a, 13c, we assessed MIs in young adult hermaphrodites (L4 + 24 hours at 25°C), following the established procedure outlined in previous studies (Narbonne et al., 2015, 2017). Briefly, we captured three-dimensional images of the distal gonad. For DAPI staining, we employed a 353 nm excitation wavelength and a 465 nm emission wavelength. The fluorophores Alexa 488 was excited at 493 nm and emitted at 517 nm, while the fluorophores Alexa 546 were excited at 557 nm and emitted at 572 nm. Images for all fluorophores (Alexa 488, Alexa 546) and DAPI were obtained at each micron interval, utilizing a Plan-Apochromat 40x/1.4 oil objective. In figures 14a and 14b, we examined the expression pattern of PIP_3 during the A1 stage

using a Deltavision microscope with 60x objective Oil, and stitching was done with ImageJ.

For figure 12 and 15a, DIC and epifluorescence images and video were acquired using a Plan-Apochromat 40x/1.4 oil objective. Epifluorescence signals were overlaid to the DIC images using Fiji.

2.10 STATISTICAL ANALYSIS

For parametric datasets, the one-way ANOVA was used, and followed by Tukey multiple comparisons. For non-parametric datasets, the Kruskal-Wallis test was used, and followed by Dunn multiple comparisons, adjusted according to the family-wide error rate procedure of Holm, and then by the false discovery rate procedure of Benjamini-Hochberg. Graphs were generated, and data were analysed using GraphPad Prism 8. Three asterisks indicate statistical significance ($P<0.0001$), two asterisks indicate statistical significance ($P<0.01$) and one asterisks indicate statistical significance ($P<0.05$) to all other samples. ns, not significant. Statistical details, including sample sizes, can be found in the figure legends.

CHAPTER Ⅲ

RESULT

3.1 Oocytes and GSC proliferation arrest independently from germline PTEN

3.1.1 Generation of a germline-rescuing DAF-18 transgene in the *fog-1; daf-18* double mutant background

To unravel the relationship between *daf-18* and oocyte accumulation, we conducted rescue experiments by reintroducing *daf-18* in the *fog-1; daf-18* double mutation. Our objective was to identify the specific tissue in which *daf-18* is required to arrest oocyte.

Given the previously identified functions for germline DAF-18 in downregulating germline MPK-1 and preventing oocyte maturation [174, 191], we hypothesized that germline DAF-18 was responsible for oocyte quiescence in the absence of sperm signals. Using CRISPR/Cas9, we introduced a single-copy of a GFP::DAF-18(+) transgene [182, 183], driven by the *mex-5* germline-specific promoter [192], in the genome of *fog-1; daf-18(ø)* mutants, to generate a feminized strain expressing DAF-18 specifically in the germline, henceforth *fog-1; germline::DAF-18* (Figure. 3.1). Since *daf-18* is under maternal control for dauer entry [193], the larval progeny of *germline::DAF-18* animals are expected to carry diluted somatic DAF-18 activity in addition to robust germline expression (Figure. 3.1)

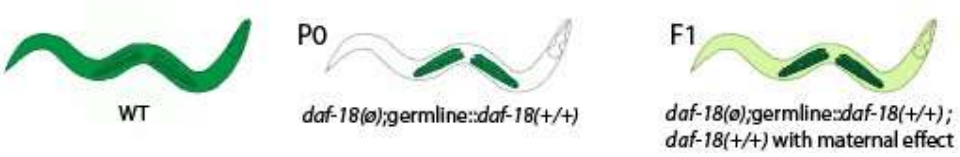

Figure. 3. 1 Schematic representation of the germline::DAF-18 rescue

In the WT, *daf-18* was expressed throughout *C. elegans* [167], and *daf-18(ø); germline:: daf-18(+/+)* expressed *daf-18::GFP* in the germline. However, the progeny of *daf-18(ø); germline::daf-18(+/+)* exhibited a maternal effect, having received maternal DAF-18 protein in the oocyte, this protein was diluted as the animal grew during larval stages. Here, DAF-18 is shown in green shades, with the intensity approximating the expected variations in its concentration across different areas.

3.1.2 Oocytes arrest in the absence of sperm independently from germline DAF-18

Young wild-type *C. elegans* adult hermaphrodites exhibit approximately 7 oocytes in the proximal somatic gonad. In sperm-less *fog-1* mutant hermaphrodite, the absence of MSP caused oocytes to arrest and accumulate, with the animals typically piling up to 15-20 arrested oocytes (Figure. 3.2). As reported previously, in the *fog-1; daf-18*(ø) double mutant, oocytes are continually ovulated as in the wild-type. Unexpectedly, when we rescued DAF-18 expression in the germline of *fog-1; daf-18*(ø) double mutants, these animals still exhibited oocyte wastage similar to *fog-1; daf-18(ø)* mutants (Figure. 3.2).

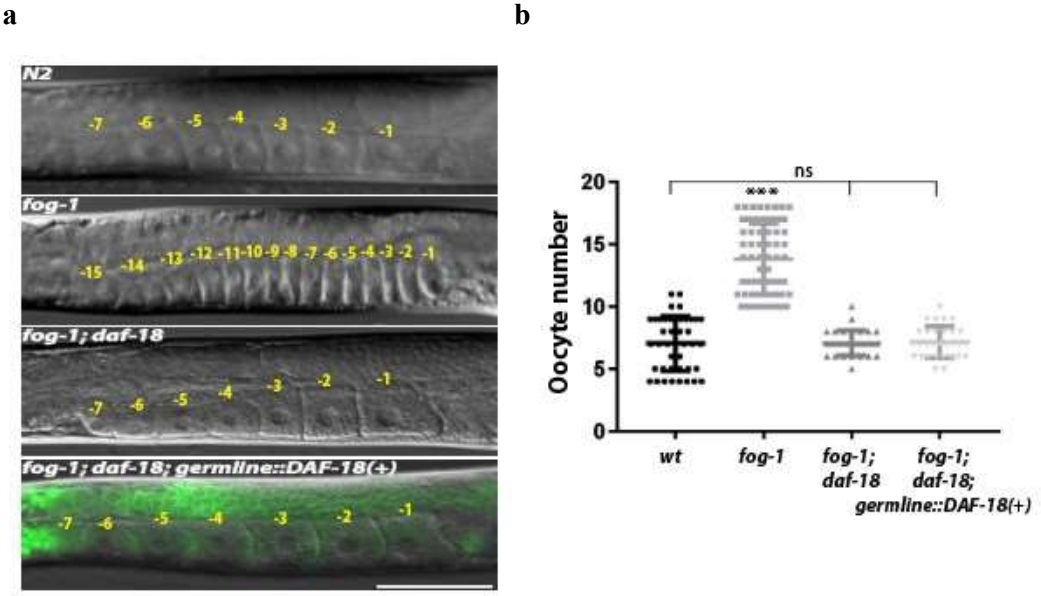

Figure. 3. 2 Oocytes arrest in the absence of sperm independently from germline DAF-18

(a) Representative day-1 adults (A1; see methods) of the indicated genotypes were imaged using Differential Interference Contrast (DIC). The expression of *daf-18* in the germline area is labelled with [GFP::DAF-18]. The yellow number indicates the area occupied by oocytes. The anterior is on the left, and dorsal is up. Scale bar: 50 μm **(b)** The average number of diakinesis-stage oocytes per gonad arm in A1 hermaphrodites of the indicated genotypes was measured. The sample sizes (n) were 42, 70, 30, and 29. Lines mark averages (± standard deviation), dots represent the whole sample. Three asterisks indicate statistical significance ($P<0.0001$, ANOVA with Tukey HSD multiple comparisons) to all other samples. ns, not significant. **(a and b)** Alleles: *fog-1(q253)*, *daf-18(ok480)*.

3.1.3 GSC proliferation slows in the absence of sperm independently from germline DAF-18

To test if germline DAF-18 could restore the inhibition of GSC proliferation, we used the GSC mitotic index (MI) as an evaluation measure (see methods). In simple terms, the MI reflects the division of G2/M-phase nuclei in the proliferating progeny of GSCs

[59, 154, 185, 194]. Our results show that *fog-1; germline::DAF-18* adults maintained a high MI, like the wild-type and *fog-1; daf-18(ø)* controls (Figure. 3.3). This indicates that the downregulation of GSC proliferation in the absence of sperm is independent of germline DAF-18.

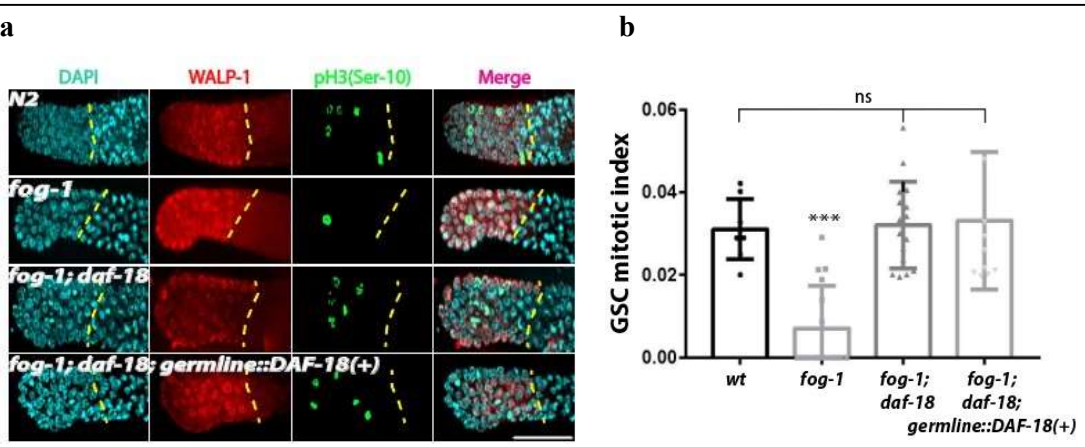

Figure. 3. 3 Oocytes arrest in the absence of sperm independently from germline DAF-18

(a) Representative distal germ lines dissected from A1 animals of the indicated genotypes, stained with DAPI (DNA; blue), anti-phospho[ser10] histone H3 (G_2/M-phase marker; green) and anti-WALP-1 (proliferation maker; red). Distal is on the left. Scale bar: 50 μm. **(b)** The GSC MIs of A1 hermaphrodites of the indicated genotypes were determined. N=8,16,16,11. Column mark averages, the error bar mark ± standard deviation, dots represent the whole sample **(a and b)** Three asterisks indicate statistical significance (P<0.0001, Kruskal-Wallis followed by Dunn) to all other samples. ns, not significant. **(a and b)** Alleles: *fog-1(q253)*, *daf-18(ok480)*.

3.2 Germline DAF-18 promotes dauer formation exclusively maternally, and in a dose-dependent manner

In *C. elegans*, the single ortholog DAF-2 represents the insulin and IGF-1 receptors found in humans [195, 196]. Initially identified through mutation screens aimed at

inducing constitutive development into the dauer larval stage, the *daf-2* gene has proven instrumental in uncovering factors that influence dauer entry. Numerous hypomorphic temperature-sensitive alleles of *daf-2* have been discovered, enabling constitutive dauer formation at 25°C while allowing for reproductive development at 15°C [197-200].

In our previous findings, we concluded that the presence of germline DAF-18 is unable to maintain oocyte arrest and promote oocyte accumulation while also suppressing the proliferation of GSCs. It was demonstrated that *daf-18(ø)* mutants exhibited defective dauer formation, while *daf-2* null mutants were temperature-sensitive and fully entered the dauer stage at 25°C [201]. To verify these unexpected negative results, and that our transgene was really rescuing DAF-18 in the germline, we conducted further investigations to determine if our transgene could rescue dauer development in *daf-2; daf-18(ø) Daf-d* mutants, since this is under maternal (and thus under the parent's germline) control.

3.2.1 Partial dauer formation in *daf-2; daf-18(ø); Germline::DAF-18(+)*

As anticipated, we observed that *germline::DAF-18* successfully restored the ability to form dauers in the *daf-2; daf-18(ø)* background (Figure. 3.4). It is important to note that *daf-18* is a maternal gene, meaning it exerts its effects on the progeny through maternal inheritance. Therefore, this positive outcome could be attributed to two factors: the rescue of *daf-18* in the germline itself, and/or to the DAF-18 protein maternally provided to the oocyte.

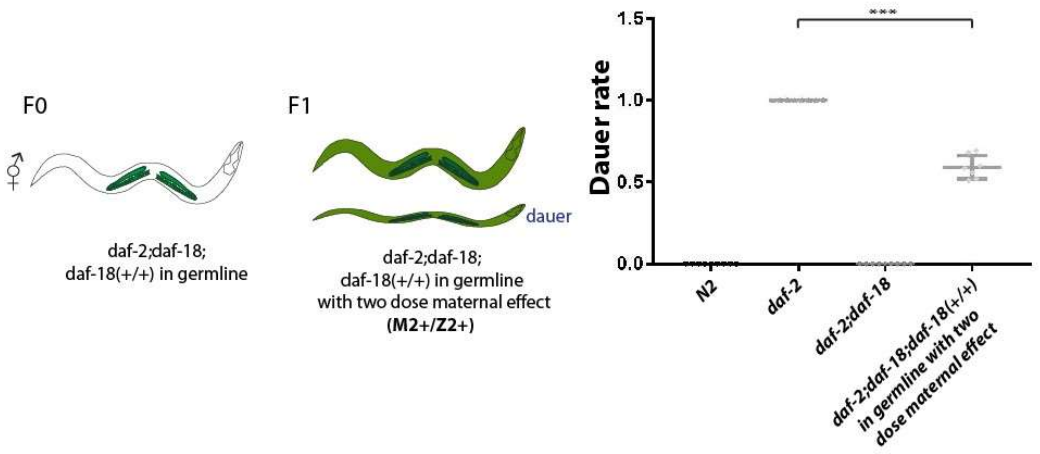

Figure. 3. 4 *daf-2; daf-18(ø); Germline::DAF-18* show partly dauer formation

Germline re-expression of DAF-18(+) rescues dauer formation in *daf-2; daf-18(ø)* mutants. Strategy to generate animals with two maternal and two zygotic (M2+; Z2+) copies of germline::DAF-18 is illustrated. N= 9, 8, 9, 7. Lines mark averages (± standard deviation). Dots represent the whole sample. Three asterisks indicate statistical significance (P<0.0001, T-test) to all other samples. Alleles: *daf-2(e1370), daf-18(nr2037), narSi5[Pmex-5::GFPo::DAF-18(+) + unc-119(+)]*.

3.2.2 Zygotic only germline re-expression of DAF-18(+) does not rescue dauer formation in *daf-2; daf-18(ø)* mutants

In order to assess the role of zygotic germline *daf-18(+)* alone in promoting dauer formation, we conducted a cross between *daf-2; daf-18(ø)* mutant hermaphrodites and *daf-2; daf-18(ø);* Germline::*DAF-18* males. This cross resulted in the generation of *daf-18* heterozygous progeny that lacked maternal *daf-18(+)* but expressed zygotic *daf-18(+)* (referred to as Mø/Z1+). To examine their dauer formation capabilities, we subjected these progenies to a 25℃ incubation. Surprisingly, we observed no appearance of dauers, suggesting that zygotic *daf-18(+)* alone is insufficient to support dauer formation (Figure. 3.5).

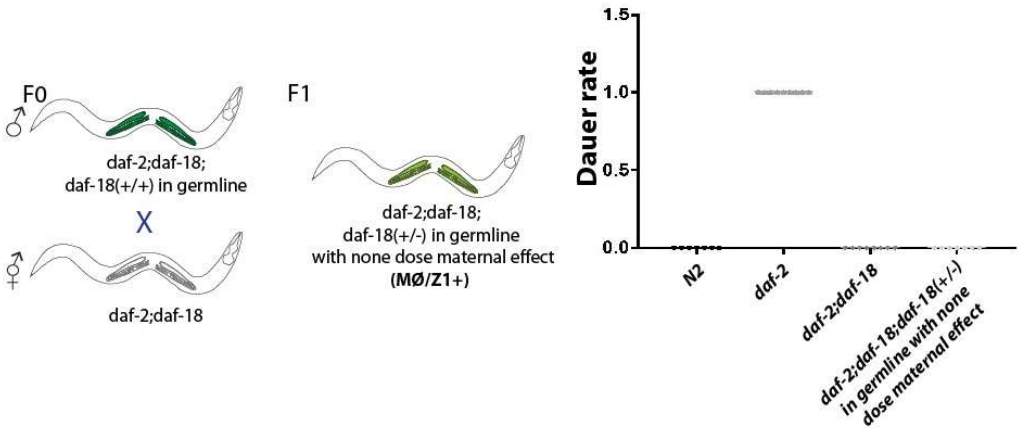

Figure. 3. 5 Zygotic only germline re-expression of DAF-18(+) does not rescue dauer formation in *daf-2; daf-18(ø)* mutants

Zygotic only germline re-expression of DAF-18(+) does not rescue dauer formation in *daf-2; daf-18(ø)* mutants. Strategy to generate Mø; Z1+ by crossing *daf-2; daf-18(ø);* germline::DAF-18(+) males with *daf-2; daf-18(ø)* hermaphrodites is shown. N= 8, 9, 8, 7. Lines mark averages. Dots represent the whole sample. The resulting F1 progeny carries one wild-type copy of germline::DAF-18(+) in the absence of maternally-provided DAF-18. Alleles: *daf-2(e1370), daf-18(nr2037), narSi5[Pmex-5::GFPo::DAF-18(+) + unc-119(+)]*.

3.2.3 Maternally-provided DAF-18 promotes dauer formation in a dose-dependent manner

We proceeded to investigate whether maternal *daf-18(+)* alone could induce dauer formation. To do so, we conducted crosses between hermaphrodites *daf-2; daf-18(ø); Germline::DAF-18* transgene and *daf-2; daf-18(ø)* males. This resulted in the generation of *daf-18* heterozygous progeny possessing two copies of maternal *daf-18 (2+)* while also expressing zygotic *daf-18(+)* (referred to as M2+Z1+). These progenies were then examined for dauer formation under a 25°C incubation. Interestingly, the results demonstrated a partial rescue of the dauer-defective phenotype observed in *daf-2; daf-18* mutants that depended solely on maternal *daf-18(+)* activity (Figure. 3.6).

Moreover, we conducted further investigations by examining the progeny derived from *daf-18(+)* heterozygous mothers with two copies of maternal *daf-18(2+)* (as described above). The progeny that expressed or did not express zygotic *daf-18(±) but* possessed one copy of maternal *daf-18(1+)* (referred to as M1+Z1±), displayed approximately half the level of dauer formation compared to M2+Z1+ progeny (Figure. 3.6). Therefore, we conclude that dauer formation is dependent on maternal DAF-18 dosage.

Additionally, we performed DAPI staining to assess the GSC numbers in dauers, since *daf-18* is required to suppress GSC proliferation during dauer development [190]. Interestingly, there were no significant differences observed in GSC numbers between *daf-2;daf-18;daf-18(+/+)* progeny with two copies of maternal effect (M2+Z2+), *daf-2;daf-18;daf-18(+/-)* progeny with two copies of maternal effect in the germline (M2+Z+), and *daf18(±/±)* progeny with one copy of maternal effect (M1+Z±): they all had extra GSCs compared with control dauers (Figure. 3.6).

Taken together, as expected, germline::DAF-18 maternally rescued dauer formation in a *daf-2; daf-18(ø)* background, in an allelic dosage-dependent manner, while zygotic germline expression was not sufficient to promote dauer entry (Figure. 3.6). Despite rescuing dauer formation, germline::DAF-18 did not suppress GSC over proliferation during dauer development (Figure. 3.6), which is prevented by somatic gonad DAF-18 [60]. This is consistent with germ-specific transgenic expression, and establishes that this defect is not maternally rescued. Therefore, we conclude that germline DAF-18 is not responsible for ensuring oocyte arrest in the absence of sperm signals. Moreover, since a maternal contribution from germline::DAF-18 to all somatic tissues was insufficient to ensure oocyte arrest, it further suggests that this regulation requires significant levels of DAF-18 protein, acting in somatic tissues.

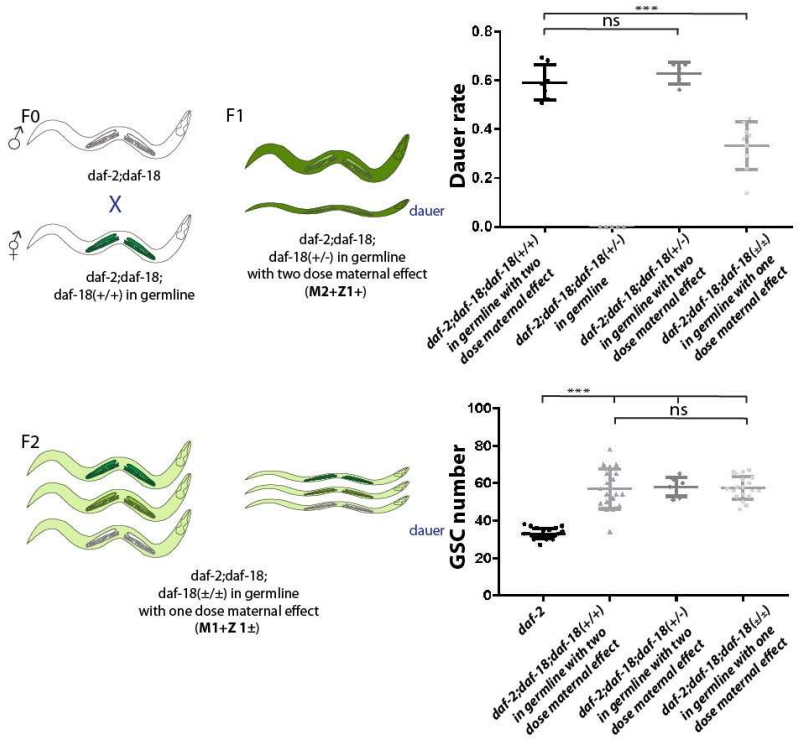

Figure. 3. 6 Maternally-provided DAF-18 promotes dauer formation in a dose-dependent manner

Strategy to generate M2+; Z1+ (F1) and M1+; (¼Z2+; ½Z1+; ¼Zø) (F2) by crossing *daf-2; daf-18(ø)* males with *daf-2; daf-18(ø);* germline::DAF-18(+) hermaphrodites is shown. There were no significant differences in dauer rates between animals having received two maternal doses of DAF-18(+), whether they carried one or two zygotic copies of germline::DAF-18(+). However, dauer rates dropped by a half when the mother was heterozygous for germline::DAF-18(+), even though ¾ of the animals carried at least one zygotic copy. We further evaluated the germline requirements for DAF-18 in the suppression of GSC proliferation during dauer formation [60]. We found that *daf-2; daf-18(ø);* germline::DAF-18(+) dauers had extra germ cells compared to *daf-2* controls, and that the severity of the defect was not affected by zygotic or maternal copy numbers. N= 7, 5, 5, 9 (dauer rate); N=22, 19, 7, 19 (GSC number). Lines mark averages (± standard deviation), dots represent the whole sample. Three asterisks indicate statistical significance (P<0.0001, ANOVA with Tukey HSD multiple

comparisons) to all other samples. ns, not significant. Alleles: *daf-2(e1370), daf-18(nr2037), narSi5[Pmex-5::GFPo::DAF-18(+) + unc-119(+)]*.

3.3 Muscle DAF-18 prevents unwanted ovulation and restores the downregulation of GSC proliferation

3.3.1 Muscle DAF-18 prevents unwanted ovulation

We already concluded that DAF-18 is not required within the germline to arrest oocytes and permit their accumulation – therefore it must work cell non-autonomously from the animal's soma. So, we next rescued *daf-18* in the main somatic tissues of the animal. To identify the somatic tissue(s) from which DAF-18 promotes oocyte arrest in the absence of sperm, we used transgenes to drive GFP::DAF-18(+) expression in specific somatic tissues within *fog-1; daf-18(ø)* animals. We used the *unc-54*, *nhr-72*, *elt-7*, and *unc-119* promoters for specific expression in non-pharyngeal muscles, seam cells, intestine and nervous system, respectively [167, 202-204]. Expression of GFP::DAF-18(+) in muscles partially rescued oocyte arrest and accumulation, while expression in hypodermal seam, intestinal or neuronal cells had no effect (Figure. 3.7 a and b). This result was confirmed using a second muscle-specific promoter, *Pmyo-3*(Fig. 7 a and b) [204].

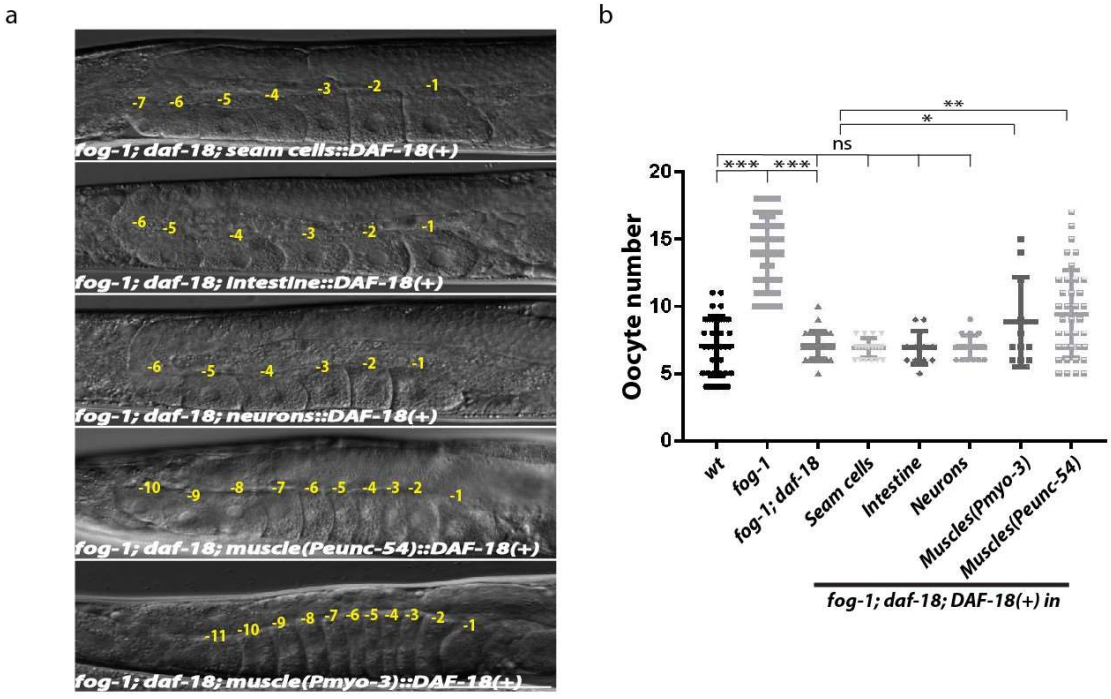

Figure. 3. 7 Muscle DAF-18 prevents unwanted ovulation

(a) Representative germlines of A1 animals of the indicated genotypes imaged using DIC. A yellow number highlight the oocytes number. Dorsal is to the up. Scale bar: 50 µm. **(b)** Average number (±standard deviation) of diakinesis-stage oocytes per gonad arm in A1 hermaphrodites of the indicated genotypes. N= 42, 68, 30, 19, 12, 17, 11, 37. Lines mark averages (± standard deviation), dots represent the whole sample. Three asterisks indicate statistical significance (P<0.0001, ANOVA with Tukey HSD multiple comparisons), two asterisks indicate statistical significance (P<0.01, ANOVA with Tukey HSD multiple comparisons) and one asterisks indicate statistical significance (P<0.05, ANOVA with Tukey HSD multiple comparisons) to all other samples. ns, not significant. Alleles: *fog-1(q253), daf-18(ok480).*

3.3.2 Muscle DAF-18 restores the downregulation of GSC proliferation

Since oocyte accumulation may be sufficient to activate homeostatic feedback and reduce GSC proliferation, we measured the GSC MI within all transgenics. GFP::DAF-

18(+) expression specifically in muscles was sufficient to promote GSC quiescence, while expression in other tissues had no effect (Figure. 3.8 a and b). We therefore conclude that, in the absence of sperm, DAF-18 expression in non-pharyngeal muscle tissues is sufficient to non-autonomously ensure that oocytes arrest and accumulate in the proximal somatic gonad, and for the concomitant homeostatic downregulation of GSC proliferation.

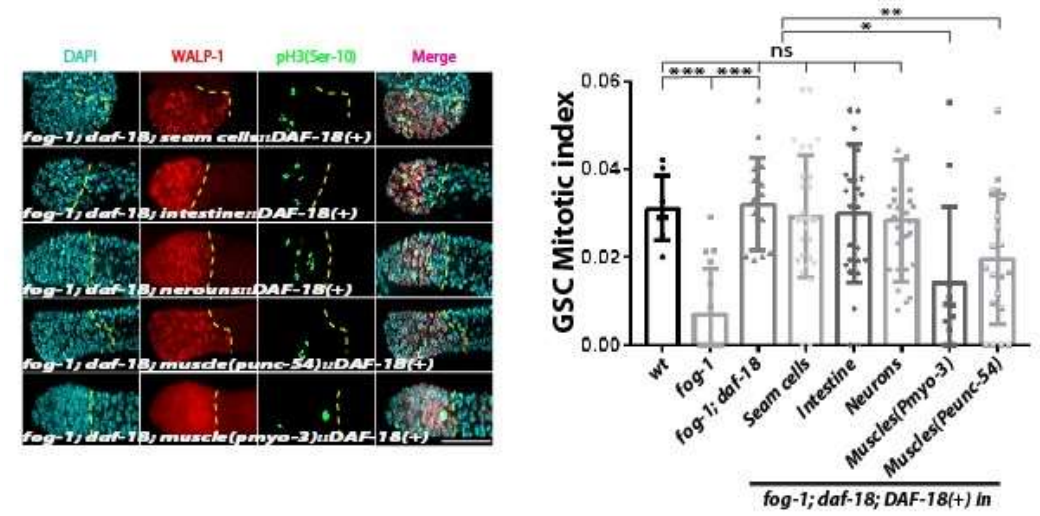

Figure. 3. 8 Muscle DAF-18 prevents unwanted ovulation

(a) Representative distal germ lines dissected from A1 *fog-1; daf-18(ø)* mutants carrying *daf-18* rescuing transgenes specifically expressed in the non-pharyngeal muscles (*Pmyo-3*, *Peunc-54*), seam cells (*Pnhr-72*), intestine (*Pelt-7*), and nervous system (*Punc-119*) ::DAF-18(+) A1 animals of the indicated genotypes, stained with DAPI (DNA; blue), anti-phospho[ser10]-histone H3 (G_2/M-phase marker; green) and anti-WALP-1 (proliferation maker; red). Distal is on the left. Scale bar: 50 µm. **(b)** The GSC MIs of A1 hermaphrodites of the indicated genotypes were determined. N= 8, 16, 16, 31, 29, 30, 11, 20. Column mark averages, the error bar mark ± standard deviation, dots represent the whole sample. Three asterisks indicate statistical significance (P<0.0001, Kruskal-Wallis followed by Dunn), two asterisks indicate statistical significance (P<0.01, Kruskal-Wallis followed by Dunn) and one asterisks indicate statistical significance (P<0.05, Kruskal-Wallis followed by Dunn) to all other samples. ns, not significant. Alleles: *fog-1(q253), daf-18(ok480).*

3.3.3 The *myo-3* and *eunc-54* muscle-specific promoters drive expression in the uterus, spermatheca and gonadal sheath myoepithelial

The *C. elegans* adult hermaphrodite muscular system consists of 20 pharyngeal and 95 body wall muscle cells, in addition to a few other specialized muscles, including the vulva, uterine and anal muscles [205]. While both the *myo-3* and *unc-54* promoters do not express in pharyngeal muscles [206, 207], it was conceptually difficult to hypothesize how DAF-18 expression in body wall muscles could promote oocyte arrest. On the other hand, the spermatheca and gonadal sheath cells are smooth muscle-like contractile cells that have been heavily implicated in the control of oocyte maturation and ovulation [105, 109]. We therefore examined more closely DAF-18 expression from the *myo-3* and *unc-54* promoters, and detected weak expression in the uterus, spermatheca and sheath cells from both promoters (Figure. 3.9).

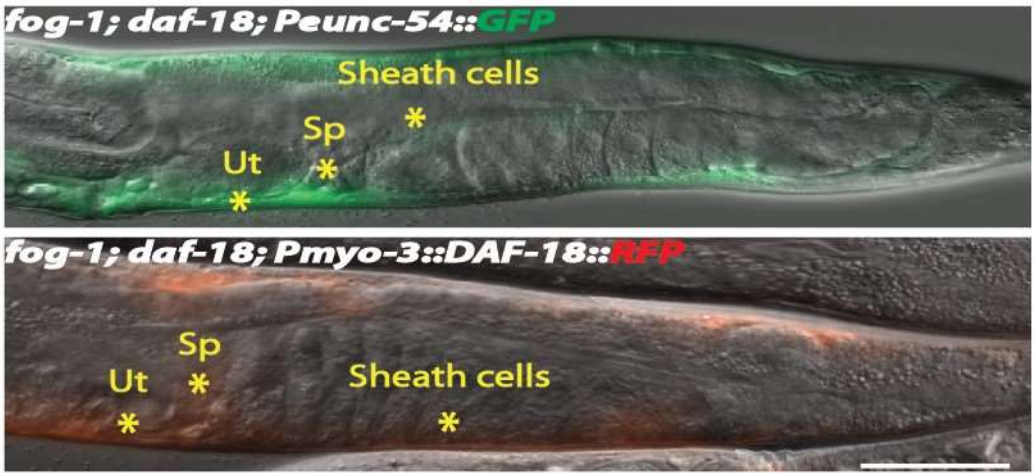

Figure. 3. 9 The *myo-3* and *eunc-54* muscle-specific promoters drive expression in the uterus, spermatheca and sheath gonadal myoepithelial

The *myo-3* and *eunc-54* (enhanced *unc-54*) promoters are reputed to drive expression specifically in non-pharyngeal muscles, and strongly label the body wall and vulva muscles [204]. We however detected fluorescence in the uterus, spermatheca and gonadal sheath cells in both of our **(A)** *myo-3* and **(B)** *eunc-54* transgenes. The yellow stars mark the location of sheath cells (SCs), spermatheca (Sp) and uterus (Ut), where fluorescence was detected. These results are consistent with the contractile, myoepithelial nature of these tissues. Scale bar: 50 µm. Alleles: *fog-1(q253), daf-18(ok480).*

3.4 Spermatheca neck DAF-18 prevents unwanted ovulation and restores the downregulation of GSC proliferation

3.4.1 Spermatheca neck DAF-18 prevents unwanted ovulation

To address whether DAF-18 may act within these contractile gonadal tissues, we first expressed GFP::DAF-18(+) specifically in the proximal gonad, comprising the spermatheca and uterus, or RFP::DAF-18(+) specifically in the gonadal sheath cells of

fog-1; daf-18(ø) animals, using the *fos-1a* and *lim-7* promoters, respectively [153, 208]. We found that GFP::DAF-18(+) expression in the proximal gonad rescued oocyte accumulation, while expression in the sheath cells had no effect accumulation (Figure 3.10). Therefore, these data indicate that the spermatheca and/or uterus is the site where DAF-18 acts to promote oocyte arrest and accumulation in the absence of sperm.

The spermatheca is the site of fertilization, and consists of three parts: an 8-cell distal neck, a 16-cell central bag, and a syncytial 4-cell sp-ut valve (Figure. 3.10a) [209]. To materialize ovulation, the gonadal sheath cells enter in a tug-of-war with the spermatheca neck until they successfully pull it open around the proximal (-1) oocyte (Figure. 3.10a) [135]. Once the oocyte enters the spermatheca, it is immediately fertilized, and the spermatheca neck and bag then contract to push the egg through the sp-ut valve and into the uterus [121, 135]. Two constrictions can therefore block the passage of oocytes to promote their accumulation: the spermatheca neck and the sp-ut valve. We therefore specifically expressed GFP::DAF-18(+) either in the spermatheca neck or the sp-ut valve of *fog-1; daf-18(ø)* animals, using the *ipp-5* and *rsef-1* promoters, respectively [210, 211]. We found that DAF-18 expression within the spermatheca neck rescued the oocyte arrest, while expression in the sp-ut valve did not (Figure. 3.10b).

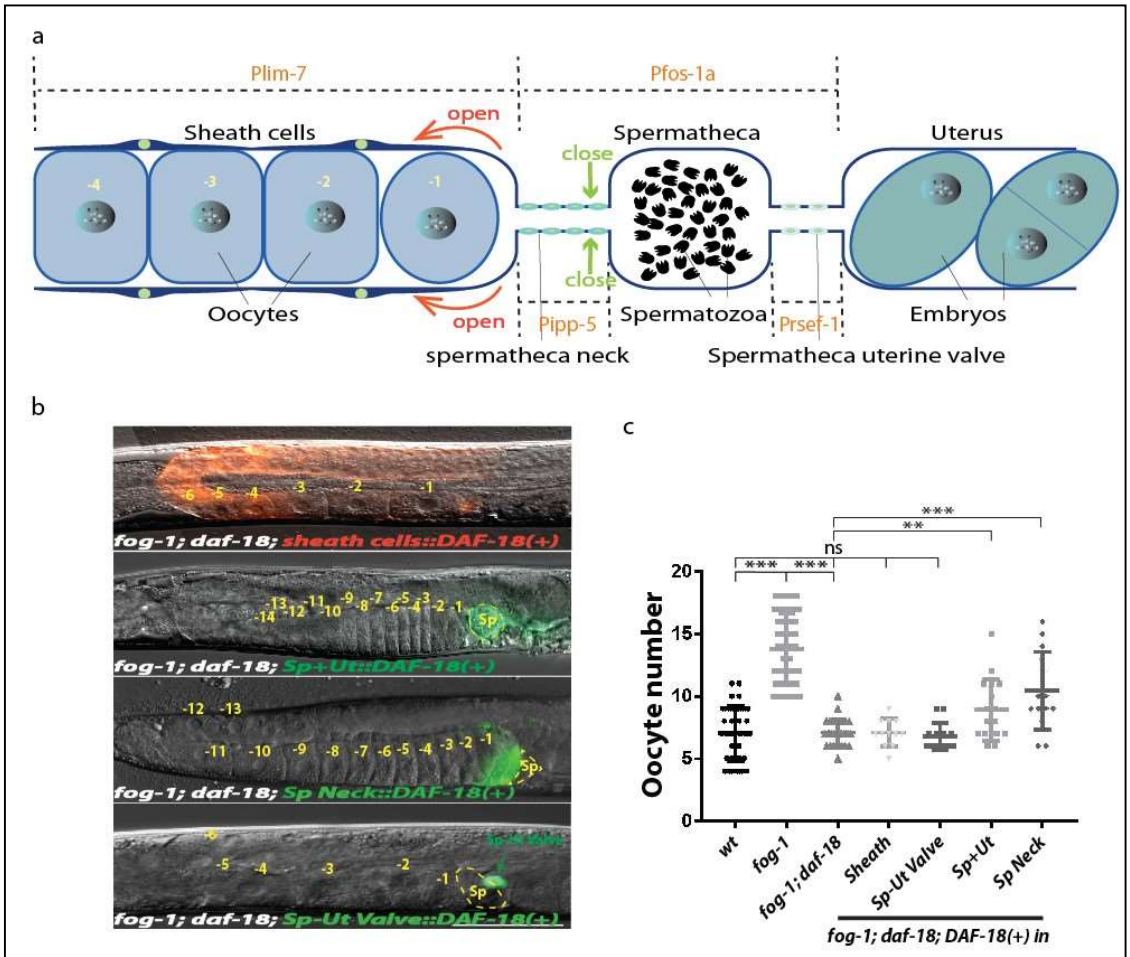

Figure. 3. 10 Spermatheca neck DAF-18 prevents unwanted ovulation

(a) Schematic of the *C. elegans* proximal gonadal sheath cells and spermatheca, itself consisting of three parts: a distal 8-cell neck, a central 16-cell bag, and a 4-cell syncytial sp-ut valve. Sheath cells contract along the distal-proximal axis (red arrows) to pull open the spermatheca neck around the -1 oocyte. The spermatheca neck is a sphincter muscle which contraction (blue arrows) resists this opening force. **(b)** Representative germlines of A1 animals of the indicated genotypes imaged using Differential Interference Contrast (DIC). The area expression of *daf-18* is labelled with [RFP::DAF-18] in *fog-1; daf-18*; sheath cells::DAF-18(+) and [GFP::DAF-18] in *fog-1; daf-18;* Sp+Ut::DAF-18(+), *fog-1; daf-18;* Sp Neck::DAF-18(+), *fog-1; daf-18;* Sp-Ut

Valve::DAF-18(+). A yellow number highlight the oocytes number. The dotted line highlights the spermatheca. The green arrows indicate the Spermatheca Neck and Sp-Ut Valve. Dorsal is to the up. Scale bar: 50 μm. **(c)** Average number of diakinesis-stage oocytes per gonad arm in A1 hermaphrodites of the indicated genotypes. Lines mark averages (± standard deviation), dots represent the whole sample. Three asterisks indicate statistical significance (P<0.0001, ANOVA with Tukey HSD multiple comparisons), two asterisks indicate statistical significance (P<0.01, ANOVA with Tukey HSD multiple comparisons) to all other samples. N=42, 68, 30, 12, 13, 17, 14. ns, not significant. Alleles: *fog-1(q253), daf-18(ok480).*

3.4.2 Spermatheca neck and sheath cell DAF-18 restore the downregulation of GSC proliferation

We already found that GFP::DAF-18(+) expression in the spermatheca neck rescued oocyte accumulation but RFP::DAF-18(+) expression in the sheath cell DAF-18 and had no effect on this defect. We measured the GSC MI within all transgenics. The results showed that GFP::DAF-18(+) expression specifically in the proximal gonad or spermatheca neck was sufficient to promote GSC quiescence, while expression in Sp-Ut valve was not (Figure. 3.11a and b).

Surprisingly, despite that RFP::DAF-18(+) expression specifically in the sheath cells had no effect on oocyte accumulation (Figure. 3.10b and c), it partially rescued the inhibition of GSC proliferation (Figure. 3.11a, b and c). This mild decrease in GSC proliferation by sheath DAF-18 expression in the absence of oocyte accumulation suggest that this tissue may not be the primary site for DAF-18 function, but can suppress GSC proliferation from this tissue independently of oocyte accumulation. Furthermore, since sheath cell MPK-1 activity can promote GSC proliferation [194], while DAF-18 suppresses MPK-1 activity [154, 191], we believe this mild and partial rescue may result from the inhibition of sheath MPK-1 by DAF-18 overexpression.

We therefore conclude that DAF-18 expression in the spermatheca neck, formed by 8 myoepithelial cells, is sufficient to non-autonomously promote oocyte arrest and accumulation in the absence of sperm, and to induce the concomitant downregulation in GSC proliferation (Figure. 3.11d).

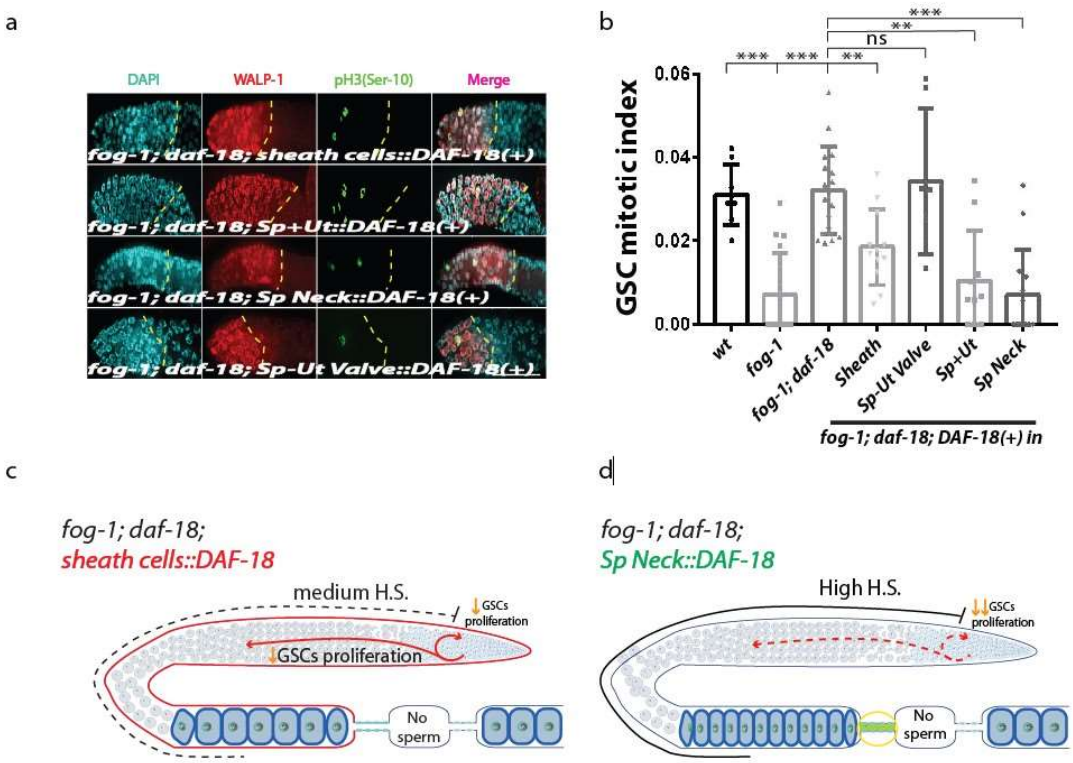

Figure. 3. 11 Spermatheca neck and sheath cell DAF-18 restore the downregulation of GSC proliferation

(a) Representative distal germ lines dissected from A1 *fog-1; daf-18(ø)* mutants carrying *daf-18* rescuing transgenes specifically expressed in the sheath cells (*Plim-7*), Sp+Ut (*Pfos-1a*), Spermatheca Neck (*Pipp-5*), and Sp-Ut Valve (*Prsef-1*) ::DAF-18(+) A1 animals of the indicated genotypes, stained with DAPI (DNA; blue), anti-phospho[ser10] histone H3 (G_2/M-phase marker; green) and anti-WALP-1 (proliferation maker; red). Distal is on the left. Scale bar: 50 µm. **(b)** The GSC MIs of A1 hermaphrodites of the indicated genotypes were determined. N= 8, 17, 16, 12, 7, 10,

14. Column mark averages, the error bar mark ± standard deviation, dots represent the whole sample. Three asterisks indicate statistical significance (P<0.0001, Kruskal-Wallis followed by Dunn) and two asterisks indicate statistical significance (P<0.01, Kruskal-Wallis followed by Dunn) to all other samples. ns, not significant. **(c)** Schematic of the *C. elegans* germline of *fog-1; daf-18*; sheath cells::DAF-18, it shows no effect on oocyte accumulation, but still partially rescued GSC proliferation. The red line highlight RFP::DAF-18 in sheath cells. **(d)** Schematic of the *C. elegans* germline of *fog-1; daf-18*; Sp Neck::DAF-18, it shows oocyte arrest and accumulation in the absence of sperm, and to induce the concomitant downregulation in GSC proliferation. The yellow cycle highlights GFP::DAF-18 in Spermatheca Neck. Alleles: *fog-1(q253), daf-18(ok480).*

3.5 DAF-18 prevents spermatheca neck relaxation to suppress unwanted ovulation

The spermatheca neck forms a sphincter muscle that is constricted between ovulation events to block the premature entrance of the large maturing proximal oocyte, despite ongoing basal rhythmic sheath cell contractions [117, 121, 135, 212]. The final maturation of the proximal oocyte, induced by MSP signalling, is however thought to provoke the release the epidermal growth factor (EGF) LIN-3 to trigger more frequent and stronger ovulatory sheath cell contractions, which eventually overcome the spermatheca neck's might and force it open while pulling it around the large, now fertilization-competent, oocyte [127, 213]. Contractility in both sheath and spermatheca is dependent on actin/myosin interactions, which are stimulated by rises in the cytoplasmic Ca^{2+} concentration, as it is released from the endoplasmic reticulum by the IP_3 receptor ITR-1 [127, 134, 135]. To dissect out how DAF-18 may work in the spermatheca neck to prevent the ovulation of unfertilized oocyte, we recorded time-lapse sequences of animals expressing the Ca^{2+} fluorescent sensor $GCaMP_3$ in the spermatheca [214]. This genetically encoded cytoplasmic Ca^{2+} sensor is a synthetic fusion between GFP, calmodulin and the M13 peptide, that fluoresces green only when

Ca^{2+} bound (Figure. 3.12a) [215]. In wild-type, as expected, the spermatheca neck was contracted before ovulation, relaxed as it was stretched-open and pulled around the mature oocyte by the sheath cells during ovulation, and then contracted again, this time stronger and together with central bag cells, to push the fertilized oocyte through the sp-ut valve and into the uterus (Figure. 3.12b). In sperm-less *fog-1* mutant however, the spermatheca neck always remained constricted, and effectively prevented oocytes to enter (Figure. 3.12b). In *fog-1; daf-18(ø)* animals, we observed that the spermatheca neck could relax normally to allow oocyte entry, and that the neck and bag then contracted to expulse it into the uterus, as in control animals. (Figure. 3.12b). Altogether these results indicate that in the absence of sperm, DAF-18 is required in the spermatheca neck to boost its contractility in order to resist sheath contractions and prevent unwanted oocyte entry.

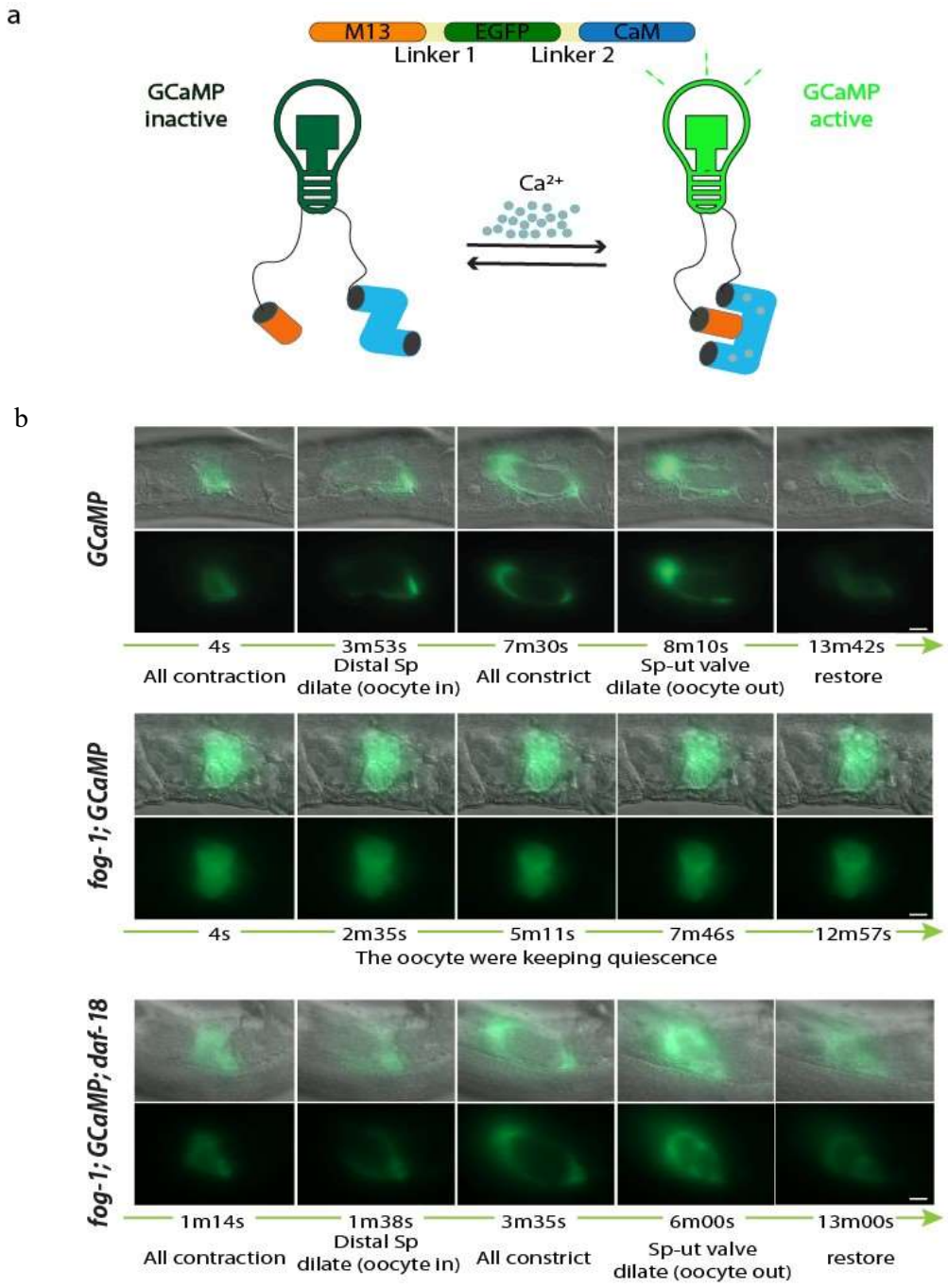

Figure. 3. 12 DAF-18 prevents spermatheca neck relaxation to suppress unwanted ovulation

(a) Representation of the GCaMP, a synthetic fusion between EGFP, calmodulin (CaM) and the M13 peptide. When Ca^{2+} bind to GCaMP, the CaM domain undergoes a conformational change and forms a strong interaction with the alpha helix of the M13 domain. This interaction effectively blocks water molecules from reaching the chromophore. Consequently, the chromophore quickly loses a proton and transitions into an anionic state, resulting in bright fluorescence similar to that of native GFP [216]. **(b)** Representative time frames showing spermatheca Ca^{2+} flows during ovulatory events in wild-type (WT) (n = 17) and *fog-1* (n=50) and *fog-1; daf-18(ø)* (n = 9) animals carrying *xbIs1101[fln-1p::GCaMP]*. Distal is left. **(b)** Scale bar: 50 µm. Alleles: *fog-1(q253), daf-18(ok480)*.

3.6 DAF-18's lipid phosphatase activity is required for oocyte retention and GSC proliferation inhibition

3.6.1 Lipid-phosphatase defective DAF-18 recapitulated the *fog-1; daf-18(ø)* phenotype and prevented oocyte accumulation and homeostatic regulation of GSC proliferation

Since DAF-18 is a dual-specificity phosphatase [175], it could block ovulation through its lipid or protein phosphatase activity, or even through a non-catalytic function. To discern the key function, we used CRISPR/Cas9 to introduce a G174E (equivalent to human G129E) transition in endogenous DAF-18, to specifically remove its lipid phosphatase activity [175, 217]. We found that *fog-1; daf-18(G174E)* mutants wasted their oocytes like *fog-1; daf-18(ø)* (Figure. 3.13a and b) and that their GSCs showed sustained proliferation (Figure. 3.13c and d). The lipid phosphatase activity of DAF-18 is likely therefore responsible for preventing ovulation in the absence of sperm, and for establishing the concomitant downregulation of GSC proliferation [176, 177].

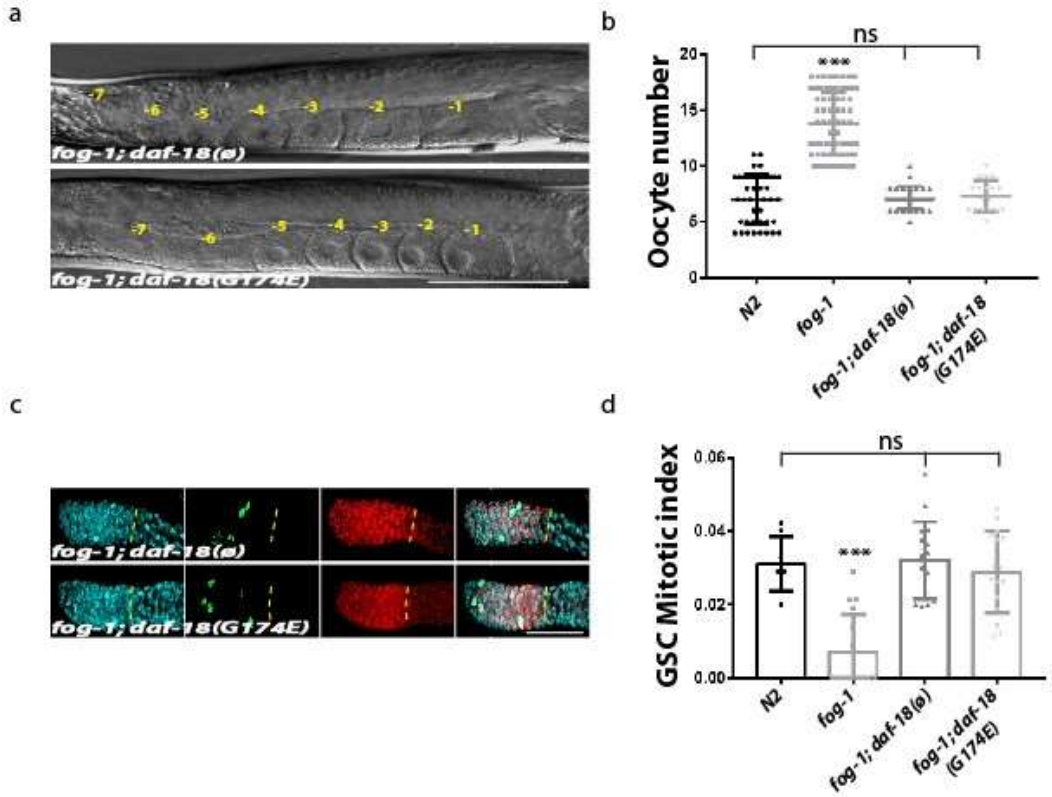

Figure. 3. 13 Lipid-phosphatase defective DAF-18 recapitulated the *fog-1; daf-18(ø)* phenotype and prevented oocyte accumulation and homeostatic regulation

(a) Representative germlines of A1 animals of the indicated genotypes imaged using DIC. A yellow number of highlights oocyte numbers. Dorsal is to the top. Scale bar: 50 μm. **(b)** Average number of diakinesis-stage oocytes per gonad arm in A1 hermaphrodites of the indicated genotypes. N=42, 68, 30, 18. Lines mark averages (± standard deviation), dots represent the whole sample. Three asterisks indicate statistical significance (P<0.0001, ANOVA with Tukey HSD multiple comparisons) to all other samples. ns, not significant. **(c)** Representative distal germ lines dissected from *fog-1; daf-18(ø)* mutants and *fog-1; daf-18(G174E)* A1 animals of the indicated genotypes, stained with DAPI (DNA; blue), anti-phospho[ser10] histone H3 (G_2/M-phase marker; green) and anti-WALP-1 (proliferation maker; red). Distal is on the left. Scale bar: 50

μm. **(d)** The GSC MIs of A1 hermaphrodites of the indicated genotypes were determined. N=, 8, 16, 16, 16. Column mark averages, the error bar mark ± standard deviation, dots represent the whole sample. Three asterisks indicate statistical significance (P<0.0001, Kruskal-Wallis followed by Dunn). ns, not significant. Alleles: *fog-1(q253), daf-18(ok480), fog-1; daf-18(nar57[G174E])*.

3.6.2 PIP_3 is relatively abundant in the spermatheca

The loss of DAF-18 activity is expected to cause an increase in PIP_3 levels. To verify this, we used antibodies to evaluate spermatheca PIP_3 levels. In wild-type gonads, we surprisingly detected little PIP_3 throughout the germline, distal tip and sheath cells, but relatively much higher PIP_3 levels on spermatheca cell membranes (Figure. 3.14). Furthermore, the results also provide a potential explanation for the specific requirement for DAF-18 in the spermatheca. Indeed, DAF-18 is present in most tissues [167, 174, 191], but its loss does not appear to weaken all muscles since the locomotion of *daf-18(ø)* mutants is superficially WT (data not shown). The specific weakening of the spermatheca may therefore arise because PIP_3 levels may only be this abundant in the spermatheca muscle, where they may allow DAF-18 to convert significant amounts into PIP_2, which could then feed into the PLC-1/Ca^{2+} pathway to promote contractility.

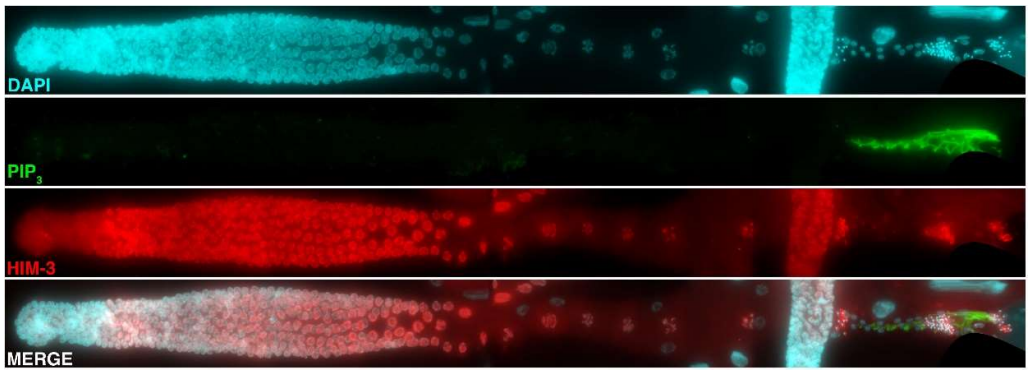

Figure. 3. 14 PIP_3 is abundant in the spermatheca

Representative distal germ lines dissected *fog-1; daf-18(G174E)* A1 animals of the indicated genotypes, stained with PIP_3 (green). Distal is on the left. Alleles: *fog-1(q253)*, *daf-18(ok480)*, *daf-18(nar57[G174E])*. Figure contribution acknowledgment: Special thanks to Patrick Narbonne for his valuable contribution to this Figure 3.14.

3.7 DAF-18 may prevent spermatheca neck dilation via PIP_2 stimulation of PLC-1/ Ca^{2+} signalling or another pathway

3.7.1 *daf-18* exacerbated the *fog-1; plc-1(ø)* phenotype

PLC-1 cleaves PIP_2 into the second messengers DAG and IP_3. IP_3 stimulates the release of Ca^{2+} from the ER through the IP_3 receptor ITR-1 [134, 136]. Loss of PLC-1 results in trapping of embryos in the spermatheca, suggesting that its neck and bag lack the ability to strongly contract and push the eggs through the sp-ut valve and expulse them into the uterus [136]. We hypothesized that the *plc-1* may be downstream of daf-18 to prevent the spermatheca neck dilation. Hence, we made *fog-1; plc-1(ø)* double mutants and *fog-1; daf-18(ø); plc-1(ø)* triples mutants.

The *fog-1; plc-1(ø)* double mutants showed a few oocytes trapped within their spermatheca (Figure 3.15). The *fog-1; daf-18(ø); plc-1(ø)* triples however accumulated obviously more oocytes trapped within their spermatheca than *fog-1; plc-1(ø)* doubles, but also had more anovulated oocytes within their proximal gonads than *fog-1; daf-*

18(ø) doubles (Figure. 3.15). The partial rescue of anovulated oocyte accumulation in the *fog-1; daf-18(ø); plc-1(ø)* triple, *vs* the *fog-1; daf-18(ø)* double, may have arisen because the loss of *plc-1* introduced a second blockade in the path of oocytes, this time at the sp-ut valve, that caused a backlog of oocytes into the proximal gonad once the spermatheca got maximally stretched. Our results show that *daf-18* exacerbates the *fog-1; plc-1(ø)* phenotype, where the spermatheca neck and spermatheca bag exhibit lower intercellular calcium levels. It has been reported that PLC-3 is also expressed in the spermatheca [213]. Consistent with our hypothesis, it implies that *daf-18* may function upstream of *plc-1/plc-3* to prevent spermatheca neck dilation. Alternative possibility is *daf-18* also may regulate another pathway, to reduce the spermatheca neck and bag contractility.

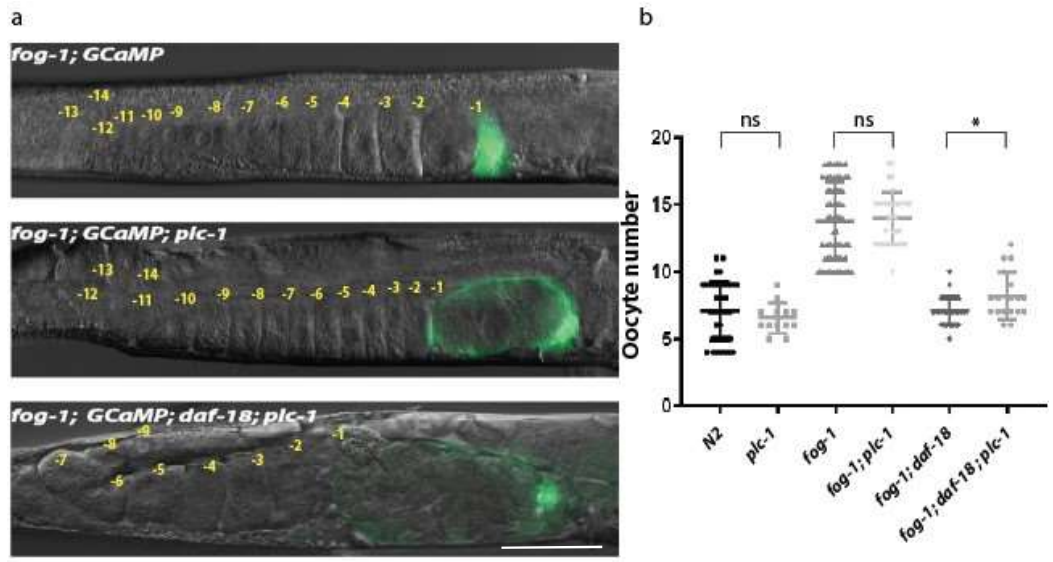

Figure. 3. 15 *daf-18* exacerbated the *fog-1; plc-1(ø)* phenotype

(a) Representative germlines of A1 animals of the indicated genotypes imaged using DIC. The area expression of Ca^{2+} is labelled with [*Pfln-1::GCaMP* + *rol-6(su1006)gf*] in *fog-1, fog-1; plc-1* and *fog-1;plc-1;daf-18*. A yellow number highlight the oocytes number. Dorsal is to the up. Scale bar: 50 μm. N= 9, 13, 6. **(b)** The average number of diakinesis-stage oocytes per gonad arm (excluding those present in the spermatheca, where applicable) in A1 hermaphrodites of the indicated genotypes was measured. The sample sizes (N) were 42, 68, 34, 18. Lines mark averages (± standard deviation), dots represent the whole sample. One asterisk indicates statistical significance ($P<0.05$, ANOVA with Tukey HSD multiple comparisons) to all other samples. ns, not significant. (a-b) Alleles: *fog-1(q253), daf-18(ok480), plc-1(rx1).*

3.7.2 The *plc-1* may be independent with *daf-18* to regulate the MI

We found that the loss of *plc-1* does not restore the *fog-1* phenotype as the double mutants still accumulates unfertilized oocytes (Figure 3.15b) accumulation and homeostatic signalling stays ON to suppress GSC proliferation but failed to make it worse since the *plc-1* alone also can reduce the GSC proliferation (Figure 3.16). And *fog-1; plc-1* MI is no significance with *fog-1*. It suggests *plc-1* may be the pathway of

fog-1 to down-regulate the GSC proliferation. Because if we assume the *plc-1* is upstream of *fog-1*, the *plc-1* may work on another pathway to aggravated *fog-1* MI value.

Daf-18 is as homeostatic signalling gene to inhibit the GSC proliferation in *fog-1* background. While, according to the *plc-1* alone MI result, *plc-1* is a gene to promote the GSC proliferation. Consists of our model, *plc-1* is positively with *daf-18*, which suggest the *plc-1* is independent with *daf-18* to regulate the GSC proliferation. Also, if we assume the *plc-1* is downstream of *daf-18*, the *fog-1; daf-18; plc-1* triple mutation should show no significant with *fog-1; daf-18*. However, our data show *plc-1* reduce the *fog-1; daf-18* MI value. It suggests that *plc-1* reduce the MI is different pathway with the *daf-18* to regulate the GSC proliferation.

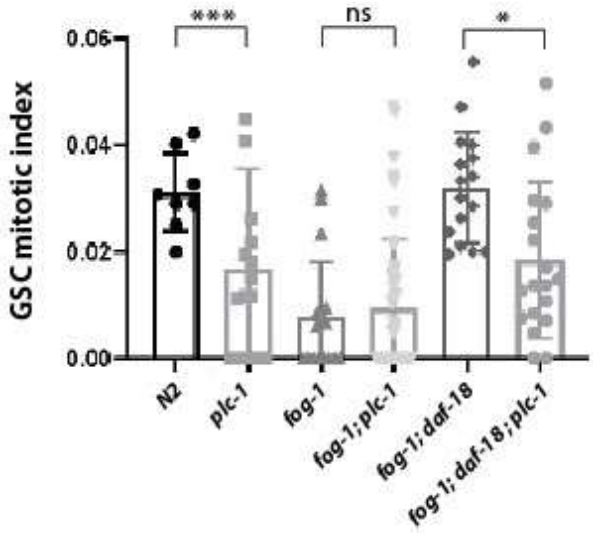

Figure. 3. 16 The *plc-1* may be independent with *daf-18* to regulate the MI

The GSC MIs of A1 hermaphrodites of the indicated genotypes were determined. N= 8, 18, 53, 19. Column mark averages, the error bar mark ± standard deviation, dots represent the whole sample. Three asterisks indicate statistical significance (P<0.0001, Kruskal-Wallis followed by Dunn) and one asterisks indicate statistical significance (P<0.05, Kruskal-Wallis followed by Dunn) to all other samples. ns, not significant. (a-b) Alleles: *fog-1(q253), daf-18(ok480), plc-1(rx1).*

3.8 Loss of *akt-1* partially restores oocyte accumulation downstream of *daf-18*

These findings imply that ovulation regulation occurs may be dependently of PIP_3's primary targets, AKT-1/2, as their activation within the spermatheca should be changed across wild-type, *fog-1* and *fog-1; daf-18(ø)* backgrounds. Hence, we investigated whether the loss of *akt-1* would modify the *fog-1*, *daf-18(ø)* phenotype. Surprisingly, our observations revealed that *akt-1(ø)* partially suppressed the *fog-1; daf-18(ø)* phenotype and promoted oocyte accumulation. These results suggest that AKT-1 activity suppresses spermatheca neck contractility, as it's removal reverses the *daf-18* defect (Figure. 3.17). DAF-18 may therefore promote spermatheca neck contractility, at least in part, by suppressing AKT-1 activation. The mechanism by which AKT-1

may in turn suppress contractility however remains to be elucidated, but is likely independent from its main downstream target, DAF-16/FOXO, since unlike DAF-18, it is not required to prevent ovulation in the absence of sperm [59, 153].

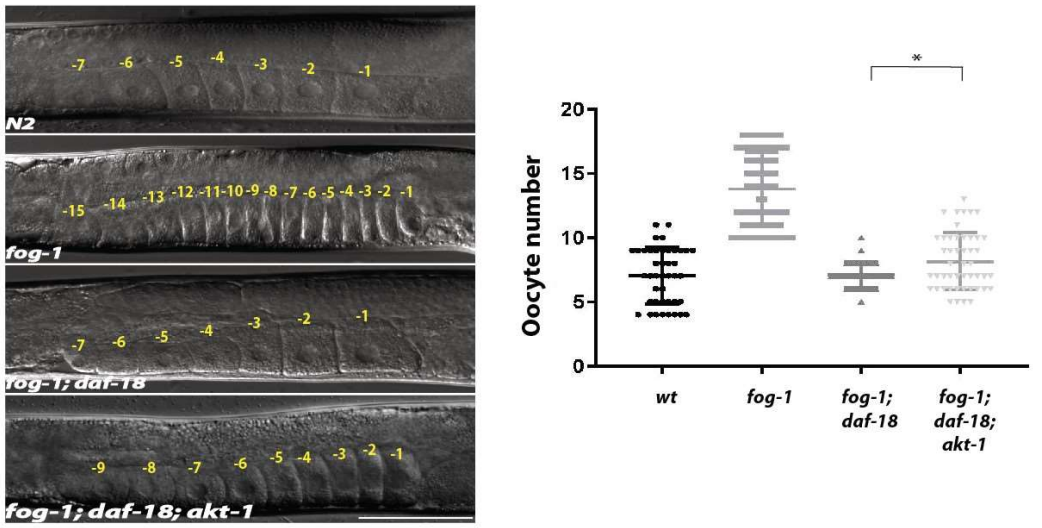

Figure. 3. 17 Loss of *akt-1* partially restores oocyte accumulation downstream of *daf-18*

(a) Representative day-1 adults (A1) of the indicated genotypes were imaged using DIC. The yellow number indicates the area occupied by oocytes. The anterior is on the left, and dorsal is up. Scale bar: 50 µm **(b)** The average number of diakinesis-stage oocytes per gonad arm in A1 hermaphrodites of the indicated genotypes was measured. The sample sizes (N) were 42, 70, 30, and 48. Lines mark averages (± standard deviation), dots represent the whole sample. One asterisk indicates statistical significance ($P<0.05$, ANOVA with Tukey HSD multiple comparisons) to all other samples. **(a and b)** Alleles: *fog-1(q253)*, *daf-18(ok480), akt-1(ok525).*

3.9 LIN-3/LET-23 may serve as the initial step in ovulation

The final maturation of the proximal oocyte is believed to provoke the release the epidermal growth factor (EGF) LIN-3 to trigger stronger ovulatory sheath cell contractions, which eventually overcome the spermatheca neck's might and force it

open while pulling it around the large, now fertilization-competent, oocyte [127, 213]. Nonetheless, direct evidence of LIN-3 release during the final maturation of the proximal oocyte is lacking. To address this, we recorded ovulation videos in animals carrying an endogenous *LIN-3::mNeonGreen* (mNG) tag [180]. As expected, we observed *LIN-3::mNG* being released during the final maturation of the proximal oocyte (Figure 3.18a). We also characterized the expression of the endogenous tagged LET-23::GFP [218] EGF receptor. We found that it was present on the sheath cells and spermetheca membranes, consistant with the models implicating it as the trigger for the sheath cell ovulatory contractions, and possibly also for triggering the spermatheca neck and bag contraction to expulse the fetilized egg into the uterus (Figure.3.18 b).

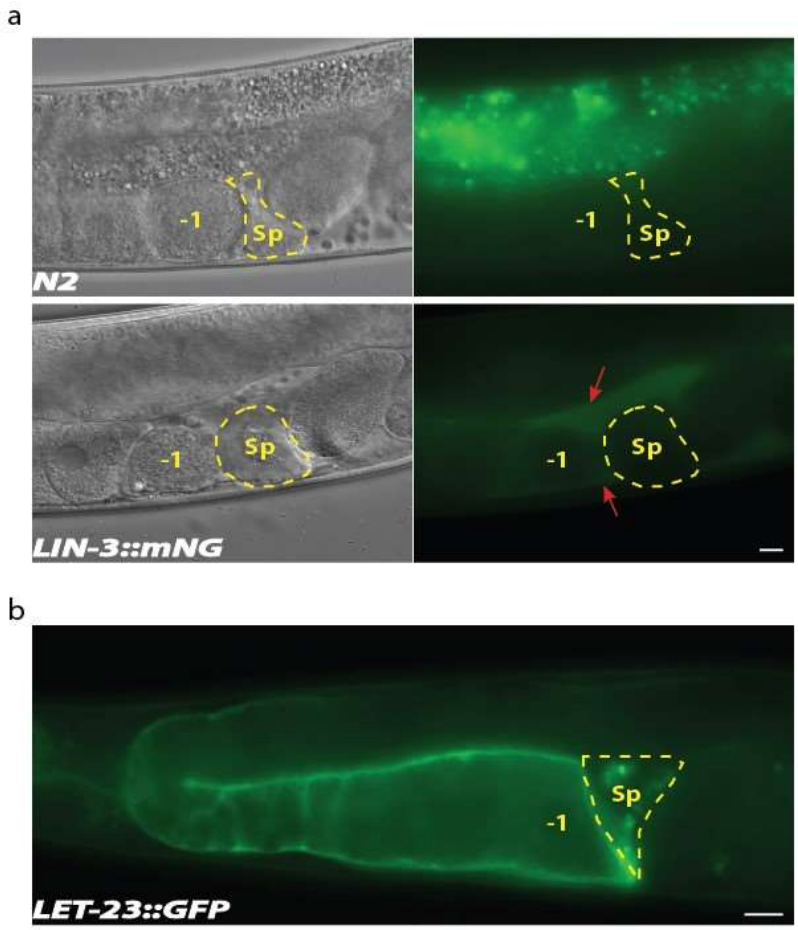

Figure. 3. 18 LIN-3/LET-23 may serve as the initial step in ovulation

(a) Representative germlines of A1 animals of the indicated genotypes imaged using DIC and *LIN-3::mNG* fluorescence. A yellow number highlight the oocytes number. The dotted line highlight the Sp. The red arrows indicate the LIN-3::mNG signal. Dorsal is to the up. Scale bar: 50 µm. **(b)** Representative germlines of A1 animals of the indicated genotypes imaged using DIC and mNG. The area expression of LET-23 is labelled with *let-23p::LET-23::GFP; unc-119(+).* Dorsal is to the up. Scale bar: 50 µm.

3.10 Loss of *daf-18* causes the formation of a differentiated benign germline tumour.

Daf-18/PTEN is considered a tumor suppressor gene. Mutations or inactivation of the *PTEN* gene are commonly associated with various human cancers and cancer predisposition syndromes [219]. One such syndrome is *PTEN* hamartoma tumour syndrome (PHTS), which results from mutations in the *PTEN* gene. In our research, we used a feminized background of *C. elegans*, such as *fog-1* mutants, where oocytes spontaneously activate upon ovulation, undergo endomitosis, and are laid. This results in the absence of tumours in *C. elegans*. Conversely, in backgrounds that prevent oocyte activation, such as *oma-1; oma-2* double mutants [220], we found that diakinesis oocytes were not laid, and hyperaccumulated inside the uterus and gonad arms of *daf-18(ø) oma-1; oma-2* triple mutants, leading to the formation of a benign oocyte tumour (Figure. 3.19), as previously observed in *aak-1(ø); oma-1; oma-2* triple mutants [154]. As such, we conclude that DAF-18 prevents the formation of benign differentiated germline tumours by non-autonomously promoting spermatheca neck contractility, and not via any cell autonomous effects. PTEN could therefore act through similar cell non-autonomous mechanisms in hµmans to prevent hamartoma formation in PHTS [142].

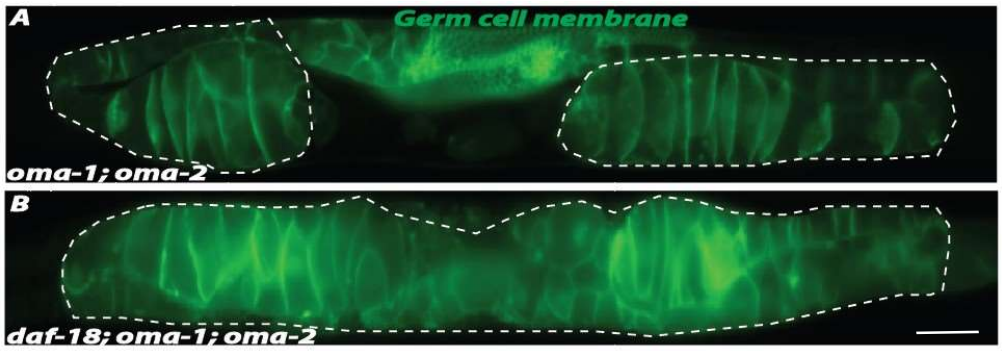

Figure. 3. 19 Loss of *daf-18* causes the formation of a differentiated benign germline tumour

(**A**) The loss of *oma-1; oma-2* prevents oocyte activation and ovulation. In response, homeostatic Signalling suppresses GSC proliferation to stall germline growth and stabilize tissue size. (**B**) In *daf-18 oma-1; oma-2* triple mutants however, oocyte still arrest but they are now ovulated, yet not laid. Homeostatic signalling is defective and does not suppress GSC proliferation, causing sustained germline growth. This leads to the disorganized hyperaccumulation of oocytes, forming a differentiated benign germline tumour [142]. **(A-B)** The region occupied by oocyte-like cells are highlighted by a white dotted line in representative A1 animals. Alleles: *oma-1(zu405te33), oma-2(te51), daf-18(ok480)*. Both strains contained the *cpSi42[Pmex-5::mNG::PLC-PH::tbb-2 3'UTR + unc-119(+)]* transgene to visualize germ cell membranes (green). Scale bar, 50 μm.

CHAPTER IV

DISCUSSION AND CONCLUSION

Considering the previously established roles of DAF-18 in suppressing germline MPK-1 activity to ensure the proper timing of oocyte growth and maturation, and potentially also to prevent the final maturation of the -1 oocyte in the absence of sperm [154, 191, 221], it would have been plausible that DAF-18 would have acted cell-autonomously within the germline to suppress MPK-1 activation and block the final maturation of the oocyte, preventing its release of LIN-3. This would have prevented the strong ovulatory contractions and ovulation, ultimately leading to oocyte accumulation [174, 191]. Contrary to this model however, we found that restoring *germline::DAF-18(+)* activity in *fog-1; daf-18(ø)* animals did not rescue oocyte accumulation.

We confirmed this unexpected negative finding by confirming the functionality of our *germline::DAF-18(+)* transgene in the *daf-2; daf-18* dauer formation model. Remarkably, we discovered that our transgene effectively restored dauer formation in *daf-2; daf-18* mutants. What's more, our analysis unveiled a crucial aspect: the restoration mechanism relies entirely on maternal contribution and adheres to a precise dosage dependency. This signifies that the capacity of germline::DAF-18 to induce dauer formation in *daf-2* mutants is exclusively attributed to the maternally-expressed DAF-18 protein, not to the zygotically-expressing DAF-18 in the germline. This result further explain that maternal *daf-18* contributions provide sufficient activity to allow *daf-2(e1370); daf-18(nr2037)* double mutants to remain dauer-constitutive which mention by Mihaylova [219]. This unexpected observation implies that *daf-18*'s function to retain oocytes and foster their accumulation in the absence of sperm does not necessitate expression in the germline. Instead, it must operate from somatic tissues in a cell non-autonomous manner.

Consistant with this, our findings showed that the reintroduction of *muscle::daf-18(+)* in the *fog-1; daf-18(ø)* background triggered oocyte accumulation and restored the downregulation of GSC proliferation. This outcome was consistently observed under two distinct muscle-specific promoters, *unc-54* and *myo-3*. Our investigation revealed that both the *unc-54* and *myo-3* promoters drive weak expression in the proximal somatic gonad. This encompasses tissues such as the sheath cells, spermatheca, and uterus – all of which exhibit contractile properties akin to muscles. These tissues have also been heavily implicated in the regulation of oocyte maturation and ovulation [105, 118, 222-224]. Building on this insight, we proceeded to express a wild-type copy of *daf-18* in the sheath cells, spermatheca, and uterus, utilizing the *lim-7* and *fos-1a* promoters, respectively. Our exploration yielded significant results: the expression of DAF-18 in the spermatheca and uterus effectively restored oocyte arrest and accumulation, while concurrently reinstating homeostatic signalling to mitigate GSC proliferation. Conversely, the introduction of *daf-18* in the sheath cells did not restore oocyte arrest but did exhibit a partial suppression of GSC proliferation. This moderate reduction in GSC proliferation due to sheath DAF-18 reexpression in the absence of oocyte accumulation suggests that this tissue is not the critical location of DAF-18 activity. Moreover, given that sheath MPK-1 activity can drive GSC proliferation [194], and that DAF-18 counteracts MPK-1 activity [154, 191], we postulate that this limited and partial rescue is likely the result of transgenic DAF-18 overexpression directly inhibiting sheath MPK-1 activation, thereby suppressing GSC proliferation. Consequently, these findings collectively suggest that the site of DAF-18's action in promoting oocyte arrest and accumulation in the absence of sperm primarily resides within the spermatheca and/or uterus. Furthermore, the expression of DAF-18 in these tissues is sufficient for the concommitant homeostatic downregulation of GSC proliferation.

In an effort to discern the precise tissue requirements for DAF-18, we further delineated its role by selectively restoring *daf-18* expression in the spermatheca neck and the spermatheca-uterus valve, utilizing the *ipp-5* and *rsef-1* promoters, respectively. Our

investigation unveiled that the presence of *daf-18* exclusively in the spermatheca neck proved sufficient to prevent spontaneous oocyte ovulation, thereby fostering their accumulation in the absence of sperm. Moreover, this localized *daf-18* expression remarkably quelled GSC proliferation. To the contrary, the expression of DAF-18 in the sp-ut valve had no discernible impact. This suggests that DAF-18 does not promote contractility of the sp-ut valve, which makes sense given that PLC-1 is not expressed in this tissue, necessitating a different mechanism of Ca^{2+} regulation from the spermathecal bag [136]. While, two recent studies aimed to explore whether the D137A and G174E alleles demonstrate overlapping effects on DAF-18 function. The findings reveal that D137A/G174E trans-heterozygotes struggle to maintain quiescence in both the somatic gonad and germ line of dauer larvae. Moreover, they are unable to enhance starvation resistance during L1 arrest. These results caution against linking a specific mutant phenotype, caused by the loss of *daf-18* activity, directly to a particular enzymatic function of DAF-18/PTEN [176, 177].

We next delved into the mechanism by which *daf-18* may operate within the spermatheca neck to ensure oocyte arrest and accumulation in the absence of sperm. Previous research has elucidated the role of PLC-1 in the spermatheca, where it instigates calcium release and initiates contractility. This cascade is stimulated upstream by PIP_2, a product stemming from the enzymatic action of DAF-18, as this enzyme is recognized for its capacity to dephosphorylate PIP_3 [134, 136, 146]. This prompted us to explore whether *daf-18* could stimulate contractility in the spermatheca neck by converting PIP_3 into PIP_2, thereby channeling into the PLC-1/ Ca^{2+} pathway. To address this hypothesis, we initially employed the GCaMP *in vivo* sensor to visualize Ca^{2+} levels within the spermatheca [225]. In a N2 context, the spermatheca neck expands, facilitating the entrance of a mature oocyte into the spermatheca. Following fertilization, the spermatheca bag contracts, propelling the oocyte into the uterus. In contrast, the *fog-1* sperm-less mutants maintain continuous contraction in the distal spermatheca, preventing any premature oocyte entry due to oocyte immaturity. Remarkably, in *fog-1; daf-18* mutants, we observed a spontaneous dilation of the distal

spermatheca, facilitating oocyte entry in the absence of sperm (Figure. 3.12). From these observations, we deduce that *daf-18* plays a pivotal role in sustaining the contracted state of the spermatheca neck, tightly intertwined with calcium signalling.

DAF-18 demonstrates a dual phosphatase activity, acting on both lipids and proteins. Specifically, its lipid function is responsible for the conversion of PIP_3 to PIP_2 [146]. To validate the pivotal role of this lipid phosphatase activity, we specifically impaired it. Our investigation revealed that the specific loss of DAF-18's lipid-phosphatase activity effectively recapitulated the *daf-18(ø)* phenotype, resulting in the prevention of oocyte accumulation and the disruption of homeostatic regulation of GSC proliferation. Considering DAF-18's ubiquitous expression across tissues, one might anticipate its absence to impact all muscles rather than solely the spermatheca. However, our insight into PIP_3 levels provides a potential solution to this puzzle. Namely, we found that PIP_3 levels remained low throughout the germline and sheath cells, but were substantially abundant in the spermatheca. This pronounced PIP_3 abundance within the spermatheca suggests that *daf-18*'s role might involve the significant conversion of PIP_3 into PIP_2, thereby facilitating contractility promotion and ovulation prevention.

To probe further into the possibility of *daf-18* prevent dilation in the spermatheca neck via the conversion of PIP_3 to PIP_2, thus engaging the PLC-1/ Ca^{2+} pathway, we conducted experiments involving the reduction of PLC-1 activity individually and in conjunction with the loss of *daf-18* in feminized hermaphrodites. Confirming previous results [134], we found that the absence of *plc-1* severely reduces contractility within the spermatheca neck and bag. Consequently, oocytes enter the spermatheca normally but become trapped in it as the neck and bag are unable to undergo the strong coordinated contraction that is required to expluse the fertilized egg in the uterus . Strikingly, oocytes do not appear to enter the spermatheca prematurely in *fog-1; plc-1* like they do in *fog-1; daf-18*, since it accumulates oocytes similar to *fog-1* single mutants. This suggests that PLC-1 is required for the spermatheca neck and bag contraction to expulse the egg into the uterus, but that its loss does not loosen the

spermatheca neck. This is why the loss of *daf-18* exacerbated the oocyte trapping defect of *plc-1* mutants, indicating independent modes of action between *daf-18* and *plc-1* in driving spermatheca neck contractility. Our data therefore suggest that DAF-18 acts to prevent spontaneous spermatheca neck dilation events independently from PLC-1, while PLC-1 ensures the strong spermatheca neck and bag contraction to expulse the egg into the uterus independently from DAF-18.

Furthermore, the loss of *akt-1* appears to improve spermatheca contractility, seemingly opposing the loss of *daf-18* in this context where *daf-18* prevents spontaneous spermatheca dilation. However, the precise mechanisms through which the loss of *akt-1* promotes spermatheca neck contraction, or by which AKT-1 promotes spermatheca neck dilation, warrant further investigation. Of note, this is not expected to occur through the inactivation of DAF-16/FOXO, since *daf-16* does not phenocopy the loss of *daf-18* [59, 153].

In addition, we aim to shed light on the complex mechanisms governing the typical ovulatory process in *C. elegans*. Our observations, which unveiled the release of LIN-3 around the final maturation of the proximal oocyte alongside the presence of LET-23 on both sheath cells and the spermatheca, provide crucial insights. Our results are consistent with the long-standing hypothesis that when the mature oocyte releases LIN-3 [127, 213], this molecule binds to the LET-23 receptor present on the sheath cells and spermatheca. This interaction is likely what triggers strong sheath ovulatory contractions [127, 213], and once the oocyte gets into the spermatheca, the strong neck and bag contraction, through PLC-1, to expulse the fertilized egg into the uterus.

Altogether, our data are consistent with a model in which DAF-18 expression in the spermatheca neck is sufficient to non-autonomously block oocyte maturation and ovulation, and for the concomitant homeostatic downregulation of GSC proliferation. We have shown that DAF-18 restricts the passage of oocytes by preventing spontaneous relaxation of the spermatheca neck. As such, the homeostatic signal linking GSC

proliferation to oocyte needs could arise either directly because of the spermatheca neck's higher contractility status, or secondary to the accumulation of arrested oocytes resulting from its increased contractility. Our study provides direct evidence supporting the secretion of LIN-3 during the final maturation of the proximal oocyte. Furthermore, the discernible presence of LET-23 on sheath cells and spermatheca strenghtens the prospective role of LIN-3/LET-23 as upstream regulators influencing PLC-1 to modulate spermatheca contractility [127]. In addition, AKT-1 emerges as a candidate gene potentially countering DAF-18 actions to maintain balanced spermatheca contractility. The exact mechanism by which AKT-1 regulates spermatheca function necessitates future comprehensive investigation (Figure. 3.19).

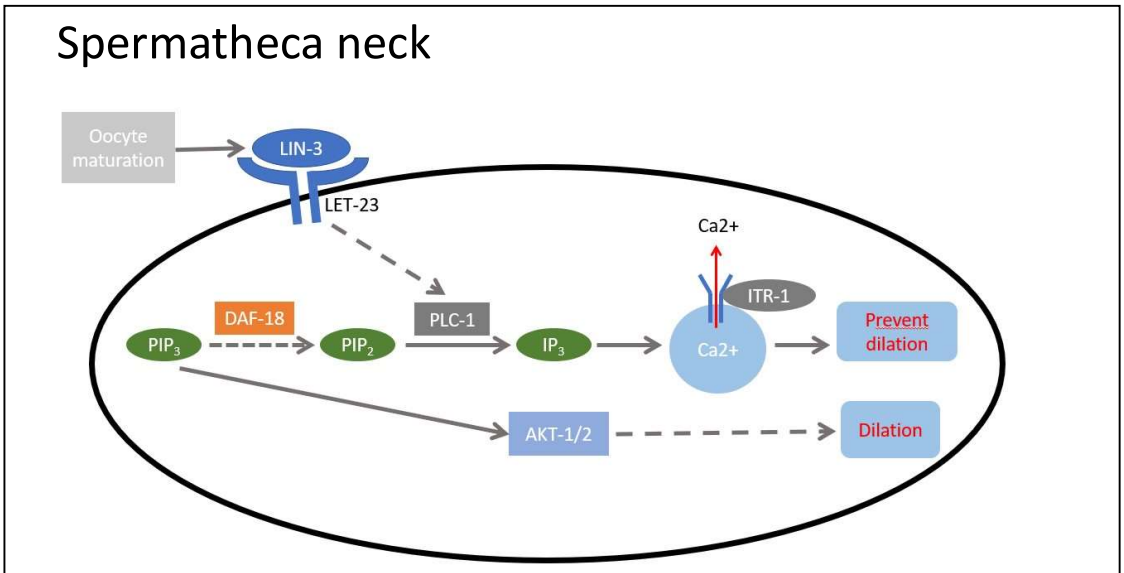

Figure. 4. 1 Model for non-autonomous regulation of oocyte maturation, ovulation and GSC proliferation by spermatheca neck DAF-18

DAF-18's established role involves the dephosphorylation of PIP_3 into PIP_2. Subsequently, PIP_2 undergoes cleavage by PLC-1, leading to the production of IP_3. This IP_3 molecule, in turn, triggers the release of calcium within the spermatheca, instigating contractility. Within this cascade, the LIN-3/LET-23 axis emerges as a potential upstream regulator, influencing the modulation of PLC-1 to govern the contractility of the spermatheca. In a parallel avenue, AKT-1 stands as another potential factor, acting as a counter-regulator for spermatheca contraction. Importantly, this regulation operates independently from *daf-18's* influence.

Future directions

Akt-1 and *Akt-2* are primary targets of PIP_3 and are highly expressed in the spermatheca [189, 226], implying that they may play a role in spermatheca function. Our results indicate that the loss of *akt-1* in the *fog-1;daf-18* strain results in partial oocyte accumulation, suggesting that AKT-1 may be involved in dilating the spermatheca to allow oocyte entry. To investigate how AKT-1 promotes spermatheca neck dilation, we are planning to create the *fog-1; daf-16; daf-18; akt-1; akt-2* quintuple mutation strain. This strain can prevent *akt-1; akt-2* from leading *C. elegans* into dauer [227]. We expect that *akt-1* null and *akt-2* null mutations in this strain could prevent spermatheca neck dilation and reduce the stronger oocyte accumulation phenotype. Additionally, through the analysis of the AKT-1 protein, we identified predicted calmodulin binding sites on AKT-1. Calmodulin appears to have four calcium binding sites. In this context, *akt-1* may prevent spermatheca neck dilation by regulating *cmd-1*, the gene encoding calmodulin.

Also, our result show that LIN-3 is secreted during the final maturation of the proximal oocyte. The released LIN-3 triggers stronger contractions in the ovulatory sheath cells, ultimately overcoming the might of the spermatheca neck and forcing it to open. However, the mechanism by which LIN-3, in combination with LET-23, dilates the spermatheca neck remains unclear. It could be a very interesting topic for further investigation [127, 213].

Overall, our study show *daf-18/PTEN*, a second tumor suppressor in humans, acts non-autonomously within the spermatheca neck to prevent oocyte ovulation in the absence of sperm; this further allows homeostatic downregulation of GSC proliferation. *PTEN* may similarly prevent tumor formation through non-autonomous mechanisms in humans, potentially involving Ca^{2+} signalling.

REFERENCES

1. Corsi, A.K., *A biochemist's guide to Caenorhabditis elegans.* Anal Biochem, 2006. **359**(1): p. 1-17.
2. Corsi, A.K., B. Wightman, and M. Chalfie, *A Transparent window into biology: A primer on Caenorhabditis elegans.* WormBook, 2015: p. 1-31.
3. Zarkower, D., *Somatic sex determination.* WormBook, 2006: p. 1-12.
4. Chasnov, J.R., *The evolutionary role of males in C. elegans.* Worm, 2013. **2**(1): p. e21146.
5. Cutter, A.D., L.T. Morran, and P.C. Phillips, *Males, Outcrossing, and Sexual Selection in Caenorhabditis Nematodes.* Genetics, 2019. **213**(1): p. 27-57.
6. Singson, A., *Every sperm is sacred: fertilization in Caenorhabditis elegans.* Dev Biol, 2001. **230**(2): p. 101-9.
7. Bargmann, C.I., *Neurobiology of the Caenorhabditis elegans genome.* Science, 1998. **282**(5396): p. 2028-33.
8. Brenner, S., *The genetics of Caenorhabditis elegans.* Genetics, 1974. **77**(1): p. 71-94.
9. Sulston, J.E. and H.R. Horvitz, *Post-embryonic cell lineages of the nematode, Caenorhabditis elegans.* Dev Biol, 1977. **56**(1): p. 110-56.
10. Kimble, J. and D. Hirsh, *The postembryonic cell lineages of the hermaphrodite and male gonads in Caenorhabditis elegans.* Dev Biol, 1979. **70**(2): p. 396-417.
11. Sulston, J.E., et al., *The embryonic cell lineage of the nematode Caenorhabditis elegans.* Dev Biol, 1983. **100**(1): p. 64-119.
12. Stiernagle, T., *Maintenance of C. elegans.* WormBook, 2006: p. 1-11.
13. Baugh, L.R., *To grow or not to grow: nutritional control of development during Caenorhabditis elegans L1 arrest.* Genetics, 2013. **194**(3): p. 539-55.
14. Hu, P.J., *Dauer.* WormBook, 2007: p. 1-19.
15. Rouault, J.P., et al., *Regulation of dauer larva development in Caenorhabditis elegans by daf-18, a homologue of the tumour suppressor PTEN.* Curr Biol, 1999. **9**(6): p. 329-32.
16. Nigon, V.M. and M.A. Felix, *History of research on C. elegans and other free-living nematodes as model organisms.* WormBook, 2017. **2017**: p. 1-84.

17. Nigon, V. and E.C. Dougherty, *Reproductive patterns and attempts at reciprocal crossing of Rhabditis elegans Maupas, 1900, and Rhabditis briggsae Dougherty and Nigon, 1949 (Nematoda: Rhabditidae).* J Exp Zool, 1949. **112**(3): p. 485-503.
18. Nigon, V., *[Experimental modifications of the sex ratio in a pseudogamous nematode].* C R Hebd Seances Acad Sci, 1952. **234**(26): p. 2568-70.
19. Haag, E.S., D.H.A. Fitch, and M. Delattre, *From "the Worm" to "the Worms" and Back Again: The Evolutionary Developmental Biology of Nematodes.* Genetics, 2018. **210**(2): p. 397-433.
20. Wenzel, D., F. Palladino, and M. Jedrusik-Bode, *Epigenetics in C. elegans: facts and challenges.* Genesis, 2011. **49**(8): p. 647-61.
21. Liang, J.J.H., I.A. McKinnon, and C.H. Rankin, *The contribution of C. elegans neurogenetics to understanding neurodegenerative diseases.* J Neurogenet, 2020. **34**(3-4): p. 527-548.
22. Saito, R.M. and S. van den Heuvel, *Malignant worms: what cancer research can learn from C. elegans.* Cancer Invest, 2002. **20**(2): p. 264-75.
23. Hubbard, E.J.A. and T. Schedl, *Biology of the Caenorhabditis elegans Germline Stem Cell System.* Genetics, 2019. **213**(4): p. 1145-1188.
24. Blackwell, T.K., et al., *TOR Signaling in Caenorhabditis elegans Development, Metabolism, and Aging.* Genetics, 2019. **213**(2): p. 329-360.
25. Carretero, M., G.M. Solis, and M. Petrascheck, *C. elegans as Model for Drug Discovery.* Curr Top Med Chem, 2017. **17**(18): p. 2067-2076.
26. Gerstein, M.B., et al., *Comparative analysis of the transcriptome across distant species.* Nature, 2014. **512**(7515): p. 445-8.
27. Culetto, E. and D.B. Sattelle, *A role for Caenorhabditis elegans in understanding the function and interactions of human disease genes.* Hum Mol Genet, 2000. **9**(6): p. 869-77.
28. White, J.G., et al., *The structure of the nervous system of the nematode Caenorhabditis elegans.* Philos Trans R Soc Lond B Biol Sci, 1986. **314**(1165): p. 1-340.
29. Hunt, P.R., *The C. elegans model in toxicity testing.* J Appl Toxicol, 2017. **37**(1): p. 50-59.
30. Apfeld, J. and S. Alper, *What Can We Learn About Human Disease from the Nematode C. elegans?* Methods Mol Biol, 2018. **1706**: p. 53-75.

31. Kapp, M.B., *Ethical and legal issues in research involving human subjects: do you want a piece of me?* J Clin Pathol, 2006. **59**(4): p. 335-9.
32. Parker, M.P. and K.R. Peterson, *Mouse Models of Erythropoiesis and Associated Diseases.* Methods Mol Biol, 2018. **1698**: p. 37-65.
33. Platt, R.J., et al., *CRISPR-Cas9 knockin mice for genome editing and cancer modeling.* Cell, 2014. **159**(2): p. 440-55.
34. Duranthon, V., et al., *On the emerging role of rabbit as human disease model and the instrumental role of novel transgenic tools.* Transgenic Res, 2012. **21**(4): p. 699-713.
35. Song, Y., et al., *Genetic deletion of a short fragment of glucokinase in rabbit by CRISPR/Cas9 leading to hyperglycemia and other typical features seen in MODY-2.* Cell Mol Life Sci, 2020. **77**(16): p. 3265-3277.
36. Ruetten, H. and C.M. Vezina, *Relevance of dog as an animal model for urologic diseases.* Prog Mol Biol Transl Sci, 2022. **189**(1): p. 35-65.
37. Feng, C., et al., *Generation of ApoE deficient dogs via combination of embryo injection of CRISPR/Cas9 with somatic cell nuclear transfer.* J Genet Genomics, 2018. **45**(1): p. 47-50.
38. Yan, S., et al., *A Huntingtin Knockin Pig Model Recapitulates Features of Selective Neurodegeneration in Huntington's Disease.* Cell, 2018. **173**(4): p. 989-1002 e13.
39. Hou, N., X. Du, and S. Wu, *Advances in pig models of human diseases.* Animal Model Exp Med, 2022. **5**(2): p. 141-152.
40. Smirnikhina, S.A., A.A. Anuchina, and A.V. Lavrov, *Ways of improving precise knock-in by genome-editing technologies.* Hum Genet, 2019. **138**(1): p. 1-19.
41. Rezazade Bazaz, M. and H. Dehghani, *From DNA break repair pathways to CRISPR/Cas-mediated gene knock-in methods.* Life Sci, 2022. **295**: p. 120409.
42. *Genome sequence of the nematode C. elegans: a platform for investigating biology.* Science, 1998. **282**(5396): p. 2012-8.
43. Stein, L.D., et al., *The genome sequence of Caenorhabditis briggsae: a platform for comparative genomics.* PLoS Biol, 2003. **1**(2): p. E45.
44. Cutter, A.D., A. Dey, and R.L. Murray, *Evolution of the Caenorhabditis elegans genome.* Mol Biol Evol, 2009. **26**(6): p. 1199-234.
45. Kaletta, T. and M.O. Hengartner, *Finding function in novel targets: C. elegans as a model organism.* Nat Rev Drug Discov, 2006. **5**(5): p. 387-98.

46. Pilarski, R., et al., *Cowden syndrome and the PTEN hamartoma tumor syndrome: systematic review and revised diagnostic criteria.* J Natl Cancer Inst, 2013. **105**(21): p. 1607-16.
47. Timmons, L. and A. Fire, *Specific interference by ingested dsRNA.* Nature, 1998. **395**(6705): p. 854.
48. Wang, J. and M.M. Barr, *RNA interference in Caenorhabditis elegans.* Methods Enzymol, 2005. **392**: p. 36-55.
49. Dickinson, D.J. and B. Goldstein, *CRISPR-Based Methods for Caenorhabditis elegans Genome Engineering.* Genetics, 2016. **202**(3): p. 885-901.
50. Paix, A., A. Folkmann, and G. Seydoux, *Precision genome editing using CRISPR-Cas9 and linear repair templates in C. elegans.* Methods, 2017. **121-122**: p. 86-93.
51. Xu, S., *The application of CRISPR-Cas9 genome editing in Caenorhabditis elegans.* J Genet Genomics, 2015. **42**(8): p. 413-21.
52. Carroll, D., *Genome engineering with zinc-finger nucleases.* Genetics, 2011. **188**(4): p. 773-82.
53. Ward, J.D., *Rapid and precise engineering of the Caenorhabditis elegans genome with lethal mutation co-conversion and inactivation of NHEJ repair.* Genetics, 2015. **199**(2): p. 363-77.
54. Paix, A., et al., *High Efficiency, Homology-Directed Genome Editing in Caenorhabditis elegans Using CRISPR-Cas9 Ribonucleoprotein Complexes.* Genetics, 2015. **201**(1): p. 47-54.
55. Dickinson, D.J., et al., *Streamlined Genome Engineering with a Self-Excising Drug Selection Cassette.* Genetics, 2015. **200**(4): p. 1035-49.
56. Mello, C.C., et al., *Efficient gene transfer in C.elegans: extrachromosomal maintenance and integration of transforming sequences.* EMBO J, 1991. **10**(12): p. 3959-70.
57. Mello, C. and A. Fire, *DNA transformation.* Methods Cell Biol, 1995. **48**: p. 451-82.
58. Barton, M.K. and J. Kimble, *fog-1, a regulatory gene required for specification of spermatogenesis in the germ line of Caenorhabditis elegans.* Genetics, 1990. **125**(1): p. 29-39.
59. Narbonne, P., P.S. Maddox, and J.C. Labbe, *DAF-18/PTEN locally antagonizes insulin signalling to couple germline stem cell proliferation to oocyte needs in C. elegans.* Development, 2015. **142**(24): p. 4230-41.
60. Tenen, C.C. and I. Greenwald, *Cell Non-autonomous Function of daf-18/PTEN in the Somatic Gonad Coordinates Somatic Gonad and Germline Development in C. elegans Dauer Larvae.* Curr Biol, 2019. **29**(6): p. 1064-1072 e8.

61. Kimble, J., *Alterations in cell lineage following laser ablation of cells in the somatic gonad of Caenorhabditis elegans.* Dev Biol, 1981. **87**(2): p. 286-300.
62. Kimble, J. and S.L. Crittenden, *Germline proliferation and its control.* WormBook, 2005: p. 1-14.
63. Metz, C.W. and C.B. Bridges, *Incompatibility of Mutant Races in Drosophila.* Proc Natl Acad Sci U S A, 1917. **3**(12): p. 673-8.
64. Bridges, C.B., *Non-Disjunction as Proof of the Chromosome Theory of Heredity (Concluded).* Genetics, 1916. **1**(2): p. 107-63.
65. Yochem, J., K. Weston, and I. Greenwald, *The Caenorhabditis elegans lin-12 gene encodes a transmembrane protein with overall similarity to Drosophila Notch.* Nature, 1988. **335**(6190): p. 547-50.
66. Kidd, S., M.R. Kelley, and M.W. Young, *Sequence of the notch locus of Drosophila melanogaster: relationship of the encoded protein to mammalian clotting and growth factors.* Mol Cell Biol, 1986. **6**(9): p. 3094-108.
67. Austin, J. and J. Kimble, *Transcript analysis of glp-1 and lin-12, homologous genes required for cell interactions during development of C. elegans.* Cell, 1989. **58**(3): p. 565-71.
68. Austin, J. and J. Kimble, *glp-1 is required in the germ line for regulation of the decision between mitosis and meiosis in C. elegans.* Cell, 1987. **51**(4): p. 589-99.
69. Greenwald, I.S., P.W. Sternberg, and H.R. Horvitz, *The lin-12 locus specifies cell fates in Caenorhabditis elegans.* Cell, 1983. **34**(2): p. 435-44.
70. Sternberg, P.W., *Vulval development.* WormBook, 2005: p. 1-28.
71. Emmons, S.W., *Male development.* WormBook, 2005: p. 1-22.
72. Herman, M.A., *Hermaphrodite cell-fate specification.* WormBook, 2006: p. 1-16.
73. Newman, A.P., J.G. White, and P.W. Sternberg, *The Caenorhabditis elegans lin-12 gene mediates induction of ventral uterine specialization by the anchor cell.* Development, 1995. **121**(2): p. 263-71.
74. Berry, L.W., B. Westlund, and T. Schedl, *Germ-line tumor formation caused by activation of glp-1, a Caenorhabditis elegans member of the Notch family of receptors.* Development, 1997. **124**(4): p. 925-36.
75. Pepper, A.S., D.J. Killian, and E.J. Hubbard, *Genetic analysis of Caenorhabditis elegans glp-1 mutants suggests receptor interaction or competition.* Genetics, 2003. **163**(1): p. 115-32.

76. Lambie, E.J. and J. Kimble, *Two homologous regulatory genes, lin-12 and glp-1, have overlapping functions.* Development, 1991. **112**(1): p. 231-40.
77. Crittenden, S.L., et al., *Regulation of the mitosis/meiosis decision in the Caenorhabditis elegans germline.* Philos Trans R Soc Lond B Biol Sci, 2003. **358**(1436): p. 1359-62.
78. Kimble, J. and P. Simpson, *The LIN-12/Notch signaling pathway and its regulation.* Annu Rev Cell Dev Biol, 1997. **13**: p. 333-61.
79. Seydoux, G. and T. Schedl, *The germline in C. elegans: origins, proliferation, and silencing.* Int Rev Cytol, 2001. **203**: p. 139-85.
80. Doyle, T.G., C. Wen, and I. Greenwald, *SEL-8, a nuclear protein required for LIN-12 and GLP-1 signaling in Caenorhabditis elegans.* Proc Natl Acad Sci U S A, 2000. **97**(14): p. 7877-81.
81. Henderson, S.T., et al., *lag-2 may encode a signaling ligand for the GLP-1 and LIN-12 receptors of C. elegans.* Development, 1994. **120**(10): p. 2913-24.
82. Fitzgerald, K. and I. Greenwald, *Interchangeability of Caenorhabditis elegans DSL proteins and intrinsic signalling activity of their extracellular domains in vivo.* Development, 1995. **121**(12): p. 4275-82.
83. Henderson, S.T., et al., *Functional domains of LAG-2, a putative signaling ligand for LIN-12 and GLP-1 receptors in Caenorhabditis elegans.* Mol Biol Cell, 1997. **8**(9): p. 1751-62.
84. Crittenden, S.L., et al., *GLP-1 is localized to the mitotic region of the C. elegans germ line.* Development, 1994. **120**(10): p. 2901-11.
85. Marin, V.A. and T.C. Evans, *Translational repression of a C. elegans Notch mRNA by the STAR/KH domain protein GLD-1.* Development, 2003. **130**(12): p. 2623-32.
86. Lee, M.H. and T. Schedl, *RNA-binding proteins.* WormBook, 2006: p. 1-13.
87. Evans, T.C. and C.P. Hunter, *Translational control of maternal RNAs.* WormBook, 2005: p. 1-11.
88. Eckmann, C.R., et al., *GLD-3 and control of the mitosis/meiosis decision in the germline of Caenorhabditis elegans.* Genetics, 2004. **168**(1): p. 147-60.
89. Hansen, D., et al., *Control of the proliferation versus meiotic development decision in the C. elegans germline through regulation of GLD-1 protein accumulation.* Development, 2004. **131**(1): p. 93-104.
90. Hansen, D., E.J. Hubbard, and T. Schedl, *Multi-pathway control of the proliferation versus meiotic development decision in the*

Caenorhabditis elegans germline. Dev Biol, 2004. **268**(2): p. 342-57.
91. Kadyk, L.C. and J. Kimble, *Genetic regulation of entry into meiosis in Caenorhabditis elegans.* Development, 1998. **125**(10): p. 1803-13.
92. Crittenden, S.L., et al., *A conserved RNA-binding protein controls germline stem cells in Caenorhabditis elegans.* Nature, 2002. **417**(6889): p. 660-3.
93. Lamont, L.B., et al., *FBF-1 and FBF-2 regulate the size of the mitotic region in the C. elegans germline.* Dev Cell, 2004. **7**(5): p. 697-707.
94. Wickens, M., et al., *A PUF family portrait: 3'UTR regulation as a way of life.* Trends Genet, 2002. **18**(3): p. 150-7.
95. Jones, A.R. and T. Schedl, *Mutations in gld-1, a female germ cell-specific tumor suppressor gene in Caenorhabditis elegans, affect a conserved domain also found in Src-associated protein Sam68.* Genes Dev, 1995. **9**(12): p. 1491-504.
96. Wang, L., et al., *A regulatory cytoplasmic poly(A) polymerase in Caenorhabditis elegans.* Nature, 2002. **419**(6904): p. 312-6.
97. Suh, N., et al., *The GLD-2 poly(A) polymerase activates gld-1 mRNA in the Caenorhabditis elegans germ line.* Proc Natl Acad Sci U S A, 2006. **103**(41): p. 15108-12.
98. Thompson, B.E., et al., *Dose-dependent control of proliferation and sperm specification by FOG-1/CPEB.* Development, 2005. **132**(15): p. 3471-81.
99. Ellis, R.E. and J. Kimble, *The fog-3 gene and regulation of cell fate in the germ line of Caenorhabditis elegans.* Genetics, 1995. **139**(2): p. 561-77.
100. Doniach, T. and J. Hodgkin, *A sex-determining gene, fem-1, required for both male and hermaphrodite development in Caenorhabditis elegans.* Dev Biol, 1984. **106**(1): p. 223-35.
101. Hodgkin, J., *Sex determination in the nematode C. elegans: analysis of tra-3 suppressors and characterization of fem genes.* Genetics, 1986. **114**(1): p. 15-52.
102. Zetka, M., *Homologue pairing, recombination and segregation in Caenorhabditis elegans.* Genome Dyn, 2009. **5**: p. 43-55.
103. Hirsh, D., D. Oppenheim, and M. Klass, *Development of the reproductive system of Caenorhabditis elegans.* Dev Biol, 1976. **49**(1): p. 200-19.
104. L'Hernault, S.W., *Spermatogenesis.* WormBook, 2006: p. 1-14.
105. McCarter, J., et al., *On the control of oocyte meiotic maturation and ovulation in Caenorhabditis elegans.* Dev Biol, 1999. **205**(1): p. 111-28.

106. Ellis, R. and T. Schedl, *Sex determination in the germ line.* WormBook, 2007: p. 1-13.
107. Ward, S., Y. Argon, and G.A. Nelson, *Sperm morphogenesis in wild-type and fertilization-defective mutants of Caenorhabditis elegans.* J Cell Biol, 1981. **91**(1): p. 26-44.
108. Smith, H., *Sperm motility and MSP.* WormBook, 2006: p. 1-8.
109. Miller, M.A., et al., *A sperm cytoskeletal protein that signals oocyte meiotic maturation and ovulation.* Science, 2001. **291**(5511): p. 2144-7.
110. Hillers, K.J., et al., *Meiosis.* WormBook, 2017. **2017**: p. 1-43.
111. Zickler, D. and N. Kleckner, *Recombination, Pairing, and Synapsis of Homologs during Meiosis.* Cold Spring Harb Perspect Biol, 2015. **7**(6).
112. Roeder, G.S., *Meiotic chromosomes: it takes two to tango.* Genes Dev, 1997. **11**(20): p. 2600-21.
113. Albertson, D.G., A.M. Rose, and A.M. Villeneuve, *Chromosome Organization, Mitosis, and Meiosis*, in *C. elegans II*, D.L. Riddle, et al., Editors. 1997: Cold Spring Harbor (NY).
114. Cheng, H., J.A. Govindan, and D. Greenstein, *Regulated trafficking of the MSP/Eph receptor during oocyte meiotic maturation in C. elegans.* Curr Biol, 2008. **18**(10): p. 705-714.
115. Miller, M.A., et al., *An Eph receptor sperm-sensing control mechanism for oocyte meiotic maturation in Caenorhabditis elegans.* Genes Dev, 2003. **17**(2): p. 187-200.
116. Govindan, J.A., et al., *Galphao/i and Galphas signaling function in parallel with the MSP/Eph receptor to control meiotic diapause in C. elegans.* Curr Biol, 2006. **16**(13): p. 1257-68.
117. Govindan, J.A., et al., *Somatic cAMP signaling regulates MSP-dependent oocyte growth and meiotic maturation in C. elegans.* Development, 2009. **136**(13): p. 2211-21.
118. Whitten, S.J. and M.A. Miller, *The role of gap junctions in Caenorhabditis elegans oocyte maturation and fertilization.* Dev Biol, 2007. **301**(2): p. 432-46.
119. Lee, M.H., et al., *Multiple functions and dynamic activation of MPK-1 extracellular signal-regulated kinase signaling in Caenorhabditis elegans germline development.* Genetics, 2007. **177**(4): p. 2039-62.
120. Han, S.M., P.A. Cottee, and M.A. Miller, *Sperm and oocyte communication mechanisms controlling C. elegans fertility.* Dev Dyn, 2010. **239**(5): p. 1265-81.
121. Yamamoto, I., M.E. Kosinski, and D. Greenstein, *Start me up: cell signaling and the journey from oocyte to embryo in C. elegans.* Dev Dyn, 2006. **235**(3): p. 571-85.

122. Ward, S. and J.S. Carrel, *Fertilization and sperm competition in the nematode Caenorhabditis elegans.* Dev Biol, 1979. **73**(2): p. 304-21.
123. Samuel, A.D., V.N. Murthy, and M.O. Hengartner, *Calcium dynamics during fertilization in C. elegans.* BMC Dev Biol, 2001. **1**: p. 8.
124. Zannoni, S., S.W. L'Hernault, and A.W. Singson, *Dynamic localization of SPE-9 in sperm: a protein required for sperm-oocyte interactions in Caenorhabditis elegans.* BMC Dev Biol, 2003. **3**: p. 10.
125. Ward, S., E. Hogan, and G.A. Nelson, *The initiation of spermiogenesis in the nematode Caenorhabditis elegans.* Dev Biol, 1983. **98**(1): p. 70-9.
126. Hall, D.H., et al., *Ultrastructural features of the adult hermaphrodite gonad of Caenorhabditis elegans: relations between the germ line and soma.* Dev Biol, 1999. **212**(1): p. 101-23.
127. Clandinin, T.R., J.A. DeModena, and P.W. Sternberg, *Inositol trisphosphate mediates a RAS-independent response to LET-23 receptor tyrosine kinase activation in C. elegans.* Cell, 1998. **92**(4): p. 523-33.
128. Xu, X., et al., *Linking integrin to IP(3) signaling is important for ovulation in Caenorhabditis elegans.* FEBS Lett, 2005. **579**(2): p. 549-53.
129. Kelley, C.A., et al., *The myosin light-chain kinase MLCK-1 relocalizes during Caenorhabditis elegans ovulation to promote actomyosin bundle assembly and drive contraction.* Mol Biol Cell, 2018. **29**(16): p. 1975-1991.
130. Pelaia, G., et al., *Molecular mechanisms underlying airway smooth muscle contraction and proliferation: implications for asthma.* Respir Med, 2008. **102**(8): p. 1173-81.
131. Sethi, K., E.J. Cram, and R. Zaidel-Bar, *Stretch-induced actomyosin contraction in epithelial tubes: Mechanotransduction pathways for tubular homeostasis.* Semin Cell Dev Biol, 2017. **71**: p. 146-152.
132. Brozovich, F.V., et al., *Mechanisms of Vascular Smooth Muscle Contraction and the Basis for Pharmacologic Treatment of Smooth Muscle Disorders.* Pharmacol Rev, 2016. **68**(2): p. 476-532.
133. Tan, P.Y. and R. Zaidel-Bar, *Transient membrane localization of SPV-1 drives cyclical actomyosin contractions in the C. elegans spermatheca.* Curr Biol, 2015. **25**(2): p. 141-151.
134. Kovacevic, I., J.M. Orozco, and E.J. Cram, *Filamin and phospholipase C-epsilon are required for calcium signaling in*

the Caenorhabditis elegans spermatheca. PLoS Genet, 2013. **9**(5): p. e1003510.
135. Castaneda, P.G., et al., *Galpha/GSA-1 works upstream of PKA/KIN-1 to regulate calcium signaling and contractility in the Caenorhabditis elegans spermatheca.* PLoS Genet, 2020. **16**(8): p. e1008644.
136. Kariya, K., et al., *Phospholipase Cepsilon regulates ovulation in Caenorhabditis elegans.* Dev Biol, 2004. **274**(1): p. 201-10.
137. LaFever, L. and D. Drummond-Barbosa, *Direct control of germline stem cell division and cyst growth by neural insulin in Drosophila.* Science, 2005. **309**(5737): p. 1071-3.
138. Shim, J., S. Gururaja-Rao, and U. Banerjee, *Nutritional regulation of stem and progenitor cells in Drosophila.* Development, 2013. **140**(23): p. 4647-56.
139. Murphy, C.T. and P.J. Hu, *Insulin/insulin-like growth factor signaling in C. elegans*, in *Wormbook*, e.T.C.e.R. Community, Editor. 2013, WormBook, doi/10.1895/wormbook.1.164.1.
140. Narbonne, P. and R. Roy, *Regulation of germline stem cell proliferation downstream of nutrient sensing.* Cell Div, 2006. **1**: p. 29.
141. Michaelson, D., et al., *Insulin signaling promotes germline proliferation in C. elegans.* Development, 2010. **137**(4): p. 671-80.
142. Valet, M. and P. Narbonne, *Formation of benign tumors by stem cell deregulation.* PLoS Genet, 2022. **18**(10): p. e1010434.
143. Tomasetti, C. and B. Vogelstein, *Cancer etiology. Variation in cancer risk among tissues can be explained by the number of stem cell divisions.* Science, 2015. **347**(6217): p. 78-81.
144. Morgan, D.E., S.L. Crittenden, and J. Kimble, *The C. elegans adult male germline: stem cells and sexual dimorphism.* Dev Biol, 2010. **346**(2): p. 204-14.
145. Cinquin, A., et al., *Intermittent Stem Cell Cycling Balances Self-Renewal and Senescence of the C. elegans Germ Line.* PLoS Genet, 2016. **12**(4): p. e1005985.
146. Liu, J. and I.D. Chin-Sang, *C. elegans as a model to study PTEN's regulation and function.* Methods, 2015. **77-78**: p. 180-90.
147. Hua, Q.X., et al., *A divergent INS protein in Caenorhabditis elegans structurally resembles human insulin and activates the human insulin receptor.* Genes Dev, 2003. **17**(7): p. 826-31.
148. Amrit, F.R. and R.C. May, *Younger for longer: insulin signalling, immunity and ageing.* Curr Aging Sci, 2010. **3**(3): p. 166-76.

149. Ogg, S. and G. Ruvkun, *The C. elegans PTEN homolog, DAF-18, acts in the insulin receptor-like metabolic signaling pathway.* Mol Cell, 1998. **2**(6): p. 887-93.
150. Murphy, C.T. and P.J. Hu, *Insulin/insulin-like growth factor signaling in C. elegans.* WormBook, 2013: p. 1-43.
151. Tissenbaum, H.A., *DAF-16: FOXO in the Context of C. elegans.* Curr Top Dev Biol, 2018. **127**: p. 1-21.
152. Lin, K., et al., *Regulation of the Caenorhabditis elegans longevity protein DAF-16 by insulin/IGF-1 and germline signaling.* Nat Genet, 2001. **28**(2): p. 139-45.
153. Qin, Z. and E.J. Hubbard, *Non-autonomous DAF-16/FOXO activity antagonizes age-related loss of C. elegans germline stem/progenitor cells.* Nat Commun, 2015. **6**: p. 7107.
154. Narbonne, P., P.S. Maddox, and J.C. Labbe, *DAF-18/PTEN signals through AAK-1/AMPK to inhibit MPK-1/MAPK in feedback control of germline stem cell proliferation.* PLoS Genet, 2017. **13**(4): p. e1006738.
155. Clark, W.H., *Tumour progression and the nature of cancer.* Br J Cancer, 1991. **64**(4): p. 631-44.
156. Humphries, A., et al., *Lineage tracing reveals multipotent stem cells maintain human adenomas and the pattern of clonal expansion in tumor evolution.* Proc Natl Acad Sci U S A, 2013. **110**(27): p. E2490-9.
157. Jones, S., et al., *Comparative lesion sequencing provides insights into tumor evolution.* Proc Natl Acad Sci U S A, 2008. **105**(11): p. 4283-8.
158. Stryker, S.J., et al., *Natural history of untreated colonic polyps.* Gastroenterology, 1987. **93**(5): p. 1009-13.
159. Li, J., et al., *PTEN, a putative protein tyrosine phosphatase gene mutated in human brain, breast, and prostate cancer.* Science, 1997. **275**(5308): p. 1943-7.
160. Steck, P.A., et al., *Identification of a candidate tumour suppressor gene, MMAC1, at chromosome 10q23.3 that is mutated in multiple advanced cancers.* Nat Genet, 1997. **15**(4): p. 356-62.
161. Li, D.M. and H. Sun, *TEP1, encoded by a candidate tumor suppressor locus, is a novel protein tyrosine phosphatase regulated by transforming growth factor beta.* Cancer Res, 1997. **57**(11): p. 2124-9.
162. Liaw, D., et al., *Germline mutations of the PTEN gene in Cowden disease, an inherited breast and thyroid cancer syndrome.* Nat Genet, 1997. **16**(1): p. 64-7.

163. Magana, M., A.P. Landeta-Sa, and Y. Lopez-Flores, *Cowden Disease: A Review.* Am J Dermatopathol, 2022. **44**(10): p. 705-717.
164. Gammon, A., K. Jasperson, and M. Champine, *Genetic basis of Cowden syndrome and its implications for clinical practice and risk management.* Appl Clin Genet, 2016. **9**: p. 83-92.
165. Pilarski, R., *Cowden syndrome: a critical review of the clinical literature.* J Genet Couns, 2009. **18**(1): p. 13-27.
166. Dragoo, D.D., et al., *PTEN Hamartoma Tumor Syndrome/Cowden Syndrome: Genomics, Oncogenesis, and Imaging Review for Associated Lesions and Malignancy.* Cancers (Basel), 2021. **13**(13).
167. Masse, I., et al., *Lifespan and dauer regulation by tissue-specific activities of Caenorhabditis elegans DAF-18.* Dev Biol, 2005. **286**(1): p. 91-101.
168. Solari, F., et al., *The human tumour suppressor PTEN regulates longevity and dauer formation in Caenorhabditis elegans.* Oncogene, 2005. **24**(1): p. 20-7.
169. Song, M.S., L. Salmena, and P.P. Pandolfi, *The functions and regulation of the PTEN tumour suppressor.* Nat Rev Mol Cell Biol, 2012. **13**(5): p. 283-96.
170. Liu, J., et al., *Insulin activates the insulin receptor to downregulate the PTEN tumour suppressor.* Oncogene, 2014. **33**(29): p. 3878-85.
171. Zhang, S., et al., *Combating trastuzumab resistance by targeting SRC, a common node downstream of multiple resistance pathways.* Nat Med, 2011. **17**(4): p. 461-9.
172. Tamura, M., et al., *Inhibition of cell migration, spreading, and focal adhesions by tumor suppressor PTEN.* Science, 1998. **280**(5369): p. 1614-7.
173. Shi, Y., et al., *PTEN is a protein tyrosine phosphatase for IRS1.* Nat Struct Mol Biol, 2014. **21**(6): p. 522-7.
174. Brisbin, S., et al., *A role for C. elegans Eph RTK signaling in PTEN regulation.* Dev Cell, 2009. **17**(4): p. 459-69.
175. Nakdimon, I., et al., *PTEN negatively regulates MAPK signaling during Caenorhabditis elegans vulval development.* PLoS Genet, 2012. **8**(8): p. e1002881.
176. Wittes, J. and I. Greenwald, *Genetic analysis of DAF-18/PTEN missense mutants for the ability to maintain quiescence of the somatic gonad and germ line in Caenorhabditis elegans dauer larvae.* G3 (Bethesda), 2022. **12**(6).
177. Chen, J., et al., *Genetic analysis of daf-18/PTEN missense mutants for starvation resistance and developmental regulation*

during Caenorhabditis elegans L1 arrest. G3 (Bethesda), 2022. **12**(6).
178. Lin, K., et al., *daf-16: An HNF-3/forkhead family member that can function to double the life-span of Caenorhabditis elegans.* Science, 1997. **278**(5341): p. 1319-22.
179. Fukuyama, M., A.E. Rougvie, and J.H. Rothman, *C. elegans DAF-18/PTEN mediates nutrient-dependent arrest of cell cycle and growth in the germline.* Curr Biol, 2006. **16**(8): p. 773-9.
180. Mereu, L., et al., *Polarized epidermal growth factor secretion ensures robust vulval cell fate specification in Caenorhabditis elegans.* Development, 2020. **147**(11).
181. Gibson, D.G., et al., *Enzymatic assembly of DNA molecules up to several hundred kilobases.* Nat Methods, 2009. **6**(5): p. 343-5.
182. Frokjaer-Jensen, C., et al., *Single-copy insertion of transgenes in Caenorhabditis elegans.* Nat Genet, 2008. **40**(11): p. 1375-83.
183. Dickinson, D.J., et al., *Engineering the Caenorhabditis elegans genome using Cas9-triggered homologous recombination.* Nat Methods, 2013. **10**(10): p. 1028-34.
184. Seydoux, G., C. Savage, and I. Greenwald, *Isolation and characterization of mutations causing abnormal eversion of the vulva in Caenorhabditis elegans.* Dev Biol, 1993. **157**(2): p. 423-36.
185. Crittenden, S.L., et al., *Cellular analyses of the mitotic region in the Caenorhabditis elegans adult germ line.* Mol Biol Cell, 2006. **17**(7): p. 3051-61.
186. Robinson-Thiewes, S., et al., *Non-autonomous regulation of germline stem cell proliferation by somatic MPK-1/MAPK activity in C. elegans.* Cell Rep, 2021. **35**(8): p. 109162.
187. Kocsisova, Z., K. Kornfeld, and T. Schedl, *Cell cycle accumulation of the proliferating cell nuclear antigen PCN-1 transitions from continuous in the adult germline to intermittent in the early embryo of C. elegans.* BMC Dev Biol, 2018. **18**(1): p. 12.
188. Korta, D.Z., S. Tuck, and E.J. Hubbard, *S6K links cell fate, cell cycle and nutrient response in C. elegans germline stem/progenitor cells.* Development, 2012. **139**(5): p. 859-70.
189. Paradis, S. and G. Ruvkun, *Caenorhabditis elegans Akt/PKB transduces insulin receptor-like signals from AGE-1 PI3 kinase to the DAF-16 transcription factor.* Genes Dev, 1998. **12**(16): p. 2488-98.
190. Narbonne, P. and R. Roy, *Inhibition of germline proliferation during C. elegans dauer development requires PTEN, LKB1 and AMPK signalling.* Development, 2006. **133**(4): p. 611-9.

191. Suzuki, Y. and M. Han, *Genetic redundancy masks diverse functions of the tumor suppressor gene PTEN during C. elegans development.* Genes Dev, 2006. **20**(4): p. 423-8.
192. Tenlen, J.R., et al., *MEX-5 asymmetry in one-cell C. elegans embryos requires PAR-4- and PAR-1-dependent phosphorylation.* Development, 2008. **135**(22): p. 3665-75.
193. Gil, E.B., et al., *Regulation of the insulin-like developmental pathway of Caenorhabditis elegans by a homolog of the PTEN tumor suppressor gene.* Proc Natl Acad Sci U S A, 1999. **96**(6): p. 2925-30.
194. Robinson-Thiewes, S., et al., *Non-autonomous regulation of germline stem cell proliferation by somatic MPK-1/MAPK activity in C. elegans.* Cell Reports, 2021. **35**(8).
195. Kenyon, C.J., *The genetics of ageing.* Nature, 2010. **464**(7288): p. 504-12.
196. Shore, D.E. and G. Ruvkun, *A cytoprotective perspective on longevity regulation.* Trends Cell Biol, 2013. **23**(9): p. 409-20.
197. Gems, D., et al., *Two pleiotropic classes of daf-2 mutation affect larval arrest, adult behavior, reproduction and longevity in Caenorhabditis elegans.* Genetics, 1998. **150**(1): p. 129-55.
198. Riddle, D.L., M.M. Swanson, and P.S. Albert, *Interacting genes in nematode dauer larva formation.* Nature, 1981. **290**(5808): p. 668-71.
199. Patel, D.S., et al., *Clustering of genetically defined allele classes in the Caenorhabditis elegans DAF-2 insulin/IGF-1 receptor.* Genetics, 2008. **178**(2): p. 931-46.
200. Kenyon, C., et al., *A C. elegans mutant that lives twice as long as wild type.* Nature, 1993. **366**(6454): p. 461-4.
201. Dorman, J.B., et al., *The age-1 and daf-2 genes function in a common pathway to control the lifespan of Caenorhabditis elegans.* Genetics, 1995. **141**(4): p. 1399-406.
202. Maduro, M. and D. Pilgrim, *Identification and cloning of unc-119, a gene expressed in the Caenorhabditis elegans nervous system.* Genetics, 1995. **141**(3): p. 977-88.
203. Miyabayashi, T., et al., *Expression and function of members of a divergent nuclear receptor family in Caenorhabditis elegans.* Dev Biol, 1999. **215**(2): p. 314-31.
204. Okkema, P.G., et al., *Sequence requirements for myosin gene expression and regulation in Caenorhabditis elegans.* Genetics, 1993. **135**(2): p. 385-404.
205. Altun, Z.F. and D.H. Hall, *Muscle system, somatic muscle.* In WormAtlas, 2009.

206. Ardizzi, J.P. and H.F. Epstein, *Immunochemical localization of myosin heavy chain isoforms and paramyosin in developmentally and structurally diverse muscle cell types of the nematode Caenorhabditis elegans.* J Cell Biol, 1987. **105**(6 Pt 1): p. 2763-70.
207. Miller, D.M., F.E. Stockdale, and J. Karn, *Immunological identification of the genes encoding the four myosin heavy chain isoforms of Caenorhabditis elegans.* Proc Natl Acad Sci U S A, 1986. **83**(8): p. 2305-9.
208. Voutev, R., et al., *Characterization of the Caenorhabditis elegans Islet LIM-homeodomain ortholog, lim-7.* FEBS Lett, 2009. **583**(2): p. 456-64.
209. McCarter, J., et al., *Soma-germ cell interactions in Caenorhabditis elegans: multiple events of hermaphrodite germline development require the somatic sheath and spermathecal lineages.* Dev Biol, 1997. **181**(2): p. 121-43.
210. Bui, Y.K. and P.W. Sternberg, *Caenorhabditis elegans inositol 5-phosphatase homolog negatively regulates inositol 1,4,5-triphosphate signaling in ovulation.* Mol Biol Cell, 2002. **13**(5): p. 1641-51.
211. Ghosh, S. and P.W. Sternberg, *Spatial and molecular cues for cell outgrowth during C. elegans uterine development.* Dev Biol, 2014. **396**(1): p. 121-35.
212. Aono, S., et al., *PAR-3 is required for epithelial cell polarity in the distal spermatheca of C. elegans.* Development, 2004. **131**(12): p. 2865-74.
213. Yin, X., et al., *Inositol 1,4,5-trisphosphate signaling regulates rhythmic contractile activity of myoepithelial sheath cells in Caenorhabditis elegans.* Mol Biol Cell, 2004. **15**(8): p. 3938-49.
214. Bouffard, J., et al., *The RhoGAP SPV-1 regulates calcium signaling to control the contractility of the Caenorhabditis elegans spermatheca during embryo transits.* Mol Biol Cell, 2019. **30**(7): p. 907-922.
215. Nakai, J., M. Ohkura, and K. Imoto, *A high signal-to-noise Ca(2+) probe composed of a single green fluorescent protein.* Nat Biotechnol, 2001. **19**(2): p. 137-41.
216. Chen, T.W., et al., *Ultrasensitive fluorescent proteins for imaging neuronal activity.* Nature, 2013. **499**(7458): p. 295-300.
217. Myers, M.P., et al., *P-TEN, the tumor suppressor from human chromosome 10q23, is a dual-specificity phosphatase.* Proc Natl Acad Sci U S A, 1997. **94**(17): p. 9052-7.

218. Haag, A., et al., *An in vivo EGF receptor localization screen in C. elegans Identifies the Ezrin homolog ERM-1 as a temporal regulator of signaling.* PLoS Genet, 2014. **10**(5): p. e1004341.
219. Mihaylova, V.T., et al., *The PTEN tumor suppressor homolog in Caenorhabditis elegans regulates longevity and dauer formation in an insulin receptor-like signaling pathway.* Proc Natl Acad Sci U S A, 1999. **96**(13): p. 7427-32.
220. Detwiler, M.R., et al., *Two zinc finger proteins, OMA-1 and OMA-2, are redundantly required for oocyte maturation in C. elegans.* Dev Cell, 2001. **1**(2): p. 187-99.
221. Das, D. and S. Arur, *Conserved insulin signaling in the regulation of oocyte growth, development, and maturation.* Mol Reprod Dev, 2017. **84**(6): p. 444-459.
222. Rose, K.L., et al., *The POU gene ceh-18 promotes gonadal sheath cell differentiation and function required for meiotic maturation and ovulation in Caenorhabditis elegans.* Dev Biol, 1997. **192**(1): p. 59-77.
223. Hiatt, S.M., et al., *Caenorhabditis elegans FOS-1 and JUN-1 regulate plc-1 expression in the spermatheca to control ovulation.* Mol Biol Cell, 2009. **20**(17): p. 3888-95.
224. McGovern, M., et al., *A role for sperm in regulation of egg-laying in the nematode C. elegans.* BMC Dev Biol, 2007. **7**: p. 41.
225. Kovacevic, I. and E.J. Cram, *Filamin and Phospholipase C-epsilon are required for calcium signaling in the Caenorhabditis elegans Spermatheca.* Worm, 2013. **2**(3): p. e25717.
226. Padmanabhan, S., et al., *A PP2A regulatory subunit regulates C. elegans insulin/IGF-1 signaling by modulating AKT-1 phosphorylation.* Cell, 2009. **136**(5): p. 939-51.
227. Hertweck, M., C. Gobel, and R. Baumeister, *C. elegans SGK-1 is the critical component in the Akt/PKB kinase complex to control stress response and life span.* Dev Cell, 2004. **6**(4): p. 577-88.